NUREG/CR-3781
EGG-2313
DRAFT

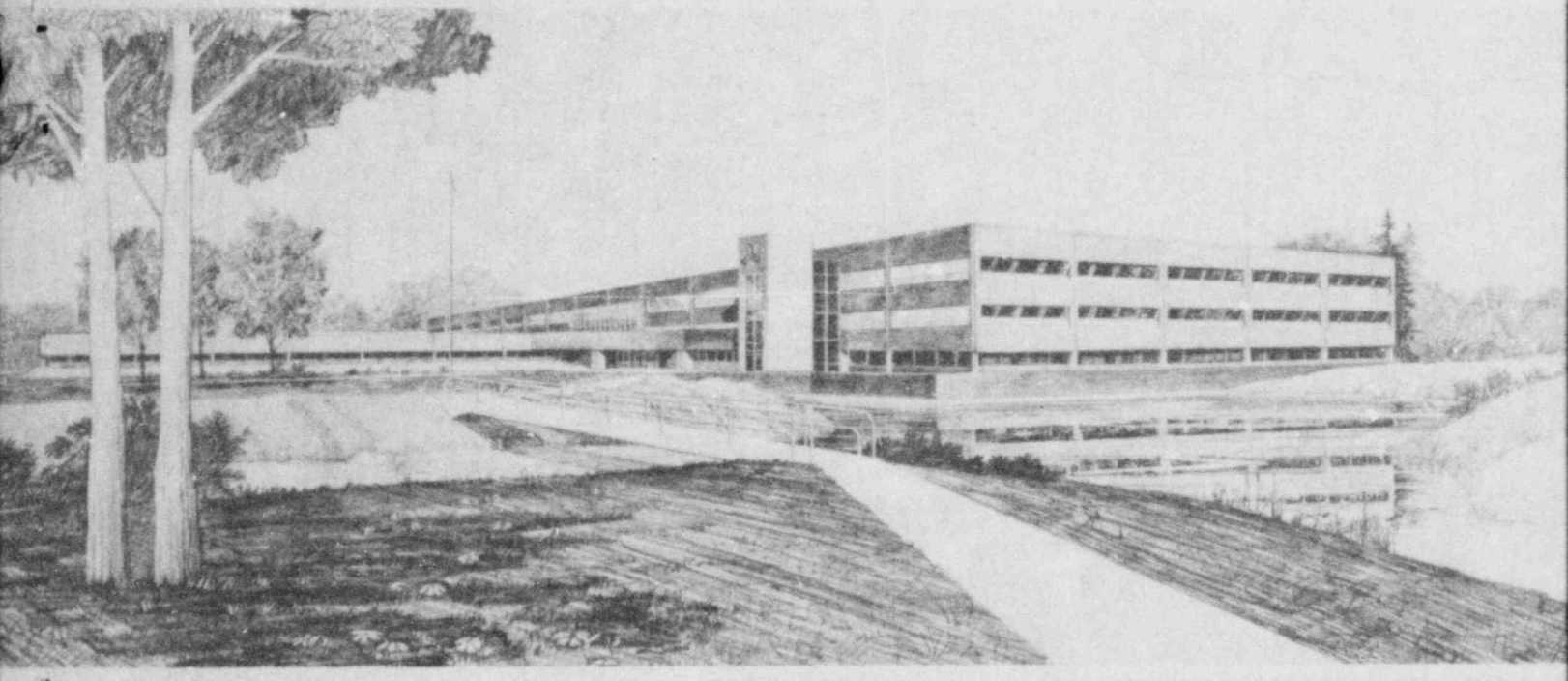

Idaho National Engineering Laboratory
Operated by the U.S. Department of Energy

PCI-Related Cladding Failures During Off-Normal Events—DRAFT

Draft Report of the USNRC PCI Review Group

R. Van Houten
M. Tokar
P. E. MacDonald

May 1984

Prepared for the
U.S. Nuclear Regulatory Commission
Under DOE Contract No. DE-AC07-76IDO1570

EG&G Idaho

UNITED STATES
NUCLEAR REGULATORY COMMISSION
WASHINGTON, D. C. 20555

Draft NUREG/CR-3781 for Comment

To those who receive copies of this draft report for comment:

Please send your comments to Dr. R. Van Houten, United States Nuclear Regulatory Commission, Mail Stop 1130 SS, Washington, D.C. 20555, to be received no later than September 15, 1984. An effort will be made to respond to significant comments by expansion or revision of the text as appropriate, and as permitted by available personnel and budgetary resources.

Sincerely,

Robert D. Van Houten

R. Van Houten
Chairman, PCI Task Force

NUREG/CR-3781
EGG-2313
DRAFT

PCI-RELATED CLADDING FAILURES DURING OFF-NORMAL EVENTS—DRAFT

Draft Report of the USNRC
PCI Review Group

R. Van Houten*
M. Tokar*
P. E. MacDonald+

Published May 1984

Prepared for the
U.S. Nuclear Regulatory Commission
Washington, D.C. 20555
Under DOE Contract No. DE-AC07-76IDO1570

* U.S. Nuclear Regulatory Commission
+ EG&G Idaho, Inc.

ABSTRACT

Pellet-cladding interaction (PCI) has long been identified as a fuel rod failure mechanism during power increases in both pressurized and boiling water reactors, and commercial guidelines have practically eliminated such failures during standard operations. A question remains regarding the possible formation of through-wall cladding cracks during several types of postulated off-normal reactor events involving power increases. Because fuel failure estimates are used as input to radiological dose calculations, the U.S. Nuclear Regulatory Commission has recently formed a task force of fuel behavior experts to study PCI, due to the NRC's concern that existing rod overheating criteria might be inadequate for evaluating transient severity in this regard. The tasks assigned to the PCI Review Group were to examine the applicable data base, to assess the potential for rod failures during representative transients of concern, and to make appropriate recommendations. This report includes preliminary findings for reactor events of the type addressed by Chapter 15 of the NRC Standard Review Plan. Specifically, the BWR turbine trip without bypass, PWR control rod withdrawal error, subcritical PWR control rod withdrawal error, BWR control blade withdrawal error, and the PWR steamline break are analyzed on the joint bases of peak rod power, power increase, ramp rate, and duration at elevated power. These Chapter 15 events are compared to numerous test reactor results and to other relevant investigations, and tentative conclusions on transient severity and data base adequacy are presented. Progress in developing computer codes for predicting PCI-induced fuel rod failures is also discussed.

CONTENTS

FIGURES

TABLES

1. INTRODUCTION

It has been recognized since at least the early 1970s that cracks in the Zircaloy cladding of water reactor fuel rods can occur during increases in reactor power.[1,2] This type of fuel rod failure mechanism,[a] which is now commonly known as pellet-cladding interaction (PCI), is generally thought to result from the tensile (hoop) stresses induced in the cladding by the thermal expansion of the UO_2 pellets during power ramps. The mechanical interaction may be combined with chemical attack or embrittlement of the cladding by aggressive fission products released from the fuel before or during the ramps, and is aggravated by irradiation damage in the Zircaloy. Although there has been considerable research of the metallurgical and mechanistic aspects of PCI (i.e., the associated physical, chemical, mechanical, thermal, and irradiation processes), the relative contributions and effects of the various phenomena involved have been difficult to quantify. This has complicated the question of how to address PCI from the standpoint of reactor regulation.

From a reactor safety or regulatory point of view, the PCI problem can be separated into two parts based on conditions of reactor operation. One part encompasses those PCI impacts that might result from overly rapid or large power increases during normal reactor power ascensions. The incidence of PCI failures under such conditions has been kept within acceptable bounds in recent years through the implementation of improved, more PCI-resistant fuel designs and the adoption of operational procedures designed to limit the magnitude and rate of power increases during normal reactor operation. These procedures, which have been in use for about 10 years, are sometimes called Pre-Conditioning Interim Operating Management Recommendations (PCIOMRs).[3] They are supplied by the vendors to their utility customers and are generally considered proprietary. These procedures and fuel design improvements have been effective in reducing the number of PCI-related fuel failures that result from power changes during

---

a. Fuel rod "failure" is defined as one or more through-wall cracks. Fuel rod "damage" is defined as non-through-wall cracks (incipient cracks).

normal operation. This part of the PCI issue has been brought into the realm of a personnel exposure and economic concern rather than an off-site, potential public hazard concern due to (a) the relatively low incidence of normal-operation, PCI-related failures and (b) the ability of failure detection systems to provide time for mitigating action should such failures occur.

Therefore, we are concerned here solely with the second portion of the PCI/reactor-operating-condition issue: viz., will PCI failures occur and should they be considered in the evaluation of the potential radiological consequences for off-normal reactor operating conditions? The type of off-normal conditions that are of concern are those power-increasing events described in Chapter 15 of the NRC's Standard Review Plan.[4] These will be described in some detail in Section 2 of this report.

Pellet-cladding interaction (PCI) is relevant to Chapter 15 reactor safety considerations for the following reasons. There is a regulatory requirement to account for fuel failures originating from any source; the common interpretation of General Design Criterion 10 is that fuel rods must not undergo (significant) failure during normal operation, including anticipated operational occurrences.[5] This means that for certain power-increasing events such as BWR turbine trip without bypass (see Reference 4, Section 15.2.2), appropiate margins are necessary to assure that specified acceptable fuel design limits (SAFDL's) are not exceeded by PCI. The principal reason that PCI is relevant to Chapter 15 safety analyses stems from the fact that it is necessary to estimate the potential radiological consequences of accidents (events of potentially greater severity, but lower frequency than moderate frequency transients) so that they may be compared with reactor siting criteria (2-hour and 30-day whole-body and thyroid dose limits) provided in 10 CFR 100.[6]

For both transient and accident conditions, the commonly used fuel failure criteria are overheating criteria, such as the departure from

nucleate boiling ratio (DNBR) for PWRs and the minimum critical power ratio (MCPR) for BWRs. It has been generally regarded by the NRC staff that if the DNBR/MCPR criteria are satisfied, i.e., if the ratios were calculated to remain above the acceptable values for a given event, then no fuel failures would be assumed for dose calculation purposes; whereas if the DNBR/MCPR criteria were violated, the number of fuel rods calculated to lie below the acceptance criteria values would be considered failed. As a corollary to these assumptions, it has been understood (assumed) that the DNBR/MCPR fuel failure criteria provide bounding estimates for the dose calculation inputs for the Chapter 15 overpower events, even though the ultimate failure mechanism may be more mechanical (PCI) than overheating in nature.

To address the question of whether PCI is adequately dealt with by the DNBR/MCPR estimates of failed fuel in the evaluation of SRP Chapter 15 overpower events, the NRC formed a task force consisting of senior reactor fuel performance experts within the agency and contractor laboratories. A list of the task force members is provided in Appendix A. Brief descriptions of the BWR and PWR SRP Chapter 15 overpower events of interest are provided in Section 2 (with more detail in Appendices B, C, D, and E). Because most of the in-reactor PCI-related cladding failure tests have been conducted at European facilities, some of the task force members and associates visited several such facilities in January 1983 to acquire data that could be used to address the PCI safety issue. The information obtained from that trip, together with other relevant information is discussed in Section 3 of this report. The PCI task force conclusions and recommendations are contained in Section 4.

2. CHAPTER 15 POSTULATED PCI EVENTS

Guidance regarding the type of information that should be supplied in plant safety analysis reports (SARs) dealing with postulated transients and accidents is provided in Chapter 15 of the NRC's Standard Review Plan (Reference 4) and Standard Format (Reference 7). The postulated Chapter 15 events are categorized and grouped on the basis of systems effects and core thermal-hydraulic or physics consequences. From the standpoint of potential fuel rod pellet-cladding interaction (PCI) failure, any rapidly increasing overpower (i.e., power-increasing) event could conceivably have an impact. However, for the purposes of this investigation, it was possible to single out certain types of events that could be considered bounding in terms of PCI potential. Those events are discussed below, with more detail provided in Appendices B through E.

In general, the events selected for primary consideration by the PCI task force were chosen because they tended to exhibit the largest power increases and hold times (i.e., times at elevated power). It cannot be overemphasized that the particular values of the parameters associated with each event, such as the change in power (ΔP) and time at elevated power, were not, and were never intended or represented to be, "bounding," "average," "realistic," etc. They are merely representative of values provided either in plant safety analysis reports or in generic study reports, and as such, the parametric values served the purpose intended: viz., to enable order-of-magnitude estimates to be made of PCI impact for the Chapter 15 events in question.

2.1 BWR Turbine Trip Without Bypass

Postulated Chapter 15 "increase in reactor pressure" events such as the BWR turbine trip without bypass (TTw/oBP), main steamline isolation valve closure, and generator load rejection are all quite alike in the sense that the plant system and core changes are very similar. That is, a turbine trip signal initiates closures of the turbine stop valves, turbine control valves, or main steamline isolation valve. The fast closure of these valves with the bypass valves in the closed position produces a rapid

increase in system pressure, which causes a significant compression of the steam voids. The positive reactivity derived from the void compression induces a sharp increase in neutron flux. The relief valves trip open when the steamline pressure exceeds the valve opening setpoints. This limits the extent of the pressure rise and, in conjunction with the scram reactivity, limits the magnitude of the neutron flux peak. The duration of the transient is on the order of a few seconds or less, unless there is a failure to scram. (A turbine trip without bypass and without scram or main steamline isolation valve closure without scram are not Chapter 15 anticipated transients.)

Turbine trip without bypass is the limiting moderate frequency transient for many BWRs because it is associated with the largest change in critical power ratio and because it has, therefore, the lowest minimum critical power ratio (MCPR). Since the MCPR is required to remain above the safety limit critical power ratio (usually about 1.07), the turbine trip without bypass or its sister event, the generator load rejection, determines the operating limit critical power ratio for full power operation. The turbine trip without bypass has, therefore, been extensively analyzed using various computer codes, which have been benchmarked with turbine trip experiments performed at the Peach Bottom II reactor.[8] As part of an NRC technical assistance program, Brookhaven National Laboratory (BNL) performed an analysis of the Peach Bottom II turbine trip tests in the late 1970s (References 9 and 10) using the BNL-TWIGL code (Reference 11). The calculated results were in good agreement with the test data. We therefore asked Brookhaven for nodalized information on linear heat generation rates versus time for a turbine trip without bypass transient. These results are reproduced in Appendix B. Salient points are summarized below.

As shown in Figure 1 and several Appendix B plots of peak linear heat generation rate versus transient time, the turbine trip without bypass is characterized by a very sharp, but short, power spike. For a given core node or block, the linear heat generation rate may increase by over an order of magnitude in less than 0.5 sec (see, for example, Figure 1, where the linear heat generation rate at approximately 0.5 sec is 7.0 kW/ft; at

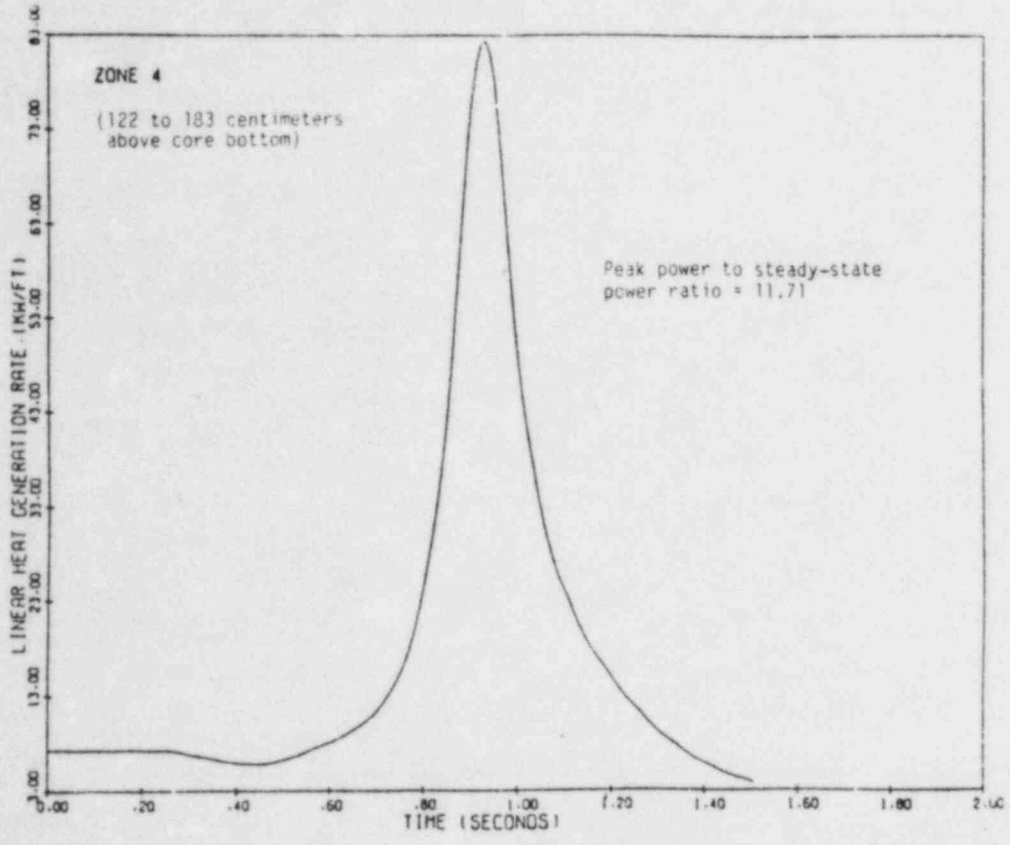

Figure 1. Brookhaven-calculated linear heat generation rates versus time at just below the core midplane for turbine trip without bypass anticipated transient.

0.92 sec is 82.8 kW/ft; and at 1.4 sec is back down to 7.2 kW/ft). These calculations are consistent with General Electric Co. predictions of neutron flux versus time as provided in numerous BWR safety analysis reports and generic topicals. As will be discussed in the next section of this report, the crucial question relevant to the likelihood for PCI damage during this event is whether the transient is too low in peak enthalpy and too short in duration for PCI cracking conditions to develop.

2.2 PWR Control Rod Bank Withdrawal Error

Whether at subcritical, low power startup, or rated power conditions, control rod withdrawal errors and misoperations are classified as Condition II, moderate frequency transients for which fuel rod failures should not be allowed to occur. In addition to the usual thermal-hydraulic acceptance criteria (for example, DNBR ≤ 1.3), the NRC's Standard Review Plan (Sections 15.4.1, 15.4.2 and 15.4.3) lists linear heat generation rate

limits that are related to UO_2 melting. PWR plants are designed to avoid UO_2 melting. In the case of BWR fuel rods, however, the UO_2 melting limit is tied to a 1% cladding strain limit; that is, UO_2 melting must be limited to the amount that would cause 1% strain due to the volumetric change involved in going from solid to liquid UO_2. The 1% strain and UO_2 centerline melt criteria are the only PCI failure criteria currently in use in LWR licensing.

Control rod withdrawals involve power increases and could thus have a PCI impact beyond the limits of 1% strain or UO_2 centerline melting. To gain insight into the potential magnitude of the impact of control rod withdrawals on PCI, the analysis of moderate frequency reactivity and power distribution anomalies presented in the San Onofre Units 2 and 3 (Combustion Engineering Co.) Final Safety Analysis Report[12] were inspected. Figures 2 and 3 present the core power level in percent of full power and the peak linear heat generation rate versus time during an uncontrolled San Onofre control element assembly bank withdrawal at high power. Note that while the core power stays below 110% of nominal full power throughout the transient (which starts at about 75% of full power), the peak linear heat generation rate increases from about 9.6 to 15.2 kW/ft--a 58% increase. Figures 4 and 5 present the San Onofre core power level in percent of full power and the peak linear heat generation rate versus time during an uncontrolled control rod bank withdrawal at low power. The core power remains below 80% of nominal full power, whereas the linear heat generation rate in the peak rod increases from zero to about 23 kW/ft in about 20 sec. The reactor coolant system pressure increases from 2000 to about 2550 psi, the minimum DNBR decreases to about 1.19, and the fuel centerline temperatures remain below the UO_2 melting point during both the low and high power, uncontrolled control rod withdrawal events.

An independent analysis of an uncontrolled control rod bank withdrawal in a Westinghouse Electric Corp.-designed PWR has been performed by Brookhaven National Laboratory. The analysis (a) assumed that the steady state relative power distribution in the reactor core remained unchanged

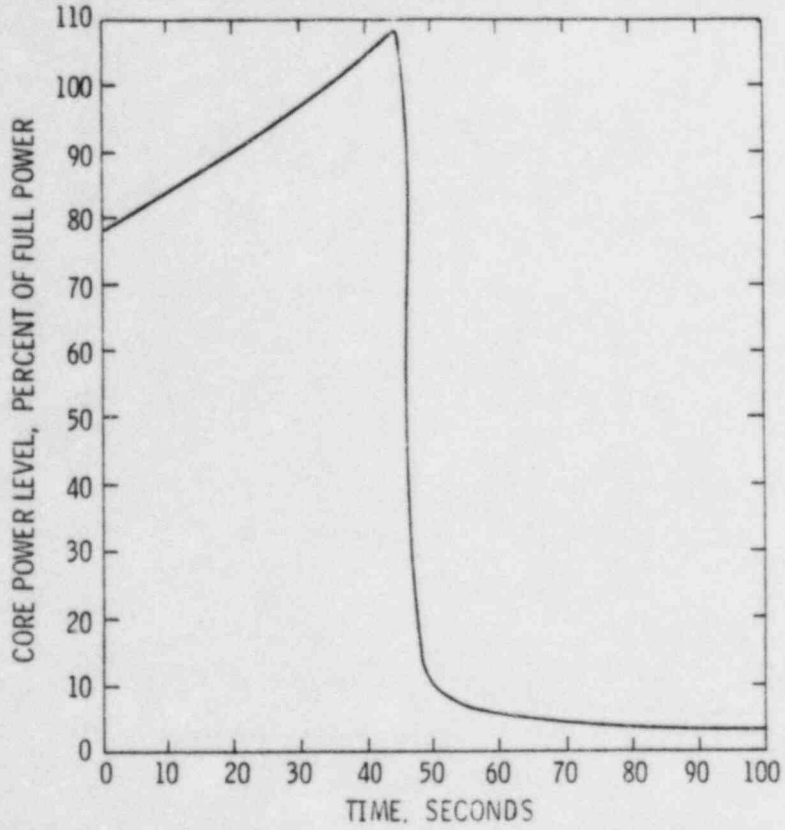

Figure 2. Core power in percent of full power versus time during a PWR uncontrolled control element assembly withdrawal at high power.

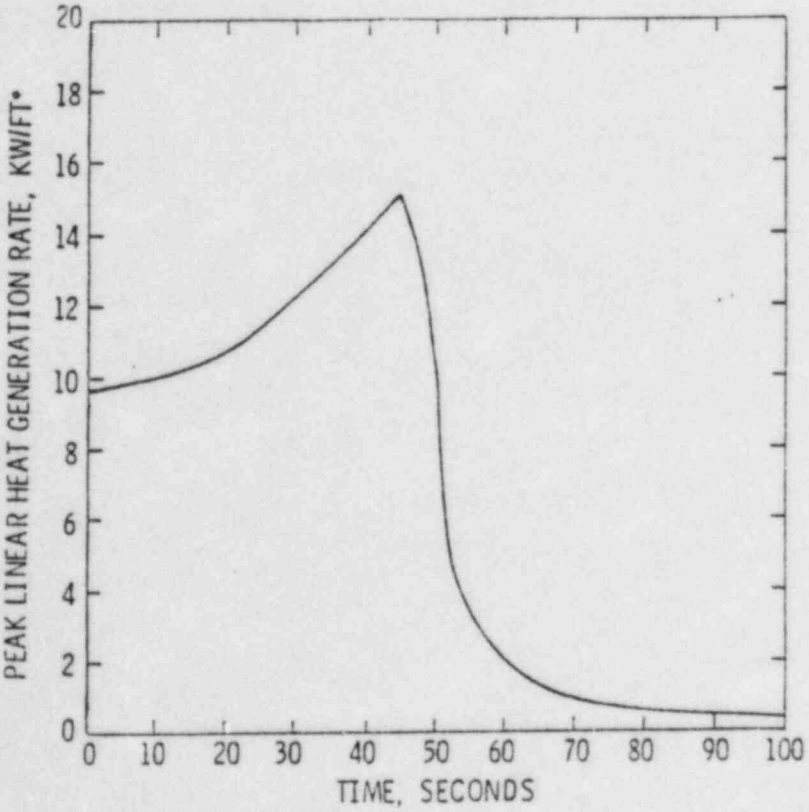

*INCLUDING FUEL Ddensification AND ENGINEERING FACTORS

Figure 3. Peak linear heat generation rate versus time during a PWR uncontrolled control element assembly withdrawal at high power.

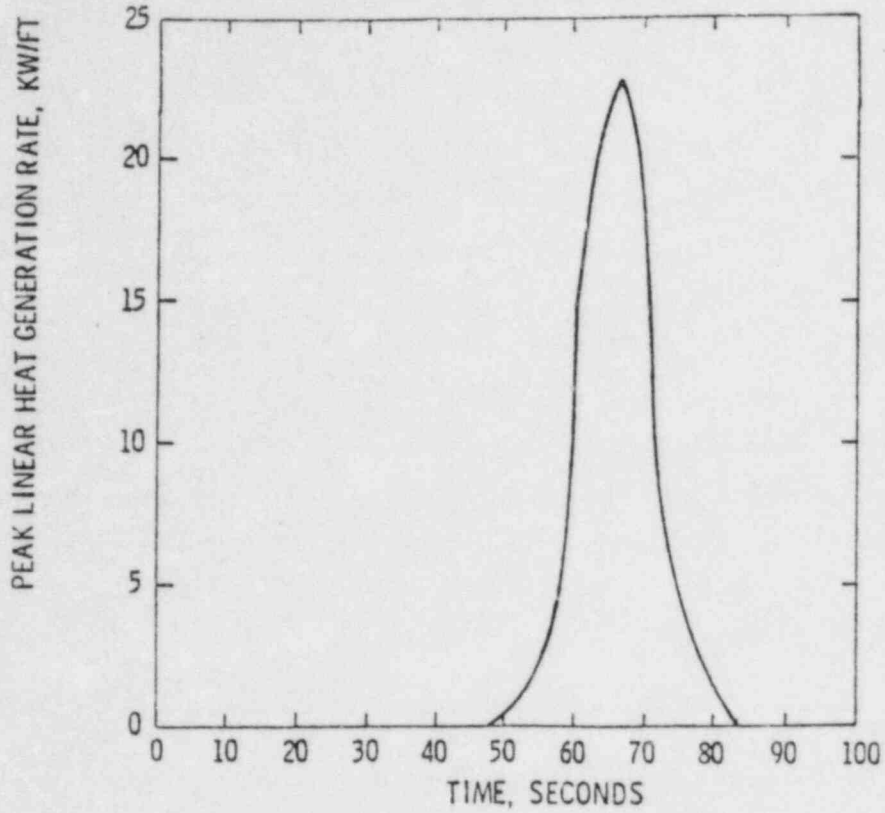

Figure 4. Core power in percent of full power versus time during a PWR uncontrolled control element assembly withdrawal at low power.

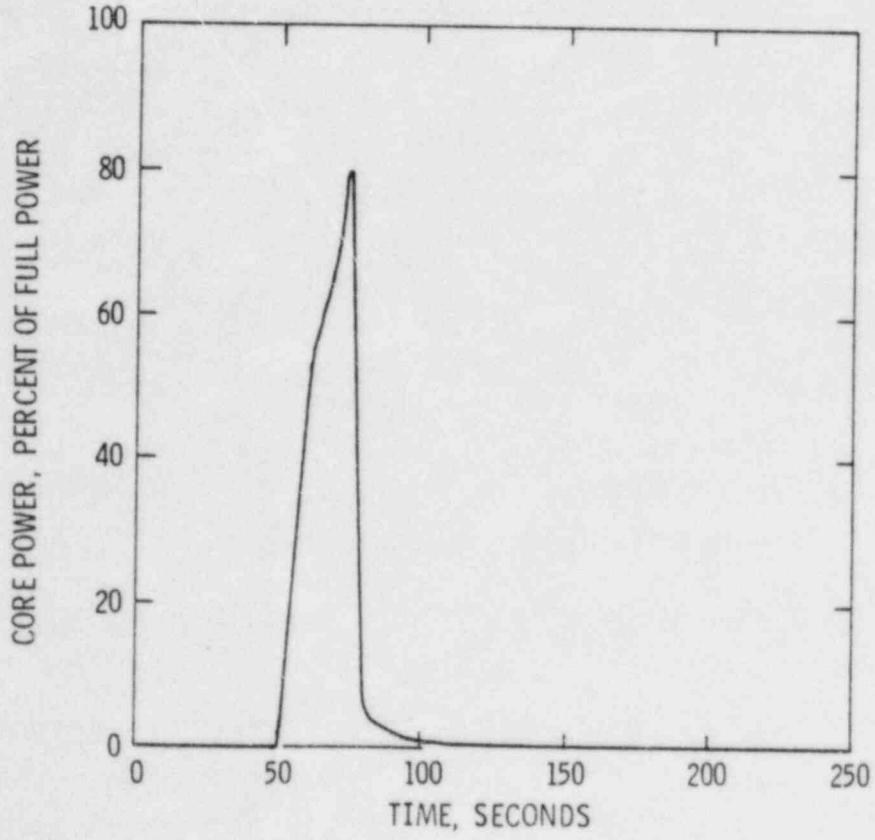

Figure 5. Peak linear heat generation rate versus time during an uncontrolled control element assembly withdrawal in a PWR at low power.

during the transient and (b) used core power distributions published by Westinghouse[13] for a 3250-MWt PWR. The Brookhaven results are presented in Appendix C.

The Brookhaven-calculated peak linear heat generation rate history of the worst radial and axial core node during an uncontrolled control rod bank withdrawal from high power is plotted in Figure 6. The peak linear heat generation rate increases about 20% (from 15 to 18 kW/ft) in about 2 sec. It should be noted that the particular transient that was analyzed by Brookhaven is a fast reactivity insertion event, assumed terminated by Westinghouse plant protection systems after 4 sec, and that the calculated core power increase is about the same as for a Combustion Engineering bank withdrawal event estimated to last about an order of magnitude longer. (Compare Figure 2 with Figure C-4 in Appendix C, for example.) However, the increase in peak linear heat generation rate calculated by Brookhaven (Figure 6) is less than the increase published in the San Onofre Final Safety Analysis Report (Figure 3). In any case, the longer, slower event is more germane than the fast withdrawal regarding potential PCI impact due to the longer time at elevated fuel temperatures. As explained in Section 3, this extended duration would prolong cladding hoop stresses and permit additional release of potentially corrosive fission products.

For comparison purposes, BNL also provided some information about an uncontrolled PWR bank withdrawal from subcritical conditions (Figure 7 and Appendix C). The core average power for that case peaked at 73% of nominal versus 120% for the hot full power core, but the rate of increase in linear heat generation rate was much greater for the transient initiated from subcritical conditions. This would be important if strain rate were a major factor in PCI cracking initiation or propagation.

2.3 BWR Control Blade Withdrawal Events

The BWR abnormal control rod withdrawal event involves only one control rod (cruciform blade), and only the fuel in the immediate vicinity

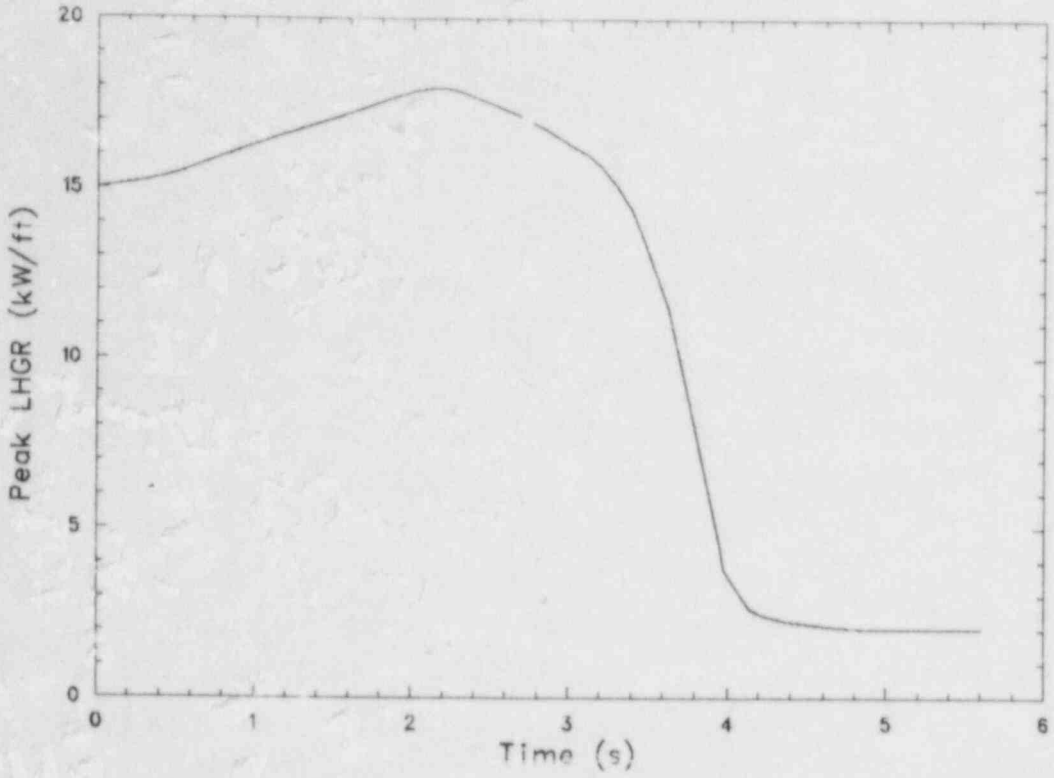

Figure 6. Brookhaven nodal worst-case projection for a PWR uncontrc withdrawal of a control rod bank at normal power.

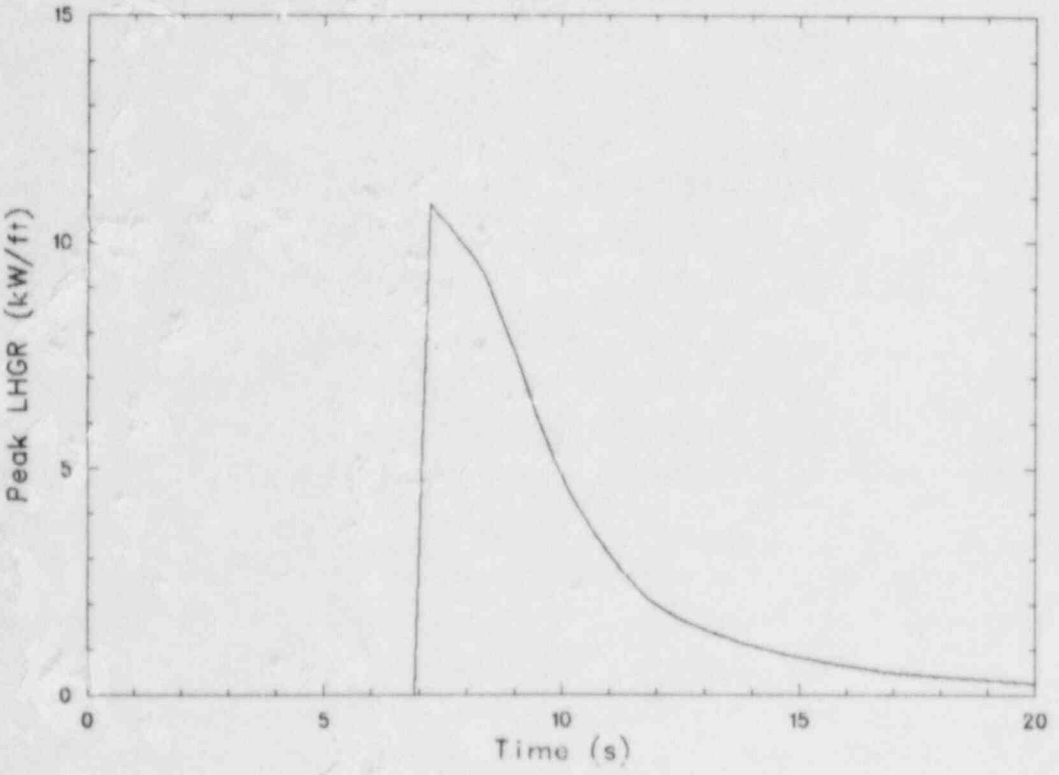

Figure 7. Brookhaven nodal worst-case projection for a PWR uncontrolled bank withdrawal at zero power.

of that control rod. The event can be divided into two categories: (1) low ("zero") power initial conditions during reactor startup and (2) operating power range initial conditions. The characteristics and analysis methods for these two categories are quite different.

The zero power event is basically similar to the corresponding PWR event, except that it involves an incorrect selection of a single control rod rather than a control bank withdrawal. Incorrect withdrawal is normally prevented by rod monitoring systems. However, these systems do not have full protection grade characteristics and, therefore, the event is assumed to occur and is analyzed with a maximum rod worth. An example of this analysis is described in the first part of Appendix D, taken from the LaSalle FSAR.[14] The analysis method is simple and conservative, neglecting important feedback and power distribution details. The event includes a few feet of rod withdrawal, excess reactivity, a rapid power level increase, and a scram which quickly shuts down the power. There is very little energy increase in the average core fuel (on the order of 1 cal/g). However, there is large power peaking (maximum local peaking factor of over 20) in the four assemblies surrounding the withdrawn rod, but only over a few (~2) feet axially in these assemblies. This region is at an appreciable power density level for less than 2 sec and the maximum energy content (by this conservative calculation) is less than 60 cal/g (initial content is 16 cal/g). The present NRC limit for this event--170 cal/g, which corresponds approximately to the point at which MCPR limits would be exceeded--is not approached.

The operating power range rod withdrawal event is quite different in its characteristics and analysis methodology. No scram is involved, but rather a rod block protection system (safety grade) is called upon in BWR3-5 designs (BWR6s use a limited rod movement system). The rod block system senses local power increases around a rod being withdrawn and stops rod movement upon high level indication. The sensitivity of the block is set via Safety Analysis Report calculations which artificially put the region surrounding a fully inserted rod on thermal limits (Technical Specification Limiting Conditions of Operation) and then provide event

termination before MCPR and MLHGR limits are reached. A typical event then proceeds (via this calculational process) with the initially fully-inserted rod withdrawn about 4 or 5 ft when blocked. The core power increase is very small (a few percent) and no scram occurs. The reactor will stay at the new condition indefinitely, until operator action is eventually required, since the reactor, while not exceeding safety limits, is above the Limiting Conditions of Operation boundary. The peak linear heat generation rate will usually change very little (see Figure 15.1.11-2 in the second section of Appendix D, taken from the Shoreham FSAR[15]) although its axial location may change via axial distribution changes. However, locally there may be big shifts (on the order of a factor of 2 increase) as controlled regions of a fuel assembly are uncovered (uncontrolled) by the rod movement. For example, power in a segment of some fuel rods may rise from an initial 4 to 6 kW/ft to a final 10 to 14 kW/ft. This would occur in a few assemblies, at most, and over an axial length of a few feet. The general transient events would occur over about 15 sec (for a 4-ft withdrawal), with the power rise in a given segment (6 in.) in a few seconds, and the new distribution would exist indefinitely, depending on operator response.

2.4 PWR Steamline Breaks

Steam system piping failures are evaluated in accordance with procedures and criteria established in Section 15.1.5 of the NRC's Standard Review Plan. As indicated therein, the increased flow resulting from rupture of a steam pipe in the main steam system will cause an increased energy removal from the reactor coolant system and will result in a reduction of the reactor coolant temperature and pressure. In the presence of a negative moderator temperature coefficient (which is most negative at end-of-cycle due to the reduction in primary coolant boron concentration), this cooldown causes an increase in core reactivity. The core reactivity increase causes a subsequent increase in power.

Steamline breaks are classified as "limiting faults" (Condition IV events). Since these are accidents, not moderate frequency transients, some fuel failure is acceptable as long as radiological consequences remain

within 10 CFR 100 guidelines. As a general rule, the NRC has traditionally required the steamline-break-calculated dose consequences to remain "well within" 10 CFR 100 guidelines: i.e., ≤25% of the 10 CFR 100 dose limits. The source term consequences of steamline breaks could be greater in the event of steam generator tube ruptures, which would allow any PCI-released fission products to bypass the containment building via the secondary coolant system.

The steamline break analyses are very plant specific because of differences in steam generator designs and other factors. In addition, the transient is sensitive to the discharge rate, so several break locations must be evaluated. Steamline break analyses are, therefore, performed for both full power and hot shutdown conditions and for a number of combinations of parameters. In most cases, the potential PCI impact for breaks occurring at power (assuming reactor trip) has appeared to be small because the power increases are small (~10%) and last for only a short time (seconds). Some consideration has, therefore, been given to the possibility that the PCI failure potential may actually be greater for a steamline break occurring from a hot standby condition because, even though the associated peak rod power may not be as large, the net power increase and power increase rate might be larger.

Because the steamline break event scenario is so varied and complex, we have not attempted to address every facet of it here. For the purpose of this study, we have chosen one example of a steamline break analysis provided in a plant FSAR (for St. Lucie 2). The event's analytical assumptions and results are discussed in detail in Reference 16; relevant portions of the St. Lucie 2 FSAR are attached as Appendix E.

The most important features of the St. Lucie 2 steamline break analysis from a PCI standpoint are illustrated in Figure 8. As shown, the core power increases by about 40% during the first 40 to 50 sec. For this particular Combustion Engineering Co. analysis, the minimum DNBR is 0.603, which corresponds to 7.6% of the fuel rods in DNB, according to a statement

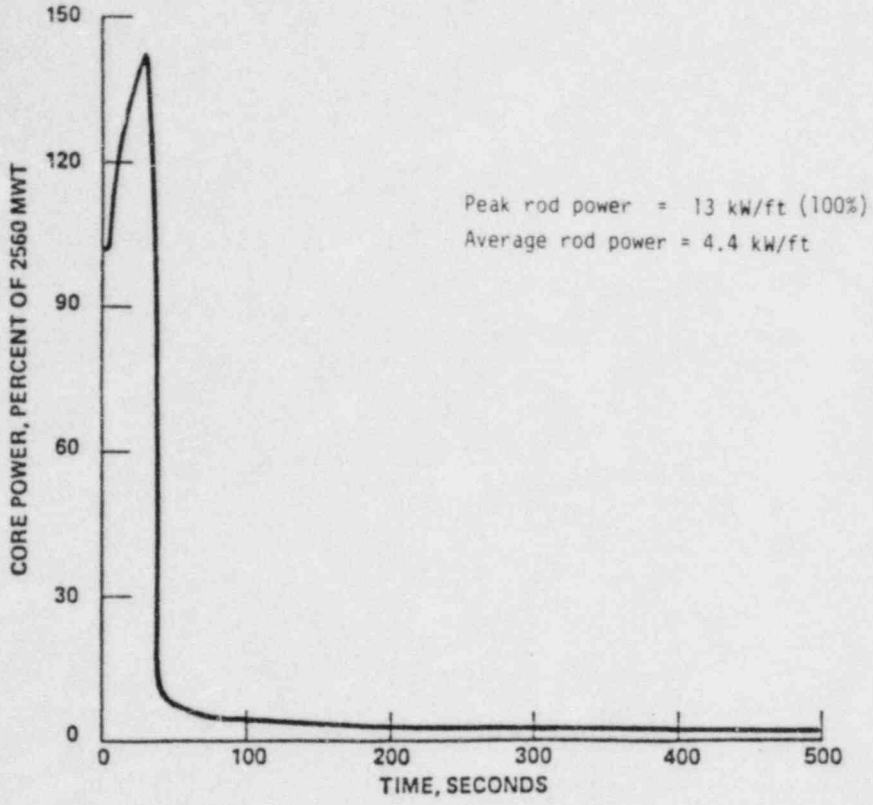

Figure 8. Core-average power during a PWR steamline break (from St. Lucie 2 FSAR).

on p. 15.1-84 of Reference 16. It is assumed that the number of fuel rods with DNBR values less than the 95/95 value is considerably higher than 7.6%, but that number has not been provided.

In summary, the most important fact with respect to estimating the potential PCI impact for this particular event is that the core power increases about 40% from hot full power over a period of 40 to 50 sec before decreasing abruptly. It cannot be overemphasized that, because of the uniqueness of the steamline break analysis on a plant-by-plant basis, the analysis and specific parameters discussed here for St. Lucie 2 are not necessarily representative for steamline breaks as a class of events. The St. Lucie 2 case is a useful one, however, to answer the question of

whether the radiological dose consequences for a Chapter 15-type accident are underestimated by using DNBR/MCPR fuel failure criteria and ignoring PCI.

3. RELEVANT PCI RESEARCH

Possibilities for PCI-induced fuel failures have historically been investigated from opposite extremes. Related nuclear safety programs have focused on the most severe power excursions wherein PCI is involved--reactivity-initiated accidents. Shortly after inception of these efforts, actual fuel rod damage attributable to PCI was observed from standard commercial power-ramping and load-following operations. Reactor manufacturers, utilities, and regulatory agencies throughout the world responded by commissioning research projects at several test reactor facilities with the objective of preventing fuel rod failures from nonaccident sources. Despite over a decade of research, these two approaches are just now converging on the relatively mild, off-normal transients of interest to the PCI task force.

As summarized in Reference 17, jointly funded power-ramping experiments have been performed at the Studsvik, Halden, and Petten facilities, among others. These studies, backed by comprehensive hot cell and laboratory investigations, have suggested thresholds for cladding cracks as functions of irradiation history, rod power, power increase, ramp rate, and transient duration. (Figure 9, from Reference 18, provides examples from several long hold-time-at-peak-power experiments.) Other variables include rod fill gas pressure, gap width, pellet size and shape, and UO_2 fabrication characteristics.[19] Various separate-effects projects have examined influences of fission product release, cladding irradiation, and cladding stresses and strains. In addition, several "remedial" BWR fuel rod designs have been tested.[20] Although many technical questions are still unanswered, design-specific guidelines have been established whereby PCI-related difficulties have been practically eliminated during standard commercial operations.

Major fuel damage and the associated release of hazardous fission products during reactivity-initiated accidents have also received considerable attention. The most probable scenario for rapid insertion of excess core reactivity is mechanical failure of control rod withdrawal hardware, followed by nearly instantaneous ejection of the control rod. In

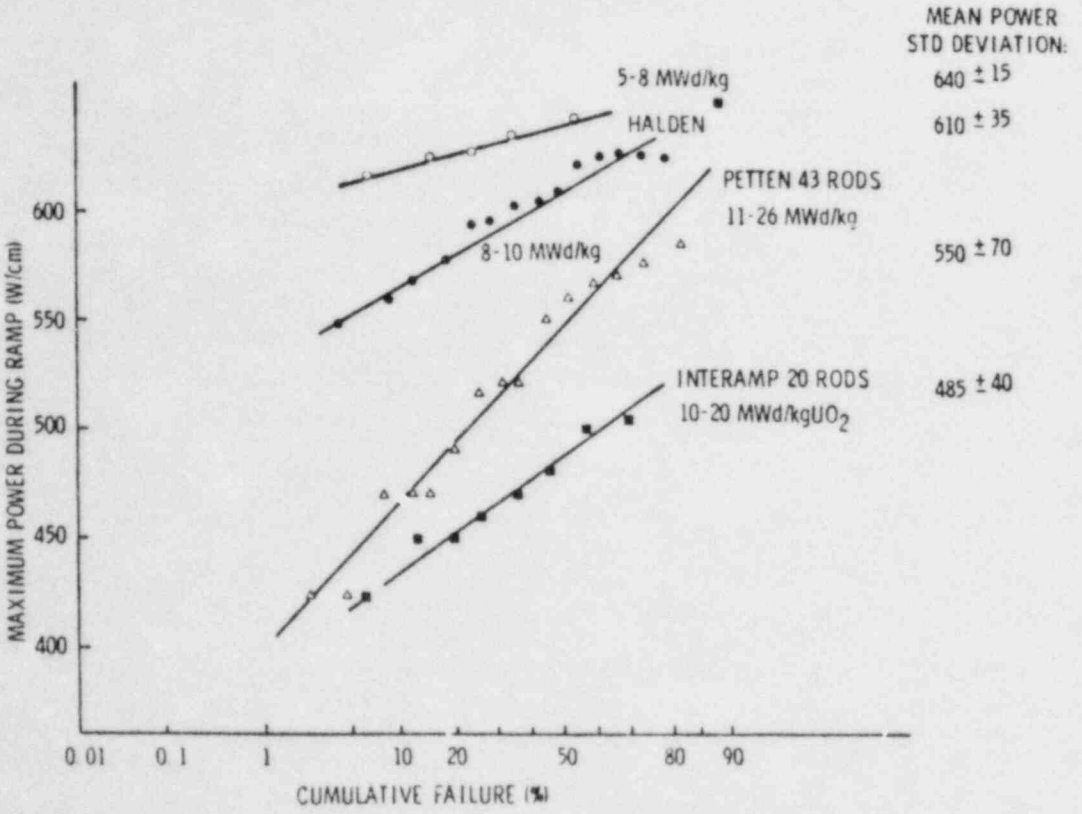

Figure 9. Failure powers for fuel rods of varying designs and burnups during several test reactor projects.

such an event, PCI-induced fracturing or tearing of cladding is only one of a number of rod failure mechanisms that can occur. Early tests at the Idaho National Engineering Laboratory's Capsule Driver Core and Transient Reactor Test Facilities, reinforced by more realistic accident simulations at the Power Burst Facility and Japanese Nuclear Safety Research Reactor, have defined the forms and extents of rod damage to be expected from various levels of deposited energy and fuel enthalpy.[21,22] The Capsule Driver Core and Power Burst Facility data suggest that there is a significant chance of failure (through-wall cracking of the cladding) when light water reactor fuel rods are subjected to a radially-averaged peak fuel enthalpy of 140 cal/g or greater.

The approximate severity of the reactor transients of interest to this committee can be indicated jointly by the peak rod power, change in rod power, maximum ramp rate, and transient duration--with special allowance for control rod extractions at zero power. Appropriate values for the six

Task Force events were estimated from Figures 1 through 8 and Appendix D and are presented in Table 1. (Note that control rod withdrawal numbers may not fully account for power peaking near control rod positions.) Related quantities from test reactor projects were obtained from References 17 and 21 and are listed in Table 2. Comparisons quickly illustrate that much of the past research is not directly applicable to the task force mission. Most of the power-ramp experiments involved long hold times to failure and slow power ramps, whereas the RIA-type experiments were too extreme in terms of peak rod powers and power increase rates.

However, the results of the OPTRAN 1-1 test conducted in the Power Burst Facility are very relevant to the turbine trip without bypass because the OPTRAN 1-1 power transients were patterned closely on General Electric calculated powers for 8 x 8 fuel subjected to such events.[23] The Mol Tribulation Program will also generate some data pertinent to fuel behavior during a PWR steamline break, when completed in 1986. The Demo-Ramp II and Trans-Ramp Projects provide data for rod damage estimates during uncontrolled control rod withdrawals in a BWR, but comparable data for PWR rods are not available.

Fortunately, well-tailored reactor experiments are not absolutely required for transient failure assessments. The relatively small number of rodlets tested in situ may not accurately simulate cladding stresses in full-length commercial rods and may not fully represent industry fabrication and power history variations. Nevertheless, PCI investigations have generated considerable information on fundamental PCI-damage mechanisms. Functional dependencies determined to date could be extrapolated toward the situations of interest, after development of appropriate models. Such a calculational approach to estimating transient severity, although perhaps incapable of supplying the absolute timing and relative influences of specific damage processes, could at least rank the task force transients in order of potential severity.

TABLE 1. PREDICTED TRANSIENT BEHAVIOR

Transient	Maximum Rod Power (kW/m)	Related Change in Rod Power (kW/m)	Maximum Ramp Rate (kW/m•s)	Approximate Duration at Elevated Power (sec)
BWR Turbine Trip without Bypass	269	269	~1000	<1
PWR Control Rod Bank Withdrawal Error at Power	50	18	0.6	45
Subcritical PWR Control Rod Bank Withdrawal Error	75	75	6.6	<15
BWR Control Rod Withdrawal Error at Power	46	20	8.0	Long
Subcritical BWR Control Rod Withdrawal Error	184	184	90	2
PWR Steamline Break[a]	59	10	1.5	35

a. The parametric values in Table 1 are representative of those provided in certain SFAR analyses and are not intended to be characteristic of all plants. (This is especially true of the steamline break parameters which are taken from the St. Lucie 2 FSAR.)

TABLE 2. TEST REACTOR RESEARCH ON PCI

Facility	Project	Maximum Rod Power (kW/m)	Maximum Ramp Rate (kW/m•s)	Hold Time at Peak Power
CDC	SPERT[a]	30,000	2.0×10^{6}	0
PBF	RIA 1-2	24,000[b]	1.8×10^{6}	0
PBF	OPTRAN 1-1 (BWR)	270	6.0×10^{2}	<15
Studsvik	Inter-Ramp (BWR)	38-65	0.07	24 hr
Studsvik	Demo-Ramp I (BWR)	40-50	0.07	24 hr
Studsvik	Demo-Ramp II (BWR)	49	0.37	0-60 min
Studsvik	Over-Ramp (PWR)	38-53	0.17	24 hr
Studsvik	Super-Ramp (BWR & PWR)	30-50	0.17	12 hr
Studsvik	Trans-Ramp (BWR)[c]	48-50	8.0	15-60 s
Riso	Fission Gas Release	32-46	$\sim 10^{-4}$	24 hr
Petten	Burnup Ramps (PWR)	38-46	0.17	10 min to 52 hr
Mol	Tribulation (PWR)[c]	32-51	2.6	1-10 min
Halden	Numerous BWR & PWR[c]	35-65	0.08	4-500 hr
PNL	High Burnup Effects[c]	30-50	1.4×10^{-4}	48 hr

a. Typical of many CDC, TREAT, and NSRR tests with radially averaged maximum fuel enthalpies near 230 cal/g UO_2.

b. Estimated for a radially averaged maximum fuel enthalpy of 185 cal/g UO_2.

c. In progress.

3.1 Fuel Behavior During Brief Power Excursions

As mentioned in Section 2, members of the PCI task force have held discussions with many prominent investigators. These conversations, coupled with an extensive survey of applicable literature, have provided an outline for relating the general fuel rod response to a short-duration, rapidly scrammed transient.

The initial consequence of the reactivity/power surge will be sudden deposition of energy within the UO_2. Heat transfer to the cladding and coolant will not be significant at first, and can be conservatively neglected for events lasting 2 sec or less. Temperature increases will be quite uniform across pellet radii, and prompt volumetric expansion will cause fuel-cladding contact at cocked pellet corners, trapped UO_2 fragments, etc. The resultant axial strains could be quite pronounced if hard mechanical interaction in upper regions of a rod prevents free axial expansion of the pellet stack. (Axial stresses near the contact point could be quite large in such a situation.) A sufficiently large power increase will force closure of the pellet-cladding gap. Hoop stresses and strains will be maximized near pellet interfaces (due to hourglassing) and along peripheral pellet cracks. Any interior cladding surface ZrO_2 layer may be fractured into tiny crack nucleation sites. Meanwhile, high temperature diffusion may release volatile fission products from the UO_2 matrix. Microcracking and fuel grain separation may release fission products trapped at grain boundaries. Releases will be highest near pellet interfaces and major pellet cracks, because these features provide the most direct pathways from the hot pellet centers.

Concentrating both chemically aggressive species and peak circumferential loads at the same locations may induce stress-corrosion cracking and, possibly, liquid metal embrittlement. Once initiated, a crack will proceed quickly through a cladding wall, unless stress fields are reduced abruptly. Water ingress appears to follow cladding perforation almost instantly, as denoted by a sharp decrease in rod elongation from the extra heat transfer by water vapor. However, escape of the fission

products through the breached cladding requires a pressure equilibrium, which may be forestalled by reactor scram. The associated stress relaxations may effectively seal the crack until the next power cycle.

Despite this broad consensus, many fundamental aspects of the PCI phenomenon are still incompletely understood: (1) The degree of corrosion protection provided by a thin, easily fractured internal cladding oxide layer is in dispute.[24,25] If fission products preferentially attack localized surface precipitates rich in Zircaloy alloying ingredients, the existence of the ZrO_2 layer may be largely irrelevant. (2) The fission product species responsible for observed brittle fractures have not been precisely identified, though iodine and cadmium are leading candidates.[26] Some researchers doubt a corrosive agent is required, pointing toward transmission-electron-microscopy evidence of ordered, oxygen-rich precipitates as the culprits in irradiated cladding.[27] (3) Many investigators believe that iodine is the active element, based on morphological similarities between in-reactor and out-of-reactor fracture surfaces. Consistent threshold amounts of iodine for stress-corrosion cracking have not been determined.[25,28,29] However, the values are many orders of magnitude higher than those derived from fission yields and thermodynamic analyses involving chemical equilibria for various fission-product species under fuel-element operating conditions.[30] Others have found no evidence of diffusion-limited behavior during 0.1- to 1000-hour laboratory tests, though this might still occur during rapid events.[31] In addition, the maximum sustainable crack propagation rates based on gaseous transport of different species (viz., I, ZrI_4, CsI) from the crack mouth to the crack tip are not consistent with the relatively rapid crack growth which apparently occurs during the time frame for PCI failures under power-ramp conditions.[30] Kinetic limitations involving complex chemical processes, as well as radiolysis of species within the fuel-cladding gap complicate analyses of Zircaloy stress-corrosion cracking during rapid transients. Alternatively, these variations may reflect back on oxide layer influences.[32] (4) Other studies have attempted to determine the respective times and stresses necessary for crack initiation and propagation as functions of rod power histories.[33,34,35] Such efforts

have encountered difficulties in separating and precisely understanding the influences of fuel burnup, fuel and cladding creepdown, cladding irradiation, cladding fabrication, crack stress intensity, and circumferential strain rate.[36,37,38]

Other separate-effects tests are underway that should shed some light on these basic questions. The Halden Project Stress-Corrosion Cracking Program, which will measure differences in failure times between intentionally precracked and undefected rods, is an example.[39] Unfortunately, the direct application of such efforts to brief, rapidly-ramped transients is yet to be demonstrated.

All of these basic uncertainties compromise development of computer models for comprehensive failure predictions. With so many variables of undefined impact, modelers have difficulty in determining the most important phenomena and the most critical interactions. It will be some time before high probabilistic accuracies are achieved on a straightforward, mechanistic basis--especially for rapid transients with a scarcity of benchmarks. Nevertheless, empirical criteria have been somewhat successful, as will be explained at the end of this section. Moreover, a nonrigorous analysis of individual transients on a time/temperature/stress basis can indicate propensities for crack formation during the events of interest to the PCI task force.

3.2 Events Considered by the Task Force

Several events which result in power increases that might cause PCI fuel rod failures were discussed in Section 2, namely:

- The Turbine Trip Without Bypass and similar BWR anticipated transients with scram (main steamline isolation valve closure, load rejection without bypass, etc.)

- PWR control rod bank withdrawal errors at full power and from zero power

- BWR control rod withdrawal errors at full power and from zero power (subcritical conditions)

- A PWR steamline break.

The maximum rod power, change in rod power, maximum ramp rate, and approximate duration at elevated power provided in some analyses of these events are listed in Table 1. Inspection of Table 1 reveals that the Subcritical BWR Control Rod Withdrawal Error event is similar to, but considerably less severe than, the BWR Turbine Trip Without Bypass event. (Therefore, the PCI implications of that event are addressed under the category of BWR Anticipated Transients below.) Also, the PWR Control Rod Bank Withdrawal Error at Power is quite similar in magnitude to the PWR Steamline Break event analyzed in the San Onofre FSAR. However, the power peaking associated with other steamline break analyses may differ from the power peaking calculated for the PWR Control Rod Bank Withdrawal Error events.

A. BWR Anticipated Transients

Information that can be used to assess the possibility of light water reactor fuel failure during a BWR anticipated transient includes results of the OPTRAN 1-1 test[23] conducted in the Power Burst Facility (PBF), and results of the Demo-Ramp and Trans-Ramp tests conducted in the R-2 reactor at Studsvik.

The OPTRAN 1-1 test consisted of four successive transients on a cluster of four, 1-m-long, previously irradiated General Electric Co. rodlets. (Two test rods were withdrawn and replaced with fresh rods after the first excursion for an incipient PCI crack examination.) Transient 1-1A closely followed the General Electric Co. core-average-power rod projections for a BWR-5 turbine trip without bypass, whereas the more severe 1-1B

transient simulated the calculated power spike at a peak power location in a BWR-5 during a turbine-trip or load-rejection-without-bypass transient. Transients 1-1C and 1-1D were run at higher peak powers and ramp rates than thought to be possible in any BWR in an attempt to establish a fuel failure threshold for a 1- to 2-sec excursion with scram. Calculated and measured test conditions are shown in Figures 10 and 11 and are listed in Table 3.

None of the OPTRAN 1-1 rods failed, as determined by elongation sensors (the only rod instruments) and the PBF fission product detection system, despite the severe nature of the successive ramps. Comprehensive postirradiation examinations included clamshelling and flattening of approximately half of the cladding length on each rod. No brittle, PCI-type incipient cladding fractures were found. No permanent hoop strains--ridges typically associated with PCI defects--were detected at pellet interfacial positions; hoop stresses and strains were small enough to stay within the region of elastic deformation. Maximum stress and strain values calculated by FRAP-T6[40] are 242 MPa and 0.6%, respectively--somewhat below thresholds for crack initiation proposed by some investigators.[24,25,33] And, the OPTRAN test rods were subjected to peak fuel enthalpies lower than the 140-cal/g threshold that has been identified for PCI failures during reactivity initiated accidents (RIAs).[21] Thus, the OPTRAN 1-1 results suggest that promptly scrammed BWR anticipated transients are benign.

The OPTRAN 1-1 results by themselves, however, are not conclusive, for a number of reasons. (a) Only six short fuel rods were tested, and low failure probabilities that could be significant in a core with 50,000 rods might not have been observed in this small sample. (b) The base irradiations were made at relatively low power levels (11 to 13 kW/m), such that the available gap inventory of corrosive fission products would have been small. (c) The modest burnups of 5 to 23 GWd/t might not have produced a "saturated" level of cladding irradiation damage or resulted in enhanced fission product release pathways. (d) Although the RIA tests mentioned above exhibited PCI-type failures only at enthalpies greater than those of the OPTRAN tests, those power bursts were of much shorter duration (~50 msec) than the OPTRAN transients. (e) The Studsvik Demo-Ramp II tests[41]

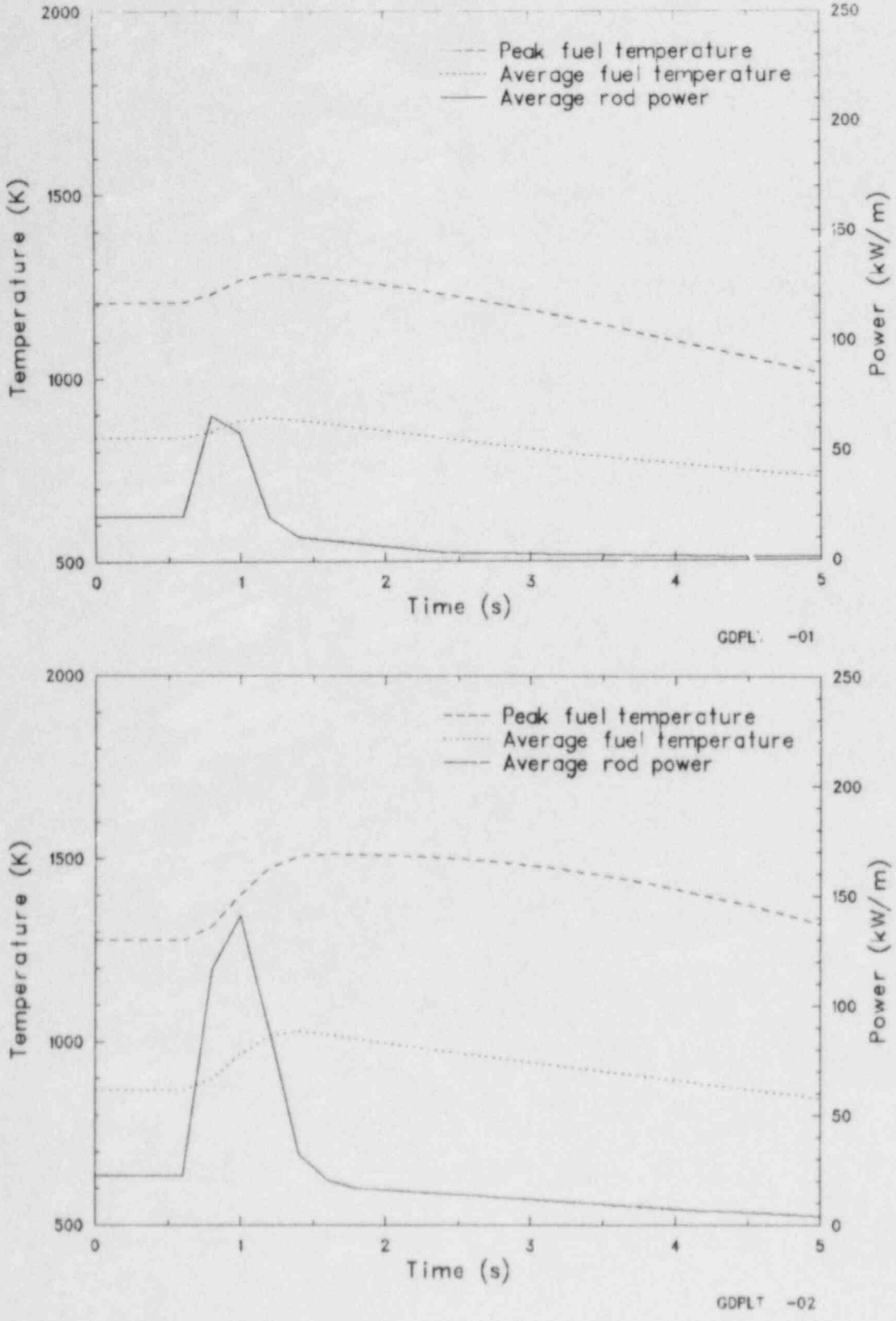

Figure 10. FRAP-T6 calculations for a BWR-6 turbine trip without bypass (OPTRAN 1-1A, top) and load rejection without bypass (OPTRAN 1-1B, bottom).

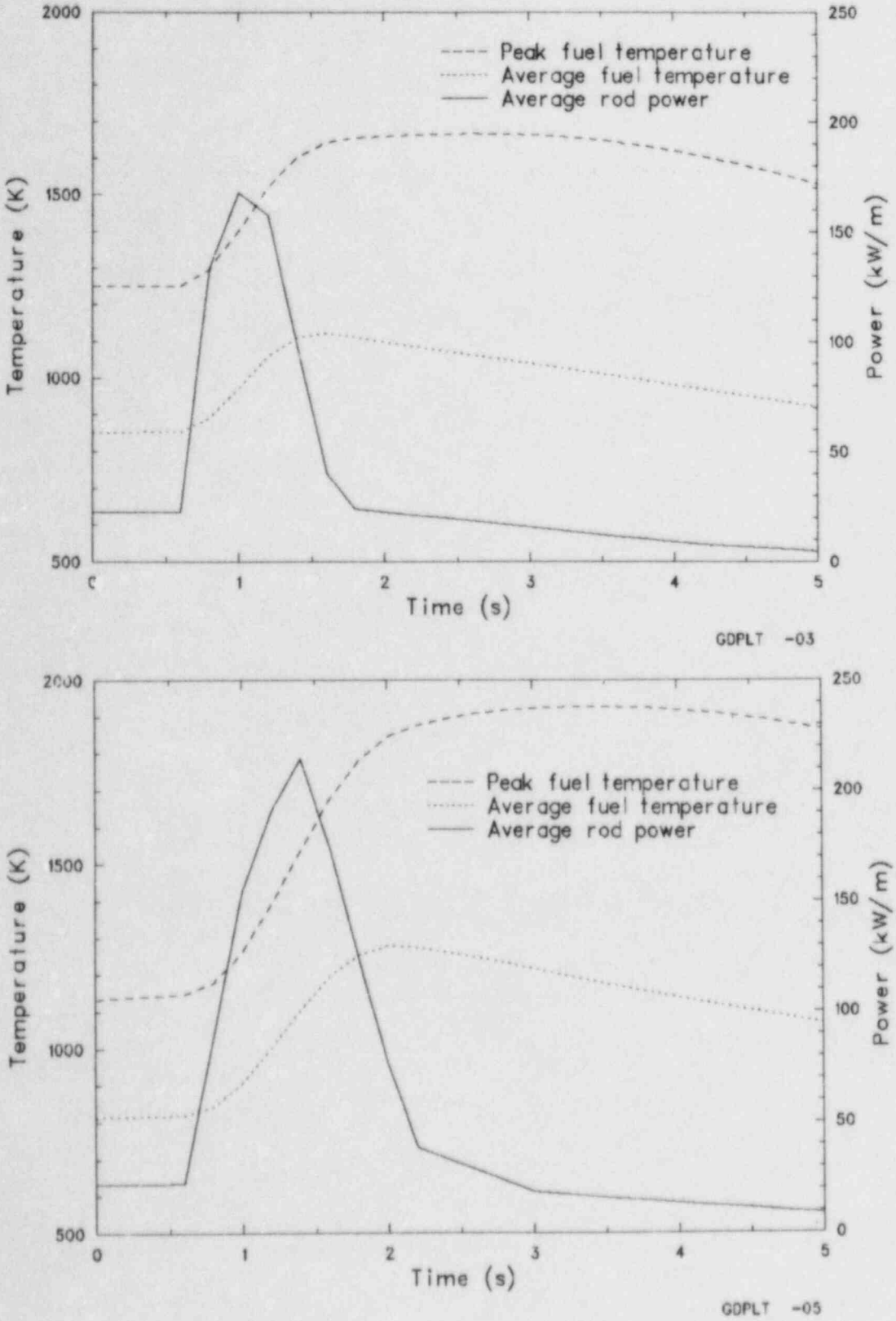

Figure 11. FRAP-T6 calculations for OPTRAN 1-1C (top) and OPTRAN 1-1D (bottom).

TABLE 3. OPTRAN 1-1 POWER TRANSIENTS

Transient	Initial Peak Rod Power (kW/m)	Maximum Peak Rod Power (kW/m)	Initial Peak Fuel Enthalpy (cal/g)	Maximum Peak Fuel Enthalpy (cal/g)	Rod-Average Energy Input (cal/g)
A	25.2	90	41.9	46.5	14.8
B	28.2	201	49.7	68.0	37.4
C	29.4	240	47.4	73.1	48.5
D	26.9	264	42.0	82.8	67.1

clearly show that PCI cracks can form very rapidly (within a minute) at power levels (~45 kW/m) that are comparable to some of the OPTRAN 1-1 transients.

The Studsvik Trans-Ramp I results (1982, 1983) provide critical insights into the incipient crack formation process, and these results seem to quantify ramp conditions below which incipient damage will not occur. Because the Trans-Ramp I tests are performed under a multiple-participant program agreement, there are a number of restrictions on public disclosure of the test results until 1986 or 1987, several years after the end of the project. However, the Task Force believes that these results, when coupled with analyses and/or additional tests of a similar nature, will show that fuel damage will not result from a promptly scrammed BWR anticipated transient. The Task Force also believes that the margins involved are not large and that delays in scram initiation of even a few seconds could reverse this conclusion. Tests that would either authenticate or disqualify this conclusion are therefore strongly recommended.

B. PWR Control Rod Bank Withdrawal Error at Power

The PWR control rod bank withdrawal error at full power (and the PWR steamline break event) is characterized by maximum rod powers of 50 to 60 kW/m, changes in rod power of 10 to 20 kW/m, maximum power ramp rates of

0.5 to 1.5 kW/m•sec, and hold times of 10 to 30 sec. Inspection of Table 2 indicates that the Studsvik Demo-Ramp II Program has conducted experiments with BWR-type fuel rods under conditions that are roughly equivalent to those listed above; additional information regarding PWR-type fuel rod behavior will be available to participants from the Tribulation Program, but not before 1986.

The Studsvik Demo-Ramp II experiment involved eight Kraftwerk Union BWR rodlets irradiated at base powers between 16 and 30 kW/m through 25- to 29-GWd/t burnups. All test rods were of the 8 x 8 unpressurized (standard) design. After preconditioning at or near 30 kW/m, these rods were ramped in the R2 Reactor to peak powers from 38 to 49 kW/m. The ramp rate used for the first four rods was 0.07 kW/m•sec, whereas the second set was subjected to ramps between 0.28 and 0.37 kW/m•sec. Detailed results are presented in Table 4. As shown, one rod failed, two were undamaged, and five contained incipient PCI cracks of varying depths. Note that Rod S30H was ramped twice without failure and that the initial power for the second ramp was 38 kW/m. Hold times at peak power ranged widely from about 0.16 min to hours.

The ramp loads in the Demo-Ramp II tests are similar to the PWR control rod withdrawal error (or to a steamline break event such as discussed in the St. Lucie 2 FSAR). The ramp rates and peak powers are close and the hold times of 0.16, 0.18, 0.25, and 0.60 min before abrupt power reduction approximate brief scrammed transients. Measured fission gas releases ranged from 0.8 to 3.0%. Only one of the four rods was free of incipient cracks; the remaining cladding contained penetrations between 10 and 60% at positions darkened by fission product deposition. These data indicate a high probability for rod damage during such events.

However, it is not clear that Studsvik data on BWR fuel can be applied directly to commercial PWR transients--at least without accounting for differences in gap width, pressurization, fuel fabrication, etc. The Overramp Program provided PWR fuel data, but did not specifically address damage or failure times.[17] Fortunately, fuel temperatures and cladding

TABLE 4. DEMO-RAMP II RESULTS

Rod	Peak Power (kW/m)	Power Change (kW/m)	Ramp Rate (kW/m s)	Duration of Ramp (m)	Hold Time at Peak Power (m)	Total Test Duration (m)	Gas Release Kr (%)	Gas Release Xe (%)	Maximum Crack Depth (%)
S30H	38.0	8.0	0.07	2.00	1440	1442	--	--	--
S30H	43.5	5.5	0.07	1.38	60	61.38	8.1	7.5	0
S31H	41.3	11.3	0.07	2.83	77	79.83	Failed		100
S38H	41.8	11.8	0.07	2.95	4.5	7.45	0.8	0.8	50
S39H	43.0	13.0	0.07	3.25	1.1	4.35	0.7	0.5	10
S29H	42.0	12.0	0.29	0.69	0.18	0.87	0.9	0.8	0
S36H	45.0	15.0	0.28	0.88	0.25	1.13	1.5	1.4	30
S27H	48.5	18.5	0.37	0.84	0.16	1.00	2.6	1.9	50
S35H	48.0	18.0	0.28	1.06	0.60	1.66	3.0	2.6	60

stresses are being calculated for PWR rods from Figures 2 and 4 by Battelle Pacific Northwest Laboratories (PNL).[42] These PNL results will facilitate discussions of transient severity on PWR fuel. In any case, it is clear that some light water reactor fuel designs may be prone to failure or damage during such events.

C. Subcritical PWR Control Rod Bank Withdrawal Error

The subcritical PWR control rod withdrawal error event is characterized by peak powers of approximately 75 kW/m, power increases of the same magnitude, maximum power ramp rates of about 7 kW/m•sec, and peak power durations of less than 5 sec. The information discussed in Section A above (BWR Anticipated Transients) can be used in part to assess the possibility of light water reactor fuel failures during this event, although the peak powers are considerably lower and the pulse width (hold time) is wider during the subcritical PWR control rod withdrawal error. However, the fuel enthalpy increases are still well below that necessary to fail the cladding by mechanical fracture, as observed in the RIA experiments, and the time span is considerably less than that apparently necessary for stress-corrosion crack initiation and propagation, as defined by the Trans-Ramp data. However, the absence of any experimental data from a simulated subcritical PWR control rod withdrawal error transient prevents any definitive conclusions.

D. BWR Control Blade Withdrawal Error at Power

The inadvertent BWR control blade withdrawal error at power event can be characterized by peak linear heat generation rates of approximately 46 kW/m, changes in local rod powers of up to 20 kW/m, local power ramp rates of up to 8 kW/m•sec, and long hold times. These conditions are similar to the local power conditions possible during planned BWR control blade movements if reactor power is not decreased sufficiently before blade movement by adjustment of the recirculation flow, as specified in General

Electric's Preconditioning Intern Operating Management Recommendations.[3] Therefore, much of the data from the previous PCI research may be appropriate for assessing failure possibilities during BWR control blade withdrawal error events. However, one experimental program, the Trans-Ramp Program discussed above, closely simulated not only the peak powers and the change in power, but also the power ramp rate associated with the BWR control blade withdrawal error event.

The Trans-Ramp data suggest that failure (or at least incipient cracking) is probable during such events. The possibility of localized failures during BWR uncontrolled control rod withdrawals at high powers is further substantiated by one commercial reactor test. In 1975, ASEA Atom of Sweden performed an experiment in the Oskarshamn-1 BWR to investigate the effects on 8 x 8 fuel of extracting a single control blade.[43] The blade was withdrawn in 10% steps from 53 to 83% over 2 hr, and then held for 24 hr. Nineteen fuel bundles were later found to contain a total of 56 leaking rods. The failure locations were generally concentrated at radial and axial positions of power peaking where maximum powers varied from 30 to 37 kW/m.

E. The PWR Steamline Breaks

Because the steamline break event scenario is so dependent on the assumptions used for break size and location, as well as other factors, we have addressed only the one example for the St. Lucie 2 FSAR analysis. For that particular event, the conditions imposed on the fuel are quite similar to those for the PWR control rod withdrawal error at power. The discussion provided in Subsection B above therefore applies for this particular event.

3.3 PCI Failure Prediction Capabilities

An ideal tool for determining PCI-induced failure probabilities during a wide variety of transients would be an integral mechanistic code. All relevant phenomena would be modeled, design differences between fuel manufacturers could be handled, and stochastic variables like fabrication

tolerances could be incorporated to produce true probabilistic predictions. Of course, accurate power/time curves (including local power peaking) and numerous experimental benchmarks would be critical to the success of failure projections.

As described earlier, several fundamental problems have prevented development of such a code. A comprehensive mechanistic understanding of PCI-induced damage has not yet been achieved and unambiguous benchmarks are scarce, especially for rapid events just coming to the forefront of investigations. Instead, efforts toward failure predictions have followed two less ambitious approaches: (a) mechanistic modeling of individual phenomena contributing to PCI defects, and (b) formulating empirical relationships from numerous commercial, test reactor, and laboratory observations.

The FASTGRASS code, developed at Argonne National Laboratory, is a mechanistic module whic provides sound, interpretable predictions of fission product releases during brief power excursions. FASTGRASS incorporates complex interactions between various gaseous and volatile fission products and UO_2 structures, including atomic and gas bubble diffusion from UO_2 grains to grain faces and then to grain edges (including the kinetics of gas atom generation and gas bubble/gas atom interactions); gas release through interconnected tunnels of fission gas-induced and fabricated porosity; chemical reactions between the various volatile fission products; and volatile fission product interactions with the noble gases. Models are included for the effects of the key variables (production of gas from fissioning nuclei, bubble nucleation and re-solution, bubble migration, bubble coalescence, gas-bubble/channel formation on grain faces, temperature and temperature gradients, interlinked porosity on grain edges, nonequilibrium effects, microcracking, and fission gas interaction with structural defects) on both the distribution of fission gas within the fuel and on the amount of fission gas released from the fuel. Although appropriate data are not available for a full assessment of FASTGRASS, this complex modeling approach has one distinct advantage over empirical techniques for treating release of aggressive chemical species,

such as the Halden gas release correlation employed in the SIROD failure prediction code.[44] That is, simple extrapolations from long-term, steady-state data may not account for purely transient effects.

Detailed model development has also been performed for cladding stress/strain predictions. For example, the FEMAXI-III code incorporates influences of fuel and cladding creep, pellet cracking, fuel relocation, fuel densification and swelling, and fuel-cladding contact conditions.[45] This code further includes a complex pellet compliance model to account for changes in pellet stiffness as a function of compressive loading. However, as with FASTGRASS, few comparisons have been made to measurements from rapidly ramped, abruptly scrammed experiments--generally as a consequence of the very limited availability of such data.

The NRC/PNL Accelerated PCI Modeling Program seeks to provide direct, quantitative relationships between reactor-operation/fuel-design variables and transient failure probabilities.[46] This program will incorporate features similar to those just described for FASTGRASS and FEMAXI III and a selection of fracture models that will bound the expected cladding damage states. This work is nearing completion and is designed especially for fast transients.

Another approach to failure assessment is represented by the PCI failure criterion developed by British Nuclear Fuels Limited. This criterion is based on a threshold cladding stress that diminishes with increased fast neutron dosage.[47] An adequate supply of fission products for stress-corrosion cracking is implicitly assumed. The SLEUTH-SEER 77 fuel performance code is used to calculate peak cladding stress; effects of pellet cracking and hourglassing are included. This method has had much success in evaluating slowly ramped experiments from several facilities. However, no claim is made for suitability to rapid, short-duration events in which fission products may not be available and in which strain rate considerations may be important. Instead, reactivity-initiated accident-type energy deposition guidelines are proposed for these situations.

Kraftwerk Union has developed an empirical technique for describing fuel rod failures, based primarily on observations from Petten, Studsvik, and Halden tests, as well as from KWU reactors. The KWU RSST approach employs separate threshold criteria for power Range, power Step, power increase Speed, and transient Time.[48] PCI-induced failure is predicted if, and only if, all four criteria are exceeded during a given reactor event. This approach has been very successful for defining desired operating limits for load-following and startup operations, both in PWRs and BWRs.[49] However, the data base for brief, rapidly terminated transients has not been sufficient to specify time criteria for transient applications.

4. CONCLUSIONS AND RECOMMENDATIONS

The principal fuel failure criteria presently used by the U.S. Nuclear Regulatory Commission and reactor vendors for both transient and accident conditions are overheating criteria. However, pellet-cladding interaction failures can and have occurred during various increases in reactor power, and it is not clear that overheating criteria will properly bound the consequences associated with such PCI-induced failures during all off-normal (Chapter 15) events. Therefore, this task force has addressed the question: Will PCI failures occur during off-normal reactor operating conditions and do PCI failures exceed DNBR/MCPR-calculated fuel failure probabilities used in the evaluation of potential radiological consequences?

Several off-normal, overpower events in commercial light water reactors may cause PCI failures. It is possible to single out certain events which are most relevant in terms of peak power, power increase, ramp rate, and duration at elevated power. The Task Force considers the following events to be appropriate for consideration:

- BWR turbine trip without bypass (transient)
- PWR control rod bank withdrawal error (transient)
- Subcritical PWR control rod bank withdrawal error (transient)
- BWR control blade withdrawal errors (transient)
- PWR steamline breaks (accident).

The first four of these events are moderate-frequency transients for which specified acceptable fuel design limits (SAFDLs) of General Design Criterion 10 in Appendix A of 10 CFR-50 must be met. The PWR steamline break events are low-probability accidents for which some small numbers of fuel failures are expected, but doses must remain below the levels of 10 CFR-100.

Unfortunately, the propensity for PCI failure during these events has not been investigated in depth, making a direct evaluation of fuel failure criteria very difficult. However, there is a body of data derived from severe reactivity-initiated accident simulations (i.e., PWR rod ejection and BWR rod drop) and from simulations of standard commercial power-ramping and load-following operations. Pellet-cladding interaction failure thresholds during normal (slow) power changes have been identified for some fuel designs and shown to be dependent on irradiation history, rod power, power increase, ramp rate, and hold time. Other variables such as rod fill gas pressure, gap width, pellet size and shape, etc., also influence PCI failure thresholds but are not thoroughly understood. The amount of deposited energy or increase in fuel enthalpy determines whether PCI failures will occur during severe reactivity initiated accident simulations. There has also been considerable research on the metallurgical and mechanistic aspects of PCI; however, the relative contributions and effects of the various phenomena have not been quantified.

The available power-ramping data, along with the results of a few tests that were designed to simulate BWR anticipated transient events, allow some conclusions to be revealed. Namely:

1. The PBF OPTRAN 1-1 test results along with the Trans-Ramp test results; the temperatures, cladding stresses, and cladding strains calculated by state-of-the-art computer models; and peak fuel enthalpy considerations suggest that failure probabilities during BWR turbine trip without bypass, load rejection without bypass, and main steamline isolation valve closure events with scram will be small.

2. The maximum rod powers, change in power, ramp rate, and transient durations associated with the PWR control rod bank withdrawal error and PWR steamline break events, such as that postulated for St. Lucie 2, are quite similar. The Studsvik Demo-Ramp II/ Trans-Ramp data suggest that BWR-type fuel rods may fail or develop incipient PCI cracks during such transients. It is not

known whether PWR-type rods are also susceptible to PCI failure during these events, but, without more information, such failures cannot be ruled out. Experiments with PWR rods would provide better insights.

3. The absence of any experimental data from a simulated subcritical PWR control rod bank withdrawal error transient prevents any definitive conclusions regarding fuel rod failure possibilities during such events.

4. The Trans-Ramp data along with the Oskarshamn-1 data suggest that PCI fuel rod failures are probable during uncontrolled BWR control blade withdrawals.

In summary, this task force has concluded that there is a reasonable chance that PCI failures will occur during some off-normal reactor operating conditions. The PCI Task Force was not able to make a quantitative comparison of PCI and DNBR/MCPR fuel rod failure numbers at this time.

ACKNOWLEDGMENT

Contributions of all task force associates to this report are acknowledged. Other special contributions by Scott Ploger and by Richard Hobbins, EG&G Idaho, in drafting various sections of this report are also acknowledged. We extend our thanks to Howard Richings, NRC, to H. Mogard, Studsvik, to A. Hanevik, Halden, to F. Wunderlich and R. von Jan, KWU, and to their associates for the contributions of data and/or suggestions.

REFERENCES

1. H. Mogard, S. Aas, and S. Junkrans, "Power Increases and Fuel Defection," in Proc. 4th United Nations International Conference on the Peaceful Uses of Atomic Energy, Geneva (1971), 10, p. 2-3.

2. H. E. Williams and D. C. Ditmore, Experience with BWR Fuel Through September 1971, General Electric Company Report NEDO-10505, May 1972.

3. H. E. Williamson, Interim Operating Management Recommendation for Fuel Preconditioning, General Electric Company Report NEDS-10456-PC, Rev. 1, June 1975.

4. Standard Review Plan for the Review of Safety Analysis Reports for Nuclear Power Plants, NRC, Office of Nuclear Reactor Regulation, Report NUREG-0800, Rev. 2, July 1981.

5. "General Design Criteria for Nuclear Power Plants," Code of Federal Regulations, 10 CFR 50, Appendix A, Government Printing Office, January 1, 1978.

6. "Determination of Exclusion Area, Low Population Zone, and Population Centerline Distance," Code of Federal Regulations, 10 CFR 100.11, U.S. Government Printing Office, January 1, 1978.

7. "Standard Format and Content of Safety Analysis Reports for Nuclear Power Plants," NRC, Regulatory Guide 1-70, Rev. 3, November 1978.

8. L. A. Carmichael and R. O. Niemi, Transient and Stability Tests at Peach Bottom Atomic Power Station Unit 2 at End of Cycle 2, Electric Power Research Institute Report, EPRI NP-564, June 1978.

9. H. S. Cheng and D. J. Diamond, Core Analysis of Peach Bottom-2 Turbine Trip Tests, Brookhaven National Laboratory Report BNL-NUREG-24903, September 1978.

10. M. S. Lu, H. S. Cheng, W. G. Shier, D. J. Diamond, and M. M. Levine, Analysis of Licensing Basis Transients for a BWR/4, Brookhaven National Laboratory Report BNL-NUREG-26684, September 1979.

11. D. J. Diamond (ed.), BNL-TWIGL, A Program for Calculating Rapid LWR Core Transients, Brookhaven National Laboratory Report BNL-NUREG-21925, October 1976.

12. Section 15.4.1.1, "Uncontrolled CEA Withdrawal from a Subcritical or Low Power Condition," and Section 15.4.1.2, "Uncontrolled CEA Withdrawal at Power," San Onofre 2 and 3 FSAR, Amendment 5, November 1977.

13. Reference Safety Analysis Report, RESAR-41, Westinghouse Nuclear Energy Systems, December 1973.

14. La Salle County Station Final Safety Analysis Report, Amendment 36, July 1978.

15. Shoreham Nuclear Power Station--Unit 1 Final Safety Analysis Report, Revision 5, March 1977.

16. Section 15.1.5.3, "Limiting Fuel Performance Event--Loss of Main Steam with Loss of Offsite Power as a Result of Turbine Trip," St. Lucie 2 FSAR, Amendment 2, Docket 50-389, May 1981.

17. H. Knaab et al., "Overview on International Experimental Programs on Power Ramping and Fission Gas Release." Paper presented at The IAEA Specialists' Meeting on Power Ramping and Cycling Behavior of Water Reactor Fuel, Petten, the Netherlands, September 8-9, 1982.

18. K. O. Vilpponen et al., "Summary of HBWR Ramp Tests." Paper presented at The Enlarged Halden Program Group Meeting on Fuel Performance Experiments and Evaluation, Hanko, Norway, HPR-229, August 1979.

19. W. Vogl et al., "The Petten Ramp Test Program of KWU/KFA during the Years 1976 to 1981." Paper presented at The IAEA Specialists' Meeting on Power Ramping and Cycling Behavior of Water Reactor Fuel, Petten, the Netherlands, September 8-9, 1982.

20. D. S. Tomalin et al., "Performance of Irradiated Cooper and Zirconium Barrier-Modified Cladding Under Simulated Pellet- Cladding Interaction Conditions," Zirconium in the Nuclear Industry: Fourth Conference, ASTM STP 681, American Society for Testing and Materials, 1979, pp. 122-144.

21. P. E. MacDonald et al., "Assessment of Light-Water-Reactor Fuel Damage During a Reactivity-Initiated Accident," Nuclear Safety, 21, 5, September-October 1980, pp. 582-602.

22. M. Ishikawa, "Tendency of Japanese Regulatory Guide on Reactivity-Initiated Events and Some Supporting Results from NSRR Experiments." Paper presented at The Enlarged Halden Program Group Meeting at Loen, Norway, May 23-27, 1983.

23. EG&G Idaho, Inc., Operational Transient Test Series, OPTRAN 1-1 and 1-2 Test Results Report, to be published.

24. R. F. Mattas et al., "Effect of Zirconium Oxide on the Stress-Corrosion Susceptibility of Irradiated Zircaloy Cladding," Zirconium in the Nuclear Industry: Fifth Conference, ASTM STP 754, American Society for Testing and Materials, 1982, pp. 158-170.

25. J. T. A. Roberts et al., "A Stress-Corrosion Cracking Model for Pellet-Cladding Interaction Failures in Light-Water-Reactor Fuel Rods," Zirconium in the Nuclear Industry: Fourth Conference, ASTM STP 681, American Society for Testing and Materials, 1979, pp. 285-305.

26. W. T. Grubb and M. H. Morgan III, "A Survey of the Chemical Environments for Activity in the Embrittlement of Zircaloy 2," Zirconium in the Nuclear Industry: Fourth Conference, ASTM STP 681, American Society for Testing and Materials, 1979, pp. 145-154.

27. H. M. Chung and F. L. Yaggee, "Deformation and Fracture Characteristics of Spent Zircaloy Fuel Cladding." Paper presented at The Sixth International Conference on Zirconium in the Nuclear Industry, Vancouver, B.C., Canada, June 28-July 1, 1982.

28. D. Cubicciotti et al., "Chemical Aspects of Iodine-Induced Stress-Corrosion Cracking of Zircaloys," Zirconium in the Nuclear Industry: Fifth Conference, STM STP 754, American Society for Testing and Materials, 1982, pp. 146-157.

29. P. Hofmann, "Influence of Iodine on the Strain and Rupture Behavior of Zircaloy-4 Cladding Tubes at High Temperatures," Zirconium in the Nuclear Industry: Fourth Conference, ASTM STP 681, American Society for Testing and Materials, 1979, pp. 409-428.

30. D. R. Olander, "A Thermodynamic Assessment of In-Reactor Iodine SCC of Zircaloy," Journal of Nuclear Materials, 110, 1982, pp. 343-345.

31. R. Williford, Battelle Pacific Northwest Laboratories, Personal Communication.

32. L. Lunde and K. Videm, "The Influence of Testing Conditions and Irradiation of the SCC Susceptibility of Zircaloy." Paper presented at The Enlarged Halden Program Group Meeting at Lillehammer, Norway, HPR-268, June 1980.

33. K. Videm and L. Lunde, "Stress-Corrosion Crack Initiation and Growth and Formation of Pellet-Clad Interaction Defects," Zirconium in the Nuclear Industry: Fourth Conference, ASTM STP 681, American Society for Testing and Materials, 1979, pp. 229-243.

34. M. Peehs et al., "Experiments to Settle an I-SCC Hypothesis for Zry Tubing." Paper presented at The IAEA Specialists' Meeting on Pellet-Cladding Interaction in Water Reactors, Riso, Denmark, September 22-26, 1980.

35. H. Stehle et al., "LWR Fuel Behavior During Operational and Overpower Transients," Paper presented at The American Nuclear Society Meeting on Reactor Safety Aspects of Fuel Behavior, Sun Valley, Idaho, August 2-6, 1981.

36. K. Pettersson et al., "Effect of Irradiation on the Strength, Ductility, and Defect Sensitivity of Fully Recrystallized Zircaloy Tube," Zirconium in the Nuclear Industry: Fourth Conference, ASTM STP 681, American Society for Testing and Materials, 1979, pp. 155-173.

37. K. Pettersson letter to editors, "Rapid Stress-Corrosion Crack Growth in Irradiated Zircaloy," Journal of Nuclear Materials, 107, 1982, pp. 116-121.

38. L. Lunde and K. Olshausen, "Stress-Corrosion Testing of Irradiated Cladding Tubes." Paper presented at The IAEA Specialists' Meeting on Power Ramping and Power Cycling of Water Reactor Fuel and Its Significance to Fuel Behavior, Arles, France, May 14-18, 1979.

39. H. Staal et al., Ramp Testing of IFA-413 and IFA-516, Halden Work Report 15, May 1981.

40. L. J. Siefken et al., FRAP-T6: A Computer Code for the Transient Analysis of Oxide Fuel Rods, NUREG/CR-2104, May 1981.

41. U. Bergenlid et al., "The Studsvik Power Transient Program Demo-Ramp II and Trans-Ramp I." Paper presented at The IAEA Specialists' Meeting on Pellet-Cladding Interaction in Water Reactor Fuel, Seattle, WA, USA, October 3-5, 1983.

42. D. Lanning, Battelle Pacific Northwest Laboratories, personal communication on efforts to support PCI Task Force.

43. S. Junkrans and O. Varnild, "ASEA Atom." Paper presented at The American Nuclear Society Topical Meeting on Water Reactor Fuel Performance, St. Charles, Ill., 1977.

44. C. Vitanza, Use of the SIROD Code for Fuel Failure Interpretation, HPR-241, May 1980.

45. T. Okubo et al., "FEMAXI III, Theory and Model Assessment." Paper presented at The Enlarged Halden Program Group Meeting at Lillehammer, Norway, HPR-268, June 1980.

46. Battelle Pacific Northwest Laboratories Quarterly Report, NUREG/CR-2716, Vol. 4, April 1983, p. 33.

47. D. Howl et al., "A Pellet-Clad Interaction Failure Criterion." Paper presented at The IAEA Specialists' Meeting on Power Ramping and Cycling Behavior of Water Reactor Fuel, Petten, the Netherlands, September 8-9, 1982.

48. W. Vogl et al., "Experimental Strategy of Fuel Performance Testing with Respect to PCI," Nuclear Engineering and Design, 65, 1981, pp. 307-312.

49. R. von Jan and W. Hering, "Experience and Plans with PCI Protection in KWU LWR Plants," Nuclear Engineering and Design, 65, 1981, pp. 313-318.

APPENDIX A
PCI TASK FORCE MEMBERS AND ASSOCIATES

APPENDIX A
PCI TASK FORCE MEMBERS AND ASSOCIATES

PCI Task Force Members

R. Van Houten, DAE/RES
M. Tokar, DSI/NRR
P. MacDonald, EG&G

PCI Task Force Associates

F. Odar, DAE/RES
H. Scott, DAE/RES
G. Marino, DAE/RES
R. Meyer, DSI/NRR
D. Fieno, DSI/NRR
H. Richings, DSI/NRR
S. Ploger, EG&G
R. Hobbins, EG&G
R. Williford, PNL
T. Kassner, ANL

APPENDIX B
LHGR DATA FOR A BWR-4 DURING A LICENSING BASIS TRANSIENT

A. Aronson and D. Cokinos

Brookhaven National Laboratory

APPENDIX B

LHGR DATA FOR A BWR-4 DURING A LICENSING BASIS TRANSIENT

This appendix provides linear heat generation rate (LHGR) data for a BWR-4 licensing basis transient. The transient consists of a turbine trip without steam bypass. The analysis performed with the two-dimensional (R,Z) core dynamics code BNL-TWIGL in conjunction with the system transient code RELAP-3B has been reported by Lu et al.[10]

The neutronic calculations in the core region were carried out with a mesh structure resulting from partitioning the core into 34 concentric cylindrical surfaces (33 radial mesh intervals) and 49 parallel axial planes (48 axial mesh intervals). However, for the purpose of this work the LHGR data have been reduced to only 11 nodes, or blocks. In the conventional (R,Z) modeling these blocks coincide with the spatial material composition of the core as shown in Figure B-1 and Table B-1. With the exception of the three peripheral blocks, 9, 10 and 11, there is no radial segmentation of the core. Since each block is composed of a relatively large integral number of neutronic nodes, the LHGR data of a block given in this memo are the result of a radial and axial integration over a volume defined by radial and axial boundaries in each of the 11 blocks.

The data preserted in this memo are based on the assumption that the average assembly has an LHGR of ~6.09 kw/ft. The data may be scaled in either direction in order to accommodate any combination of core power, core size (number of fuel assemblies) or rod array according to the following formula:

$$\frac{\text{Power in kW}}{\text{(Total No. of Rods in Core) (12 ft)}}$$

The total core power as a function of time is given in Figure B-2. Figures B-3 through B-13 show the time dependence of the LHGR in each block. The maximum LHGR in each block and the corresponding time are given in Table B-2. A frequency distribution showing number of blocks in which the peak LHGR's have values within a 10 kW/ft range plotted as a function of LHGR is given in Figure B-14. The peak LHGR data used in the frequency distribution have been obtained from a partitioning of the core into 60 blocks. Therefore, the values used in this distribution are block-averaged peaks, i.e., values obtained by adding the LHGR of each of the neutronic nodes making up each block and dividing through by the number of neutronic nodes in the block. The peak LHGR's given in Table B-2 reflect this definition of the peak for the case of the 11-block core. Table B-3 shows the initial LHGR and the volume fraction for each block.

In addition to the LHGR data for the 11-block core, data reductions have also been made for a 35-block core and a 60-block core. These more detailed data sets are also available.

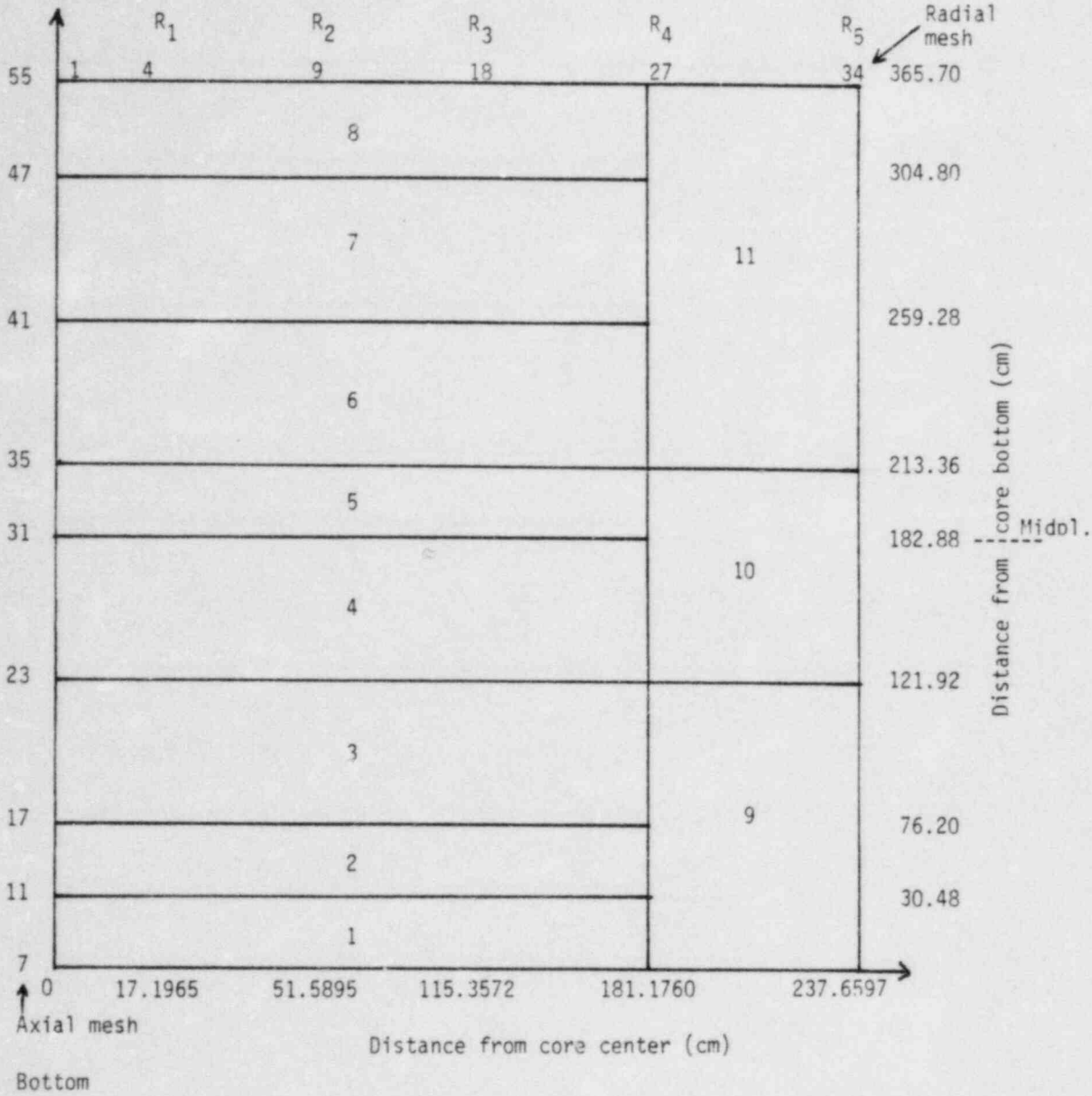

Figure B-1. The (R,Z) block structure of the 11-block core.

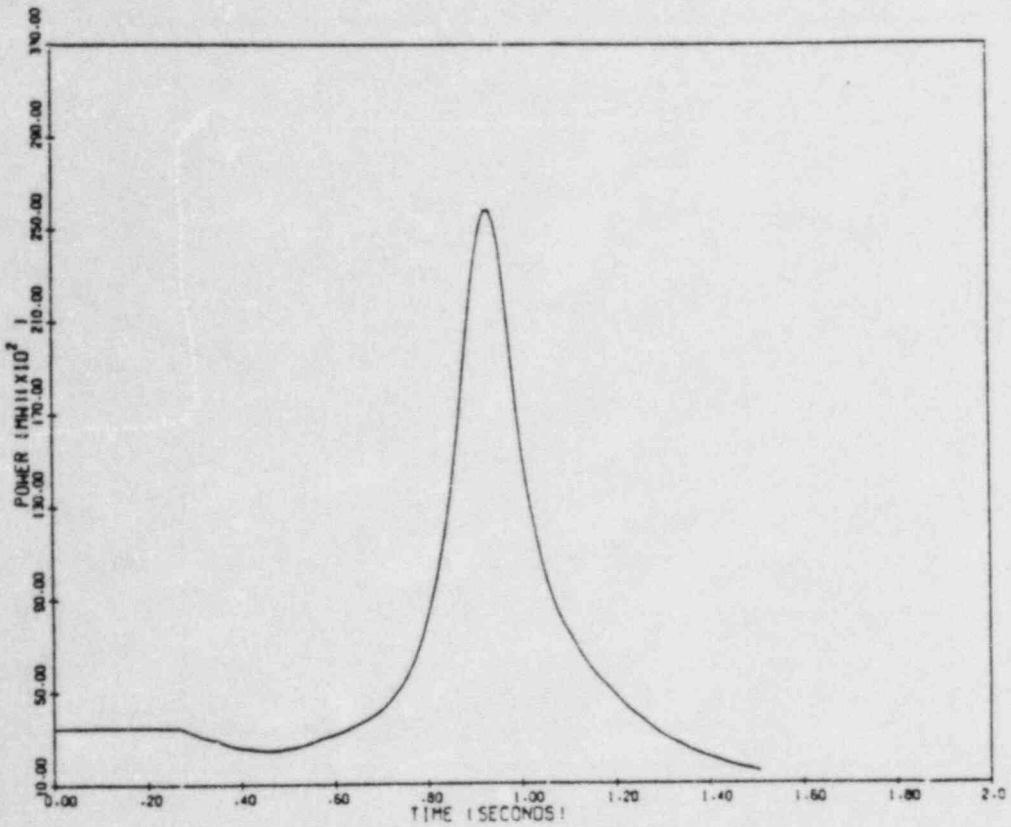

Figure B-2. Total core power versus time during a BWR/4 turbine trip without bypass.

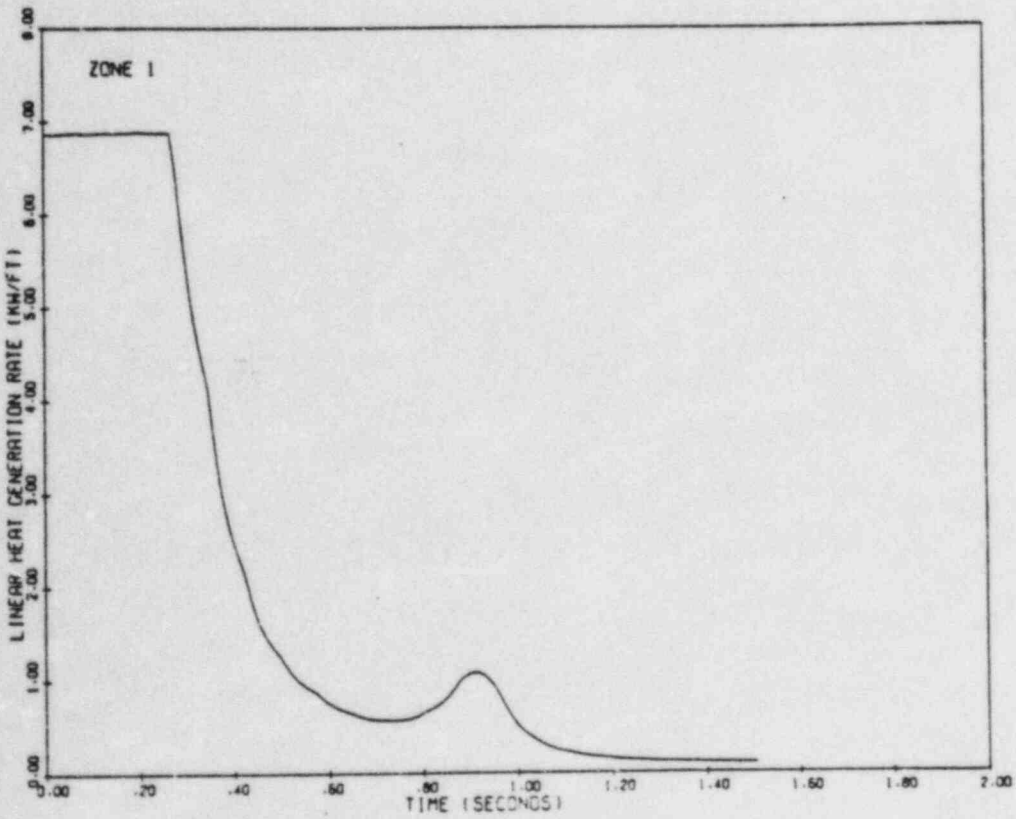

Figure B-3. Maximum linear heat generation rates versus time in Zone 1 during a BWR/4 turbine trip without bypass.

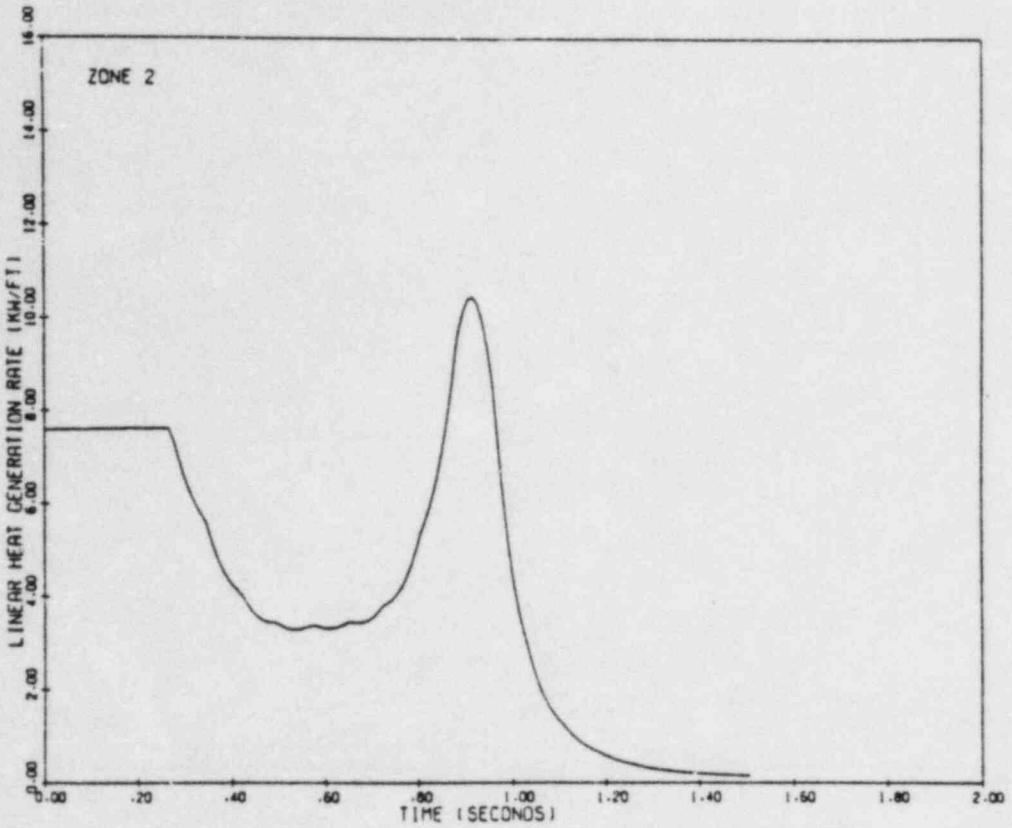

Figure B-4. Maximum linear heat generation rates versus time in Zone 2 during a BWR/4 turbine trip without bypass.

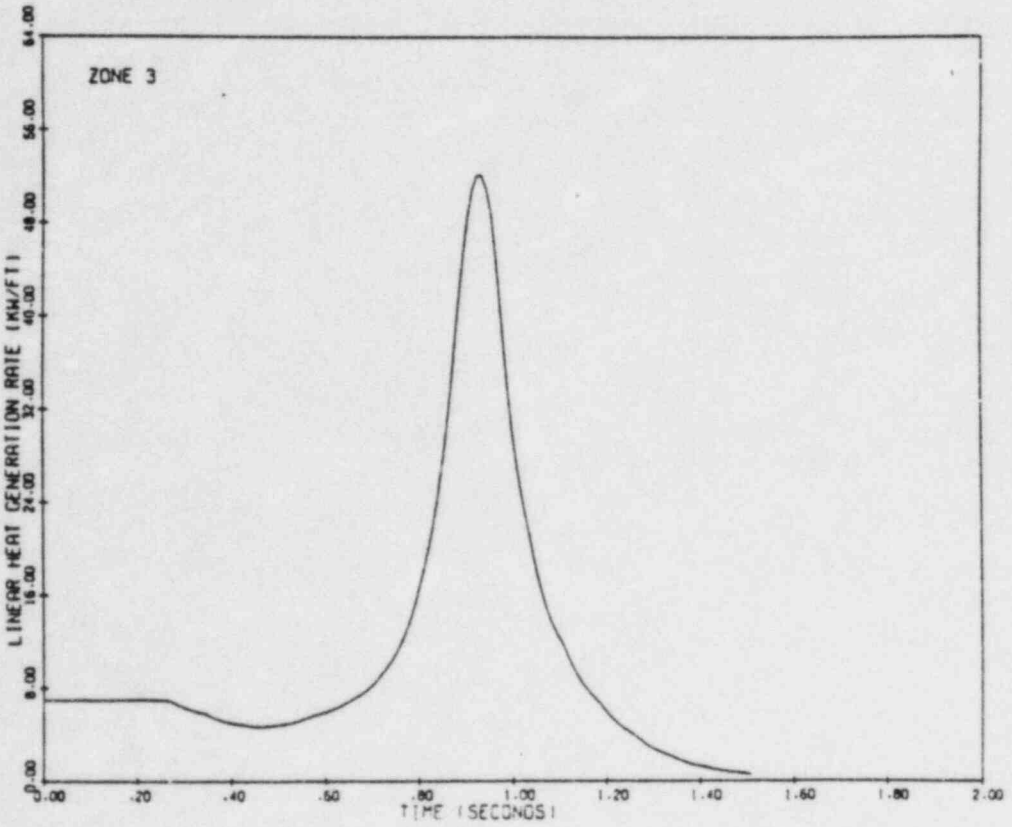

Figure B-5. Maximum linear heat generation rates versus time in Zone 3 during a BWR/4 turbine trip without bypass.

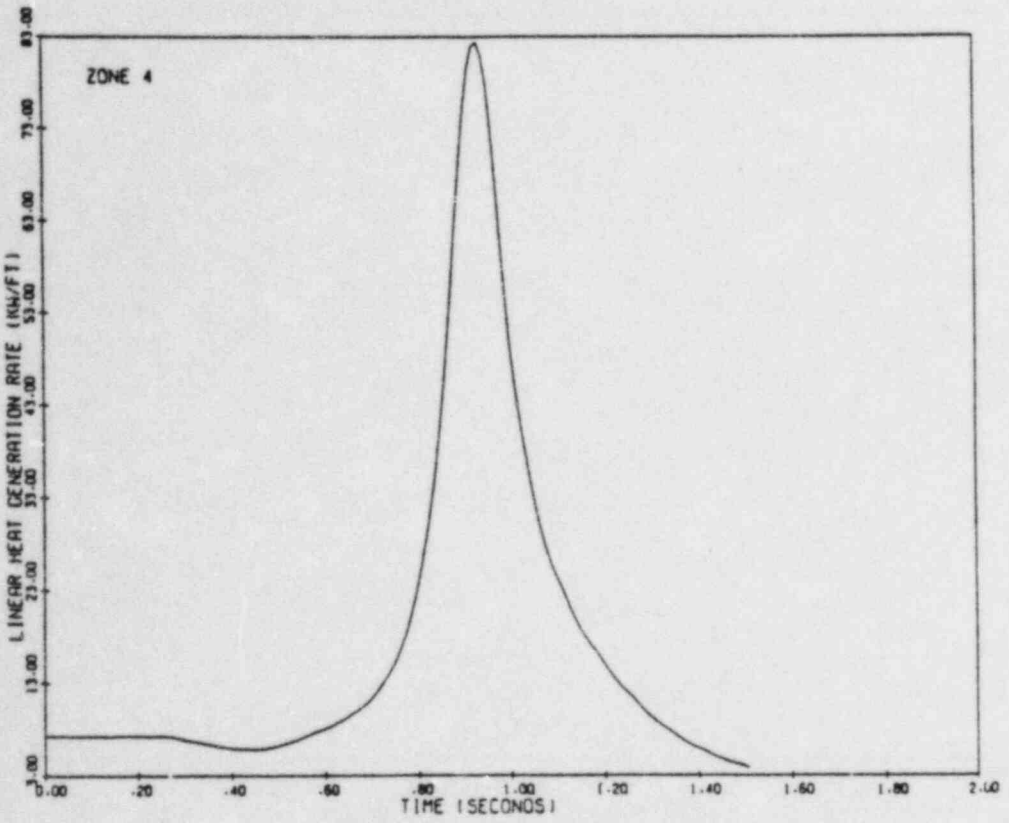

Figure B-6. Maximum linear heat generation rates versus time in Zone 4 during a BWR/4 turbine trip without bypass.

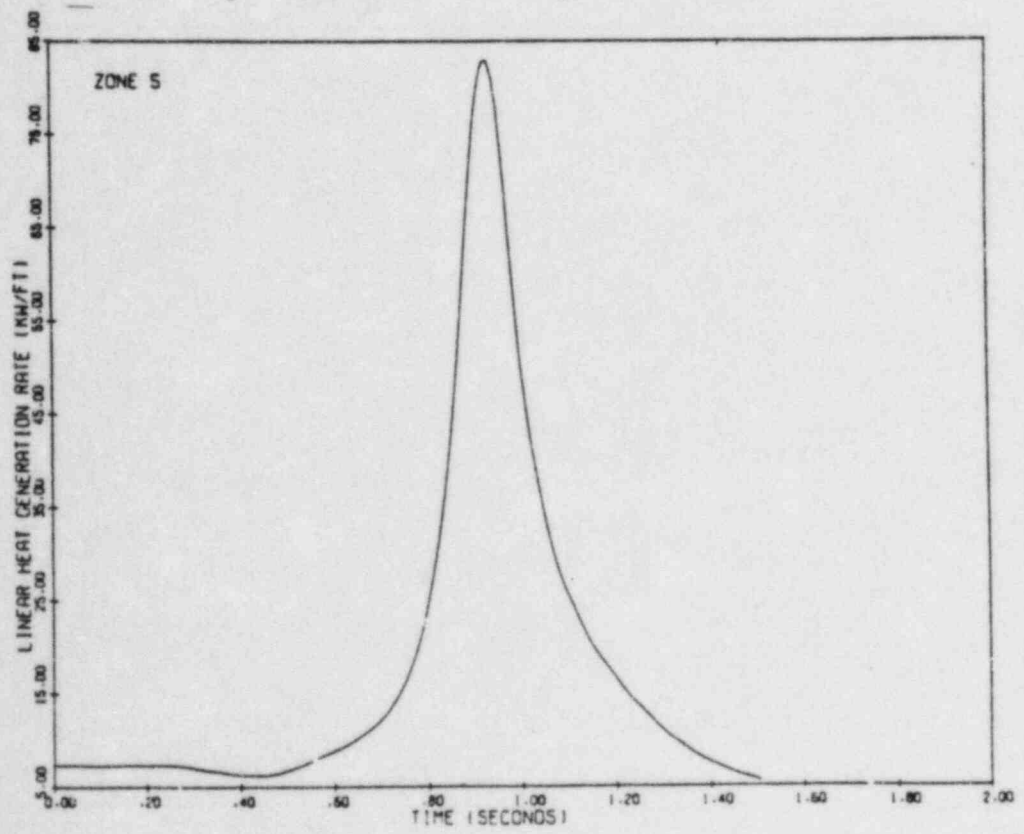

Figure B-7. Maximum linear heat generation rates versus time in Zone 5 during a BWR/4 turbine trip without bypass.

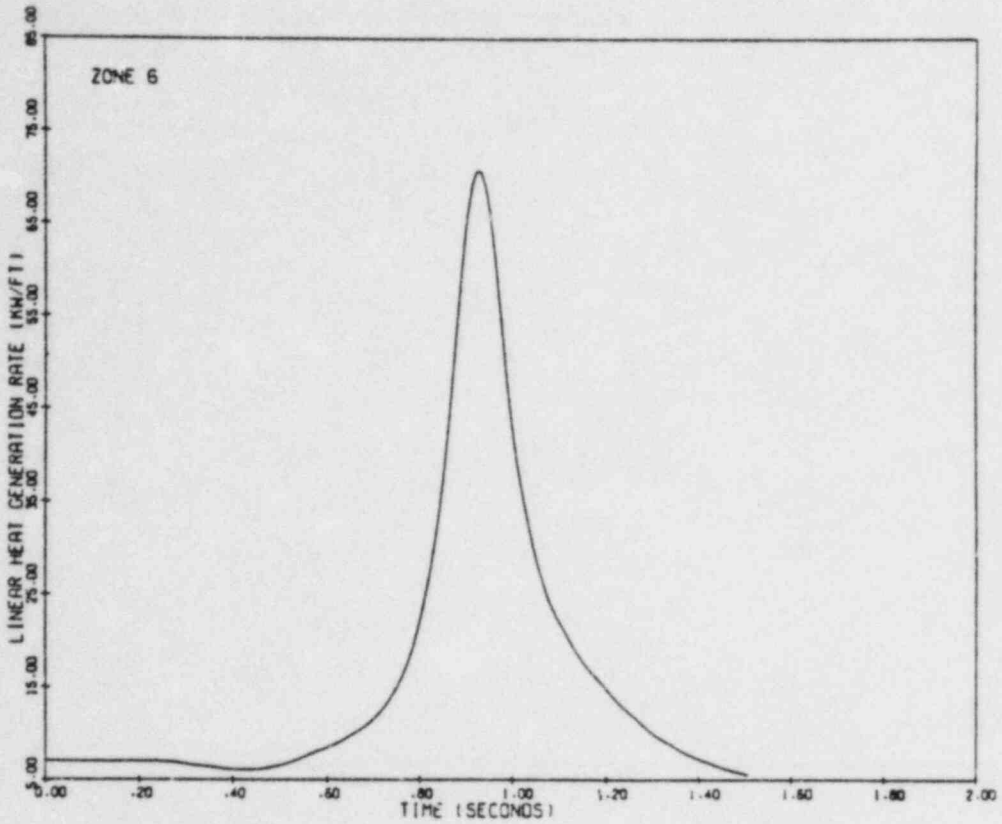

Figure B-8. Maximum linear heat generation rates versus time in Zone 6 during a BWR/4 turbine trip without bypass.

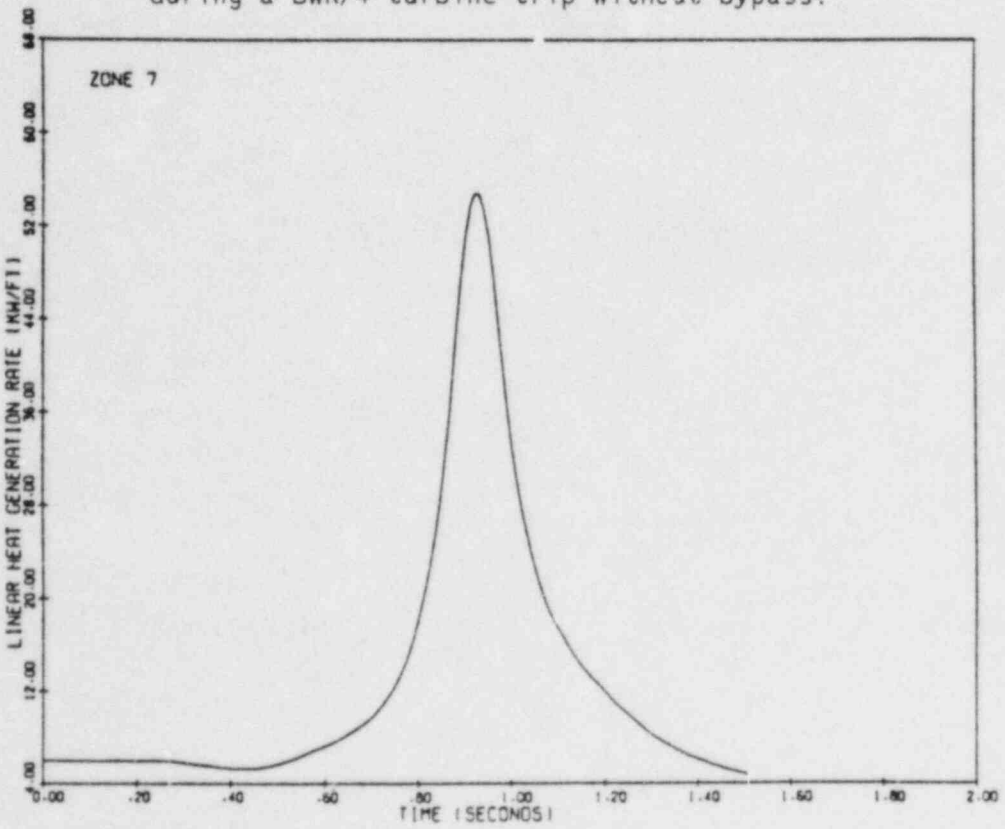

Figure B-9. Maximum linear heat generation rates versus time in Zone 7 during a BWR/4 turbine trip without bypass.

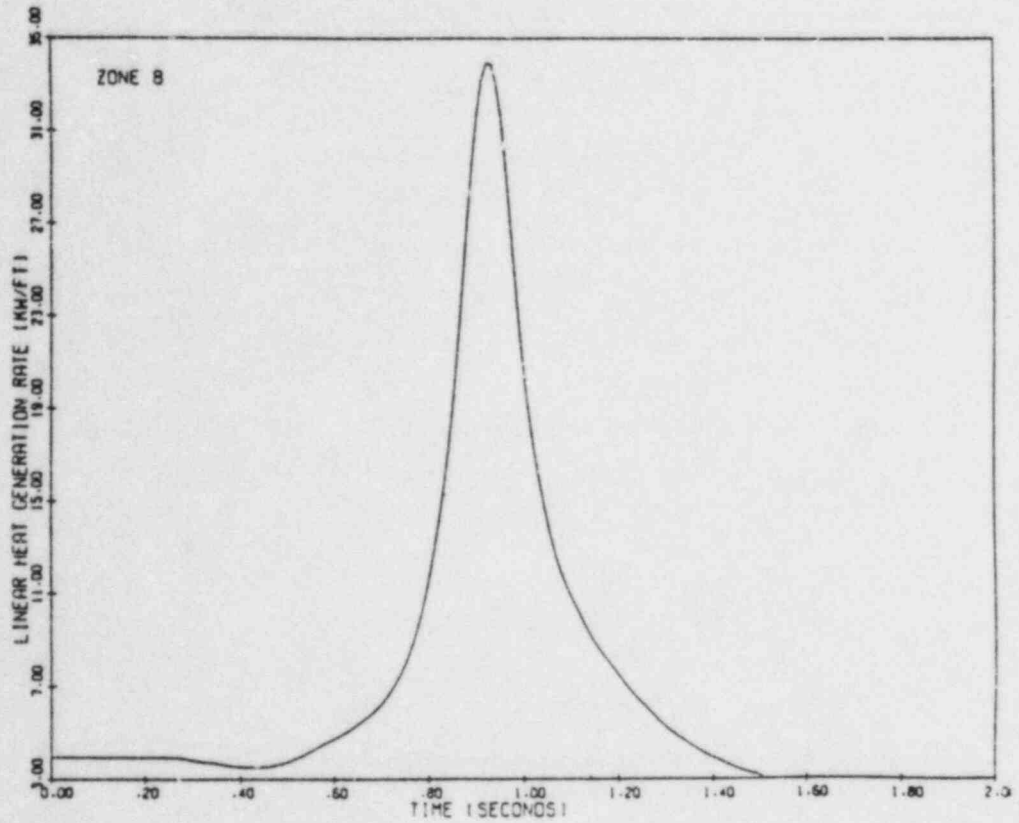

Figure B-10. Maximum linear heat generation rates versus time in Zone 8 during a BWR/4 turbine trip without bypass.

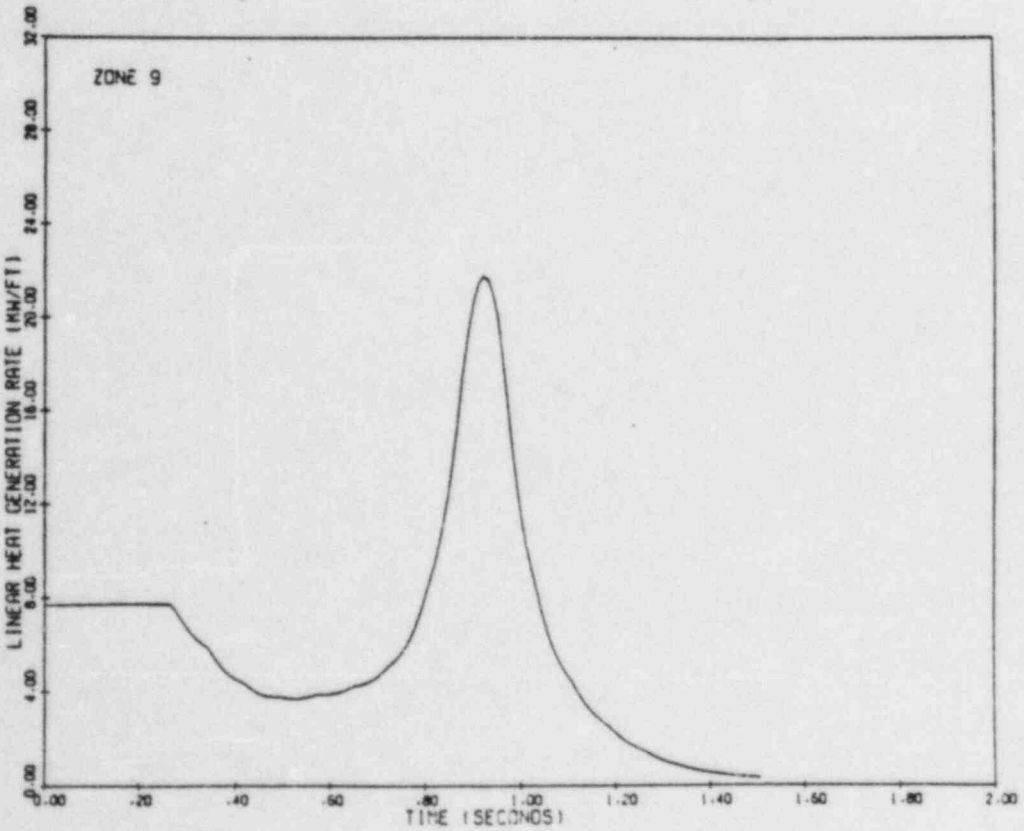

Figure B-11. Maximum linear heat generation rates versus time in Zone 9 during a BWR/4 turbine trip without bypass.

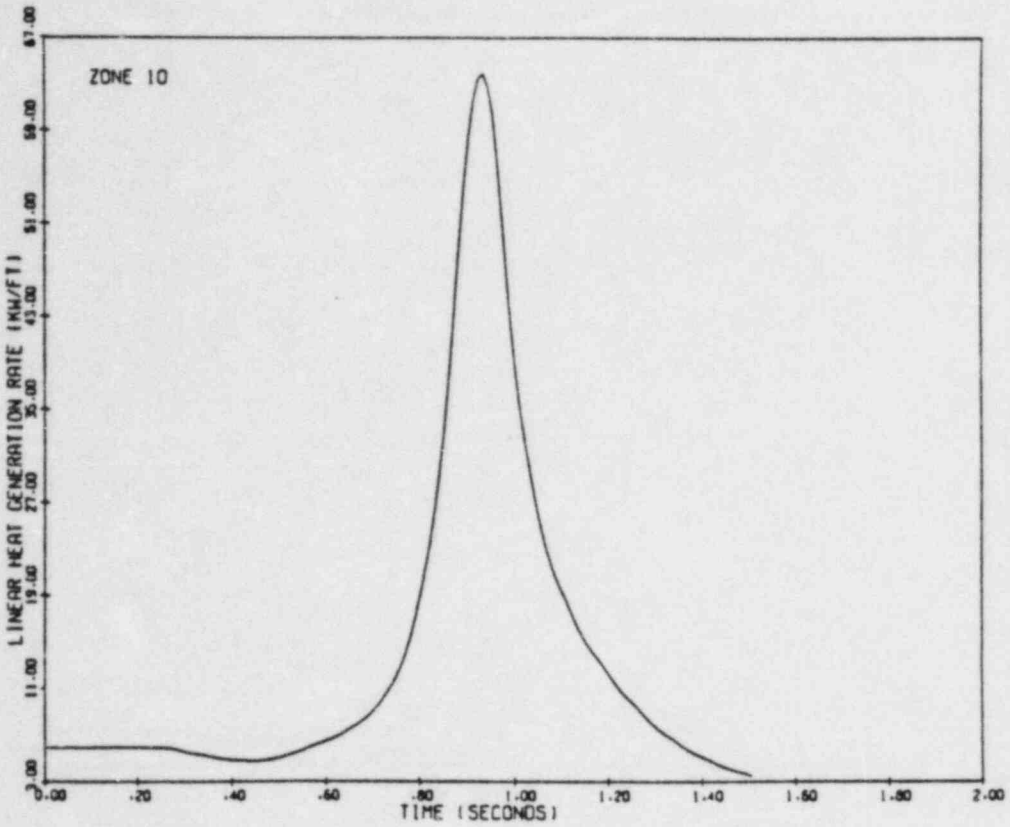

Figure B-12. Maximum linear heat generation rates versus time in Zone 10 during a BWR/4 turbine trip without bypass.

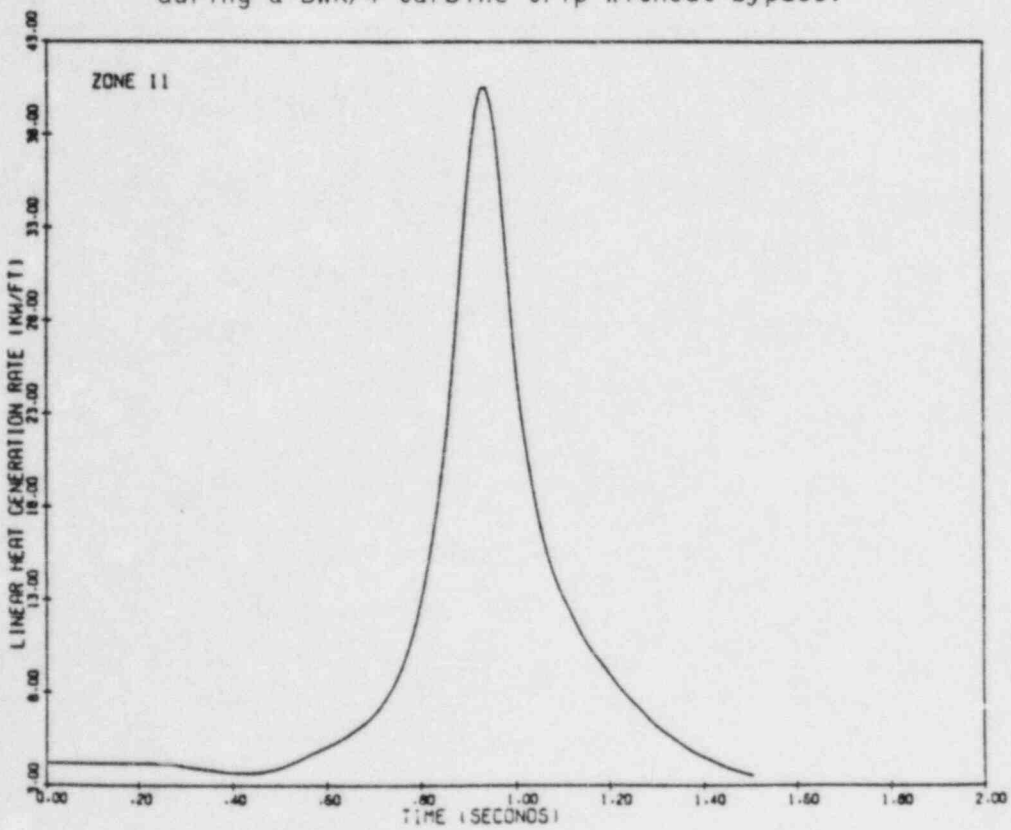

Figure B-13. Maximum linear heat generation rates versus time in Zone 11 during a BWR/4 turbine trip without bypass.

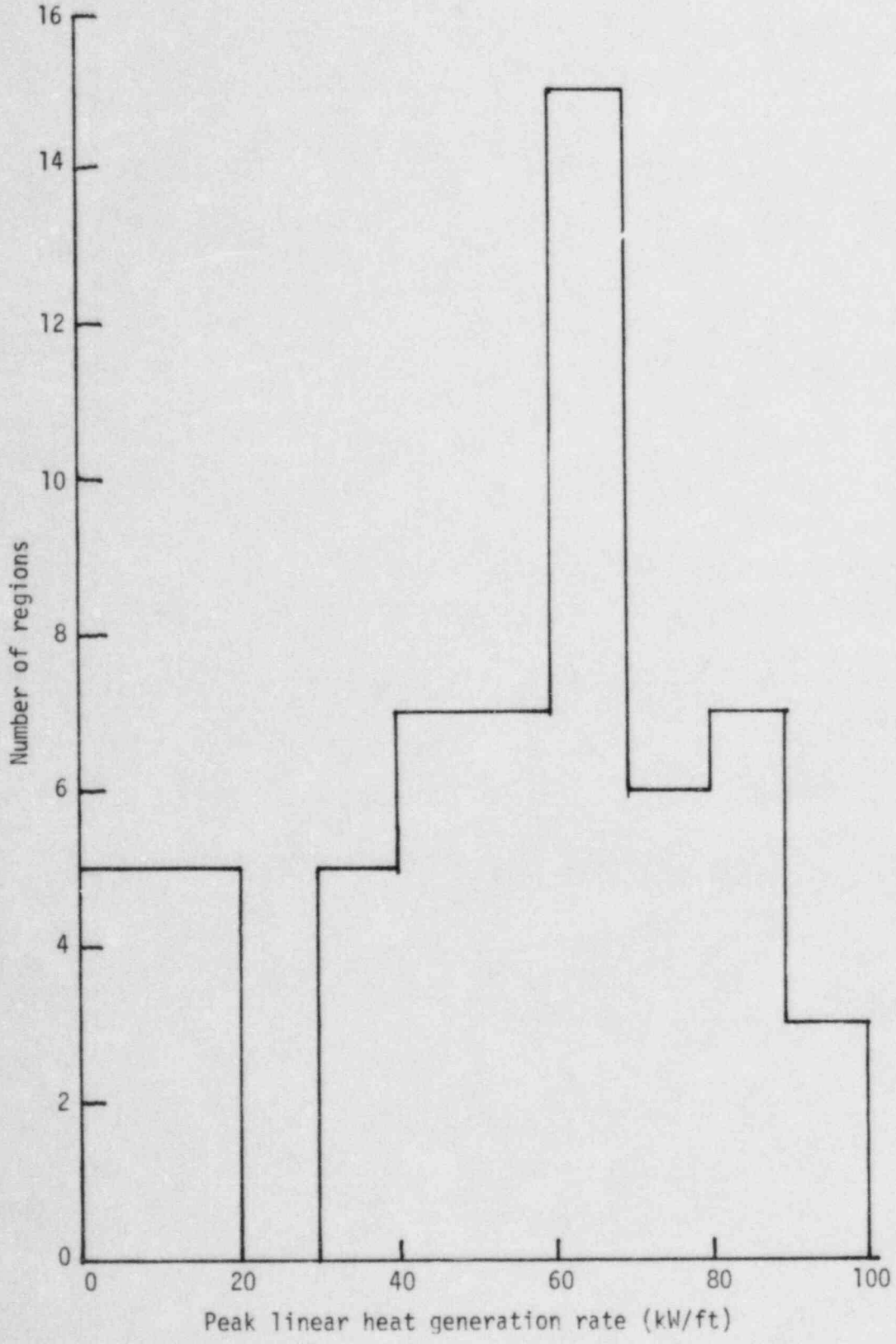

Figure B-14. Frequency distribution showing number of regions versus linear heat generation rate.

TABLE B-1. AXIAL REGION STRUCTURE: 11-BLOCK CORE

	Axial Mesh					
	From	To	Number of Intervals	Axial From	Distance To	Material Number
Central Regions	7	11	4	0	30.48	1
	11	17	6	30.48	76.20	2
	17	23	6	76.20	121.92	3
	23	31	8	121.92	182.88	4
	31	35	4	182.88	213.36	5
	35	41	6	213.36	259.28	6
	41	47	6	259.28	304.80	7
	47	55		304.80	365.70	8
Peripheral Regions	7	23	16	0	121.92	9
	23	35	12	121.92	213.36	10
	35	55	20	213.36	365.70	11

TABLE B-2. LICENSING BASIS TRANSIENT BWR/4

Zone	Peak Linear Heat Generation Rate (kW/ft)	Time (sec)
1	6.87735E+00	0.20270
2	1.04300E+01	0.91270
3	5.20845E+01	0.93270
4	8.24167E+01	0.93270
5	8.29221E+01	0.93270
6	7.04015E+01	0.93270
7	5.45330E+01	0.92270
8	3.38551E+01	0.92270
9	2.16644E+01	0.92270
10	6.37238F+01	0.93270
11	4.04228E+01	0.93270

TABLE B-3. LICENSING BASIS TRANSIENT BWR/4

Zone	Peak Linear Heat Generation Rate (kW/ft)	Volume Fraction
1	6.86181E+00	4.84294E-02
2	7.59757E+00	7.26441E-02
3	6.96212E+00	7.26441E-02
4	7.20299E+00	9.68588E-02
5	7.30495E+00	4.84294E-02
6	6.75996E+00	7.26441E-02
7	5.77694E+00	7.26441E-02
8	3.81927E+00	9.68588E-02
9	7.60396E+00	1.39616E-02
10	5.73176F+00	1.04712E-01
11	4.02201E+00	1.74520E-01
Core Average kW/ft = 6.08583E+00		

APPENDIX C
LINEAR HEAT GENERATION RATES IN A PWR UNDERGOING UNCONTROLLED BANK WITHDRAWAL

Partha Neogy

Brookhaven National Laboratory

APPENDIX C
LINEAR HEAT GENERATION RATES IN A PWR UNDERGOING UNCONTROLLED BANK WITHDRAWAL

Introduction

The uncontrolled bank withdrawal accident leads to an uncontrolled addition of reactivity to the reactor core, resulting in a power excursion. The transient is caused by a malfunction of the reactor control or control rod drive systems. The event may occur at either subcritical, hot zero power, or at power conditions. The present discussion addresses transients initiated at hot full power conditions although a discussion of the transient initiated from subcritical conditions is included. The power excursion is terminated by the high neutron flux trip, the overtemperature or overpower ΔT trips, or the high pressurizer pressure trip.

The point kinetics model is assumed to be valid. That is, the steady state relative power distribution in the reactor core is assumed to persist unchanged throughout the transient. The numerical results used are taken from a safety analysis report for a standard 3250 MW(t) PWR.

Steady State Power Distribution

The radial and axial steady state power distributions at hot full power, control bank-D 30% inserted, beginning of life conditions for a typical 4-loop PWR are presented in Figures C-1 and C-2. Figure C-3 shows an octant of the reactor core partitioned into four radial and four axial edit zones. The reactor core is thus partitioned into sixteen regions, each region being labelled by a particular radial zone and a particular axial zone.

Table C-1 lists the heat generation characteristics of the reactor core. The normalized steady state power distributions within the radial and axial edit zones are indicated in Tables C-2 and C-3, respectively. The quantity "f_R" for a radial zone is the ratio of the maximum fuel

assembly power in that zone to the average power in the zone. "f_Z" is the axial peaking factor for the edit zone of interest. The break up of the 16 edit regions in terms of the radial and axial zones, the volume fraction of each region, and the normalized power in each region are indicated in Table C-4.

Transient Results

A conservatively high reactivity insertion rate of 75×10^{-5} $\Delta k/sec$ was assumed for the transient. Conservative values of Doppler and moderator feedback coefficients were also used. A high neutron flux trip was assumed, and a point kinetics model was utilized. The core average normalized linear heat generation rate, F(t), is presented as a function of time in Figure C-4.

The linear heat generation rate for the limiting fuel rod in an edit region at any time is given by

$$\text{LHGR} = \text{(Average Linear Power Density)} \times \text{(Normalized Power} \times F(t) \times f_R \times f_z \times f_{local},$$

where f_{local} is a local peaking factor (typically 1.1) that accounts for variations in heat generation rates between fuel rods within a fuel assembly; and the other factors are those defined in Tables C-1 through C-4 and Figure C-4.

Example

As an example, let us determine the linear heat generation rate for (i) the limiting rod and (ii) the average rod in edit region #6 at 2.15 sec.

(i) $\text{LHGR} = \text{(Nominal Linear Power Density)} \times \text{(Normalized Power)} \times F(t) \times f_R \times f_Z \times f_{local}$

$= 6.722 \times 1.71 \times 1.2 \times 1.06 \times 1.03 \times 1.1$ kW/ft

$= 16.6$ kW/ft

(ii) LHGR = 6.722 x 1.71 x 1.2 x 1.0 x 1.0 x 1.0 kW/ft

= 13.8 kW/ft

Uncontrolled Bank Withdrawal From Subcritical Conditions

For comparison, the transient heat flux following uncontrolled bank withdrawal from subcritical conditions is shown in Figure C-5. The core average linear heat generation rate in this case peaks at 73% of the nominal value at ~7.5 sec into the transient, considerably lower than 120% of nominal for the hot full power case. However, the rate of change of the LHGR is much larger when the transient is initiated from subcritical conditions.

TABLE C-1. HEAT GENERATION CHARACTERISTICS OF THE REACTOR CORE

Rated Thermal Power (MW)	3250
Fraction of Thermal Power Generated in Fuel	0.974
Total Length of Fuel Columns (ft)	4.709×10^5
Average Linear Power Density (kW/ft)	6.722

TABLE C-2. RADIAL POWER DISTRIBUTION

Radial Zone #	Normalized Power	f_R
1	0.984	1.09
2	1.120	1.06
3	1.058	1.12
4	0.837	1.32

TABLE C-3. AXIAL POWER DISTRIBUTION

Axial Zone #	Normalized Power	f_Z
1	0.91	1.58
2	1.53	1.03
3	1.17	1.26
4	0.39	1.92

TABLE C-4. VOLUME FRACTIONS AND NORMALIZED POWER FOR EDIT REGIONS

Region	Radial Zone	Axial Zone	Volume Fraction	Normalized Power
1	1	1	1.165×10^{-2}	0.90
2	2	1	5.183×10^{-2}	1.02
3	3	1	9.328×10^{-2}	0.96
4	4	1	9.328×10^{-2}	0.76
5	1	2	1.165×10^{-2}	1.51
6	2	2	5.183×10^{-2}	1.71
7	3	2	9.328×10^{-2}	1.62
8	4	2	9.328×10^{-2}	1.28
9	1	3	1.165×10^{-2}	1.15
10	2	3	5.183×10^{-2}	1.31
11	3	3	9.328×10^{-2}	1.24
12	4	3	9.328×10^{-2}	0.98
13	1	4	1.165×10^{-2}	0.38
14	2	4	5.183×10^{-2}	0.44
15	3	4	9.328×10^{-2}	0.41
16	4	4	9.328×10^{-2}	0.33

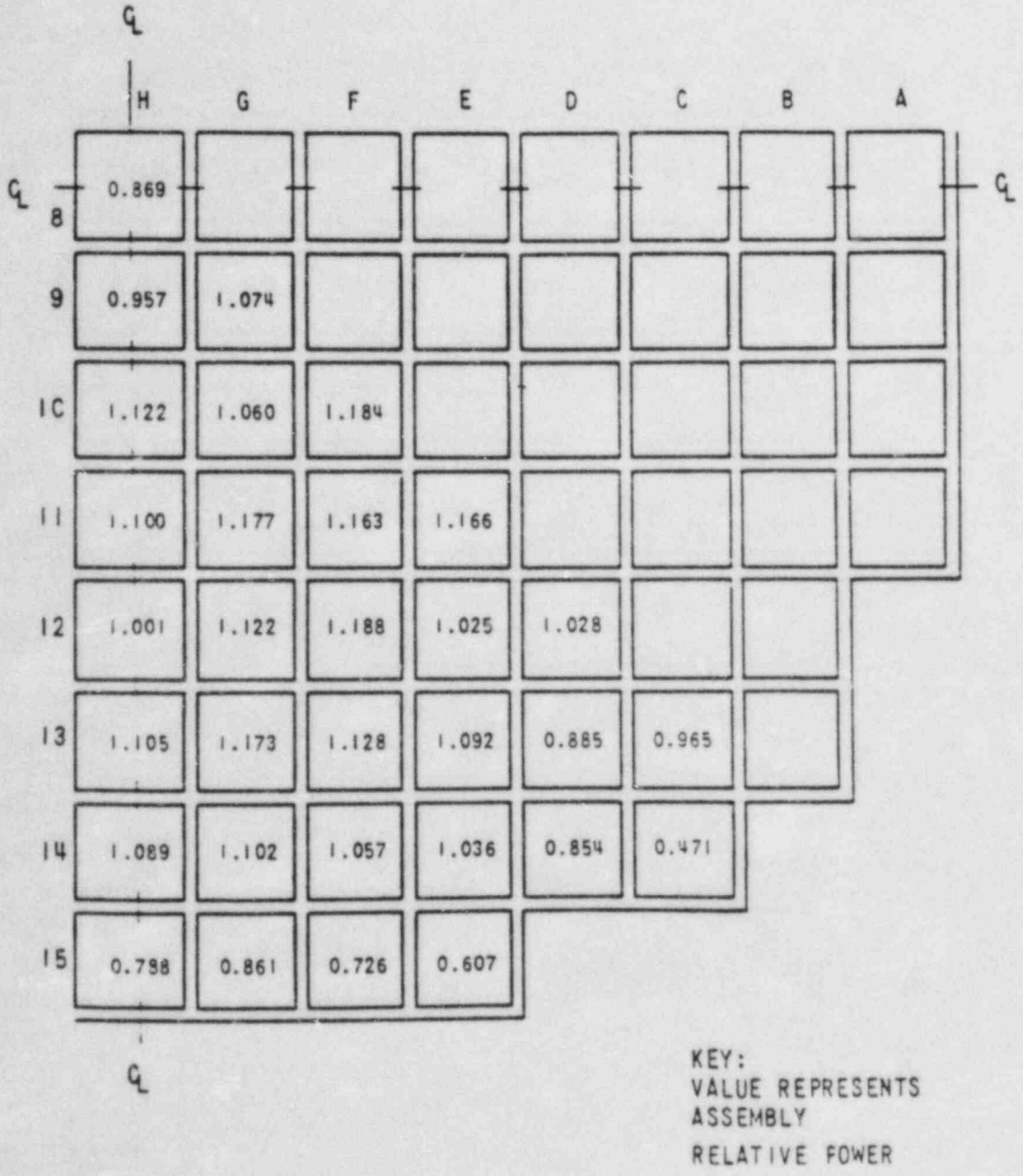

Figure C-1. Radial power distribution at steady state.

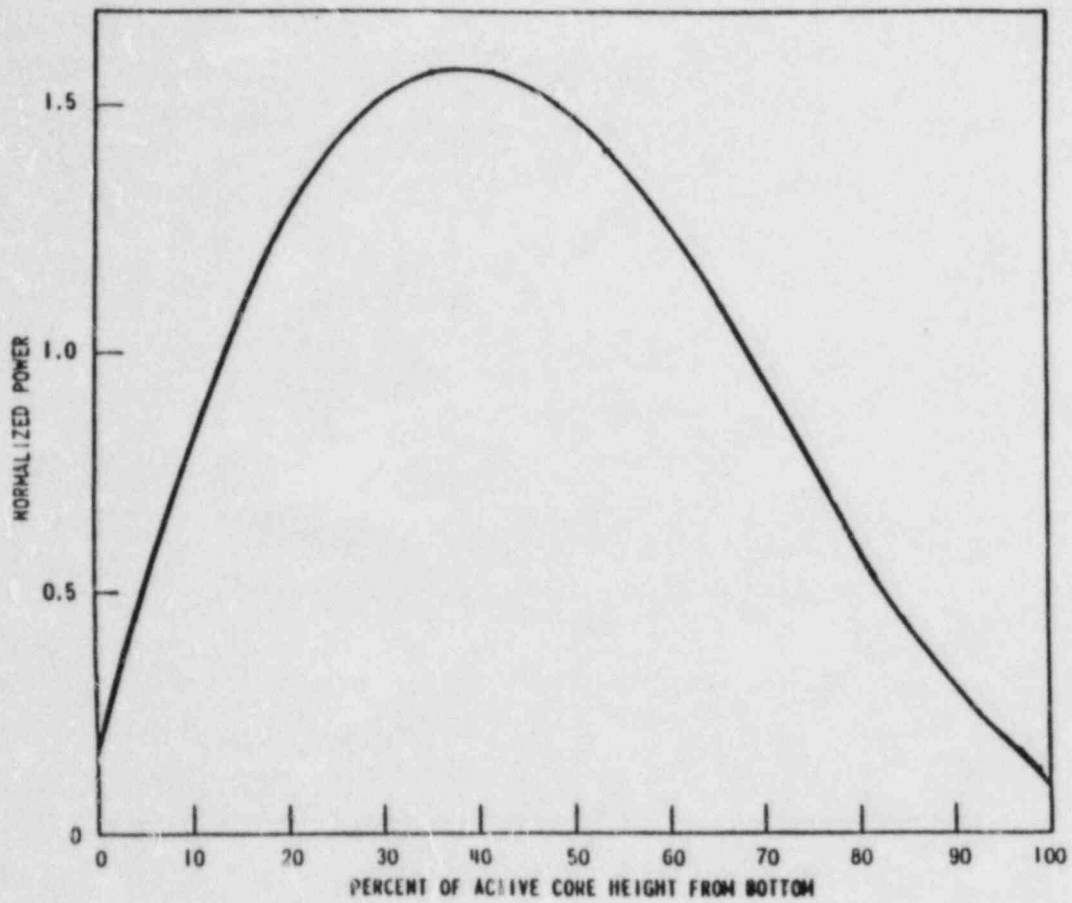

Figure C-2. Axial power distribution at steady state.

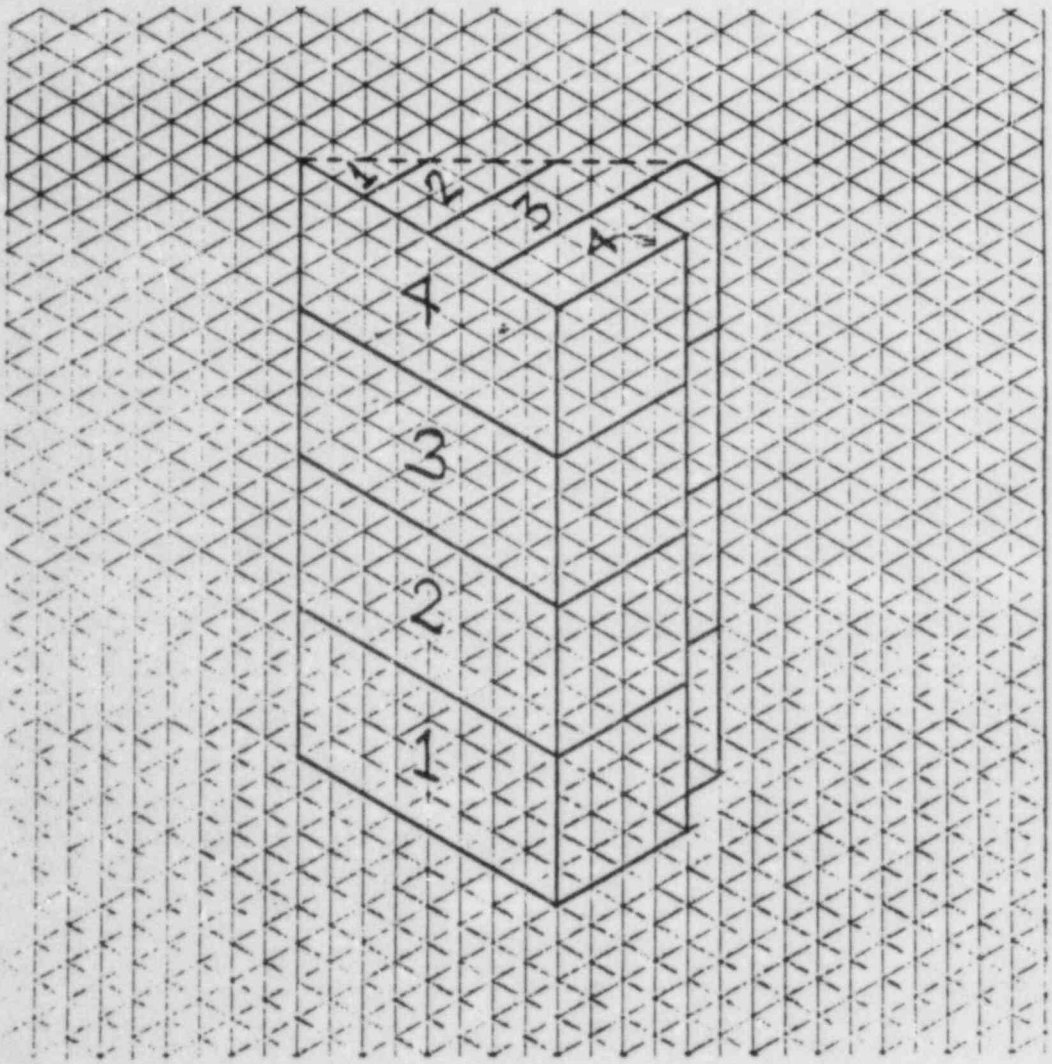

Figure C-3. An octant of the reactor core partitioned into radial and axial edit zones.

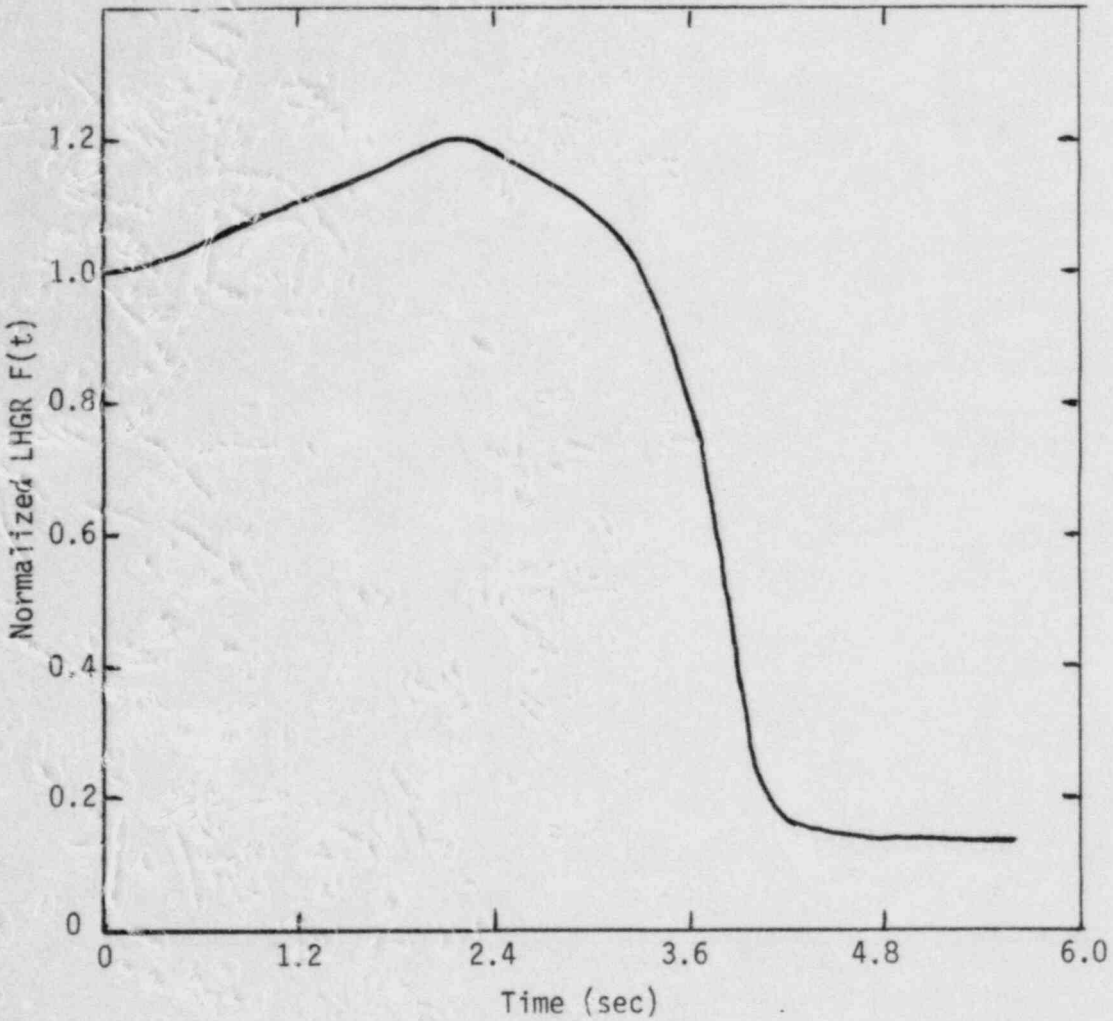

Figure C-4. Core average linear heat generation rate versus time (for fast withdrawals--slow withdrawal could be a factor of 10 longer).

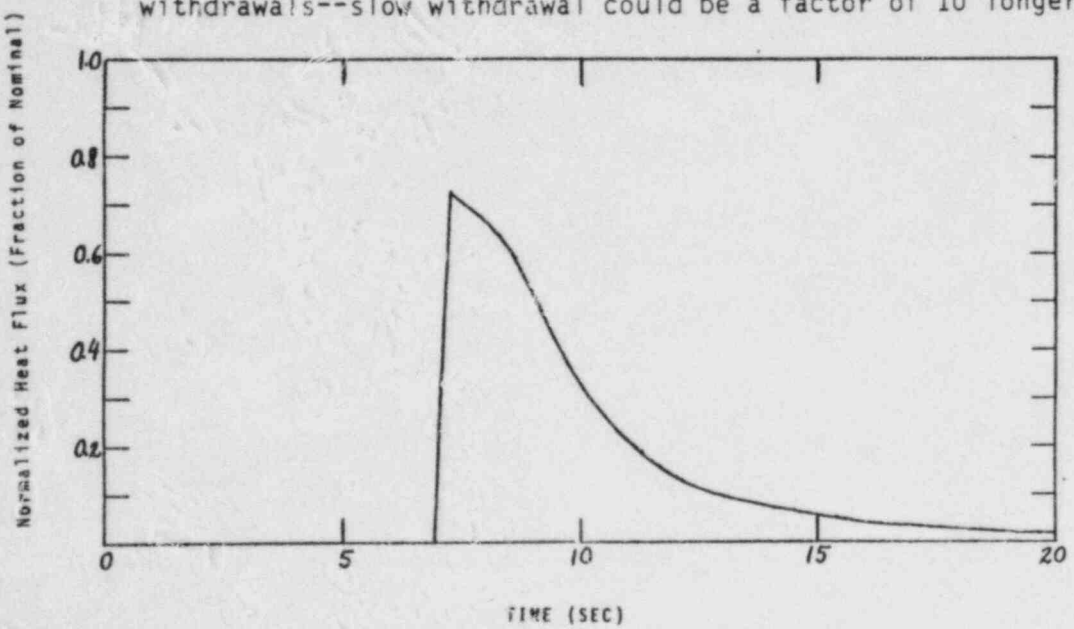

Figure C-5. Normalized heat flux versus time for rod withdrawal from subcritical conditions.

APPENDIX D

CONTINUOUS CONTROL ROD WITHDRAWL DURING A BWR STARTUP (La Salle FSAR) OR AT POWER (Shoreham FSAR)

APPENDIX D

CONTINUOUS CONTROL ROD WITHDRAWL
DURING A BWR STARTUP (La Salle FSAR)
OR AT POWER (Shoreham FSAR)

1. LA SALLE COUNTY STATION FSAR

15.4.1.2 Continuous Rod Withdrawal During Reactor Startup

15.4.1.2.1 Identification of Causes and Frequency Classification

Control rod withdrawal errors are not considered credible in the startup power range. The RSCS and the RWM prevent the operator from selecting and withdrawing an out-of-sequence control rod.

15.4.1.2.2 Sequence of Events and Systems Operation

Continous control rod withdrawal errors during reactor startup are precluded by the RSCS. In the range of 75% rod density to the low power setpoint (approximately 20% rated core power), the RSCS logic inhibits continuous rod withdrawal. In addition, since out-of-sequence control rods cannot be withdrawn, there is no basis for the continuous control rod withdrawal error in the startup power range.

The sequence of events for this event is shown in Table 15.4.1-1.

15.4.1.2.3 Core and System Performance

The performance of the RSCS and RBM prevent erroneous selection and withdrawal of an out-of-sequence control rod. Thus, the core and system performance is not affected by such an operator error.

15.4.1.2.3.1 Analysis

The continuous control rod withdrawal transient analysis in the startup range was performed to demonstrate that the licensing basis criteria for fuel failure will not be exceeded when an out-of-sequence control rod is withdrawn at the maximum allowable normal drive speed.

The rod sequence control system (RSCS) and the rod worth minimizer (RWM) constraints on rod sequences will prevent the continuous withdrawal of an out-of-sequence rod. This analysis was performed to demonstrate that, even for the unlikely event where the RWM and RSCS fail to block the continuous withdrawal of an out-of-sequence rod, the licensing basis criteria for fuel failure is still satisfied.

The methods and design basis used for performing the detailed analysis for this event, are similar to those previously approved for the control rod drop accident (CRDA) (References 1, 2, and 3). Additional simplified point model kinetics calculations were performed to evaluate the dependence of peak fuel enthalpy on the control blade worth. For the detailed calculation, the 50% control rod density pattern was selected as the initial starting condition which is consistent with the approved design basis for the CRDA (References 1, 2, and 3).

The licensing basis criterion for fuel failure is the contained energy of a fuel pellet located in the peak power region of the core shall not exceed 170 cal/gm-UO_2.

15.4.1.2.3.2 Methods of Analysis

Since the rod worth calculations using the approved design basis methods (References 1, 2,and 3) use three-dimensional geometry, it is not practical to do a detailed analysis of this event parameterizing control rod worths. Therefore, the methods of analysis employed were to perform a detailed evaluation of this event for a typical BWR and control rod worth (1.6% Δk) and to use a point model calculation to evaluate the results over the expected ranges of out-of-sequence control rod worths. The detailed calculations are performed to demonstrate (1) the consequences of this event over the expected power operating range and (2) the validity of the approximate point model calculation. The point model calculation will demonstrate that the licensing criteria for fuel failure is easily satisfied over the range of expected out-of-sequence control rod worths. These methods are described in more detail below.

The methods used to perform the detailed calculation are identical to those used to perform the design basis control rod drop accident with the following exceptions:

a. The rod withdrawal rate is 3.6 ips rather than the blade drop velocity of 3.11 fps.

b. Scram is initiated either by the IRM or 15% APRM scram in the startup range. The IRM system is assumed to be in the worst bypass condition allowed by technical specifications.

c. The blade being withdrawn inserts along with remaining drives at technical specification insertion rates upon initiation of scram signal.

Examination of a number of rod withdrawal transients in the low power startup range, using an R-Z model, has shown clearly that higher fuel enthalpy addition would result from transients starting at the 1% power level rather than from lower power levels. The analysis further shows that for continuous rod

withdrawal from these initial power levels (1% range) the APRM 15% power level scram is likely to be reached as soon as the degraded (worst bypass condition) IRM scram. Consequently, credit is taken for either the IPM or APRM 15% scram in meeting the consequences of this event. The transients for this response were initiated at 1% of power and were performed using the 15% APRM scram.

An initial point kinetics calculation was run to determine the line to scram based on an APRM scram setpoint of 15% power and an initial power level of 1%. From this time and the maximum allowable rod withdrawal speed, it is possible to show the degree of rod withdrawal before reinsertion due to the scram. From this information Figure 15.4.1-1, showing the modified effective reactivity shape, was constructed.

The point model kinetics calculations use the same equations employed in the Adiabatic Approximation described on page 4-1 of Refereince 1. The rod reactivity characteristics and scram reactivity functions are input identical to the adiabatic calculations, and the Doppler reactivity is input as a function of core average fuel enthalpy. The Doppler reactivity feedback function input to the point model calculations was derived from the detailed analysis of the 1.6% rod worth case described above. This is a conservative assumption for higher rod worths since the power peaking and hence spatial Doppler feedback will be larger for higher rod worths. As will be seen in the results section, maximum enthalpies resulted from cases initiated at 1% of rated power. In this power range the APRM will initiate scram at 15% of power; hence, the APRM 15% power scram was used for these calculations thereby eliminating the need to perform the spatial analysis required for the IRM scram. All other inputs are consistent with the detailed transient calculation.

The point model kinetics calculations results in core average enthalpies. The peak enthalpies were calculated using the following equation:

where

$\hat{h} = ho + (P/A)_T (\bar{h}_f - ho)$;

$\hat{h}$ = Final peak fuel enthalphy;

ho = Initial fuel enthalpy;

$\bar{h}_f$ = Final core average fuel enthalpy; and

$(P/A)_T$ = Total peaking factor (radial peaking) * (axial peaking) * (local fuel pin peaking).

For these calculations, the (radial x axial) peaking factors as a function of rod worth were obtained from the calculations performed in Section 3.6 of Reference 2 and are shown in Figure 15.4.1-2. It was conservatively assumed that no power flattening due to Doppler feedback occurred during the course of the transient.

15.4.1.2.3.3 Results

The reactivity insertion resulting from moving the control rod is shown in Figure 15.4.1-1 for the point kinetics calculations. The core average power versus time and the global peaking factors from Section 3.6 of Reference 2 are shown in Figures 15.4.1-2 and 15.4.1-3, respectively. The results of the point kinetics calculation are summarized in Table 15.4.1-2 along with the results of the detailed analysis.

From Figure 15.4.1-3 and Table 15.4.1-2, it is shown that the core average energy deposition is insensitive to control rod worth; therefore, the only change in peak enthalpy as a function of rod worth will result from differences in the global peaking which increases with rod worth. Comparison of the global peaking factors shown in Figure 15.4.1-2 with the values used in the detailed calculations demonstrates that the Reference 2 values are reasonable for their application in this study. For all cases, the peak fuel enthalpy is well below the licensing design criteria of 170 cal/gm.

Cases 4 and 5 of Table 15.4.1-2 show that the point kinetics calculations give conservative results relative to the detailed evaluations. The primary difference is that the global peaking will flatten during the transient due to Doppler feedback. This is accounted for in the detailed calculation but the point kinetics calculations conservatively assumed that the peaking remains constant at its initial value.

The differences in core average and peak enthalpy between cases 1 and 5 are due to the fact that for case 1 the scram was initiated by the 15% APRM scram setpoint, whereas, in case 5 the scram was intiated by the IRM's. As seen by Figure 15.4.1-4, this occurred at a core average power of 21%. Since the APRM trip point will be reached first, it is reasonable to take credit for the APRM scram.

15.4.1.2.3.4 Conclusions

From this study the following conclusions can be stated:

a. The resultant peak fuel enthalpies due to the continuous withdrawal of an out-of-sequence rod in the startup range results in peak fuel enthalpies which are significantly less than the licensing basis criteria of 170 cal/gm.

b. The point model calculations used to assess the sensitivity of peak enthalpy as a function of control rod worth are in good agreement with, and slightly conservative relative to the more detailed design basis model which is employed to evaluate the continuous rod withdrawal transient in the startup range.

15.4.1.2.4 Barrier Performance

An evaluation of the barrier performance was not made for this event since no radioactive material is released from the fuel.

15.4.1.2.5 Radiological Consequences

An evaluation of the radiological consequences was not made for this event since no radiocative material is released from the fuel.

15.4.1.2.6 References

1. C. J. Paone, et al. "Rod Drop Accident Analysis for Large Boiling Water Reactors," NEDO-10527, March 1972.

2. R. C. Stirn, et al. "Rod Drop Accident Analysis for Large BWRs," NEDO-10527, Supplement 1, July 1972.

3. R. C. Stirn, "Rod Drop Accident Analysis for Large Boiling Water Reactors Addendum No. 2 Exposed Cores," NEDO-10527, Supplement 2, January 1973.

TABLE 15.4.1-1

SEQUENCE OF EVENTS FOR CONTINUOUS ROD WITHDRAWAL DURING REACTOR STARTUP

TIME (sec)	EVENT
0	1. The reactor is critical and operating in the startup range.
>0	2. The operator selects and withdraws an out-of-sequence control rod at the maximum normal drive speed of 3.6 ips.
~4 sec	3. Both the RWM and the RSCS fail to block the selection (selection error) and continuous withdrawal (withdraw error) of the out-of-sequence rod.
4-8 sec	4. The reactor scram is initiated by the intermediate range monitor (IRM) system or the average power range monitor system (APRM).
5-9 sec	5. The prompt power burst is terminated by a combination of Doppler and/or scram feedback.
10 sec	6. The transient is finally terminated by the scram of all rods, including the control rod being withdrawn. (Technical Specification scram insertion times are assumed, 5 seconds to 90% insertion.)

TABLE 15.4.1-2

SUMMARY OF RESULTS FOR DETAILED AND POINT KINETICS EVALUATIONS OF CONTINUOUS ROD WITHDRAWAL IN THE STARTUP RANGE

CASE	CONTROL ROD WORTH (%Δk)	$\bar{h}_f$(cal/gm)	P/A [c]	$\hat{h}$(cal/gm)
1	1.6	17.3	24.2	42.7
2	2.0	17.3	30.9	50.0
3	2.5	17.2	46.0	58.5
4	1.6 [a]	18.3	19.7 [b]	56.2
5	1.6 [d]	18.3	19.7	59.6

(a) Detailed transient calculation. All other data reported are for point kinetics calculations.

(b) The P/A = 19.7 is the initial value. For the detailed analysis this value will decrease during the course of the transient since the power shape will flatten due to Doppler feedback.

(c) P/A = global peaking factor (Radial x Axial).

(d) Point kinetics calculation with IRM initiated scram and 3-D simulator global peaking.

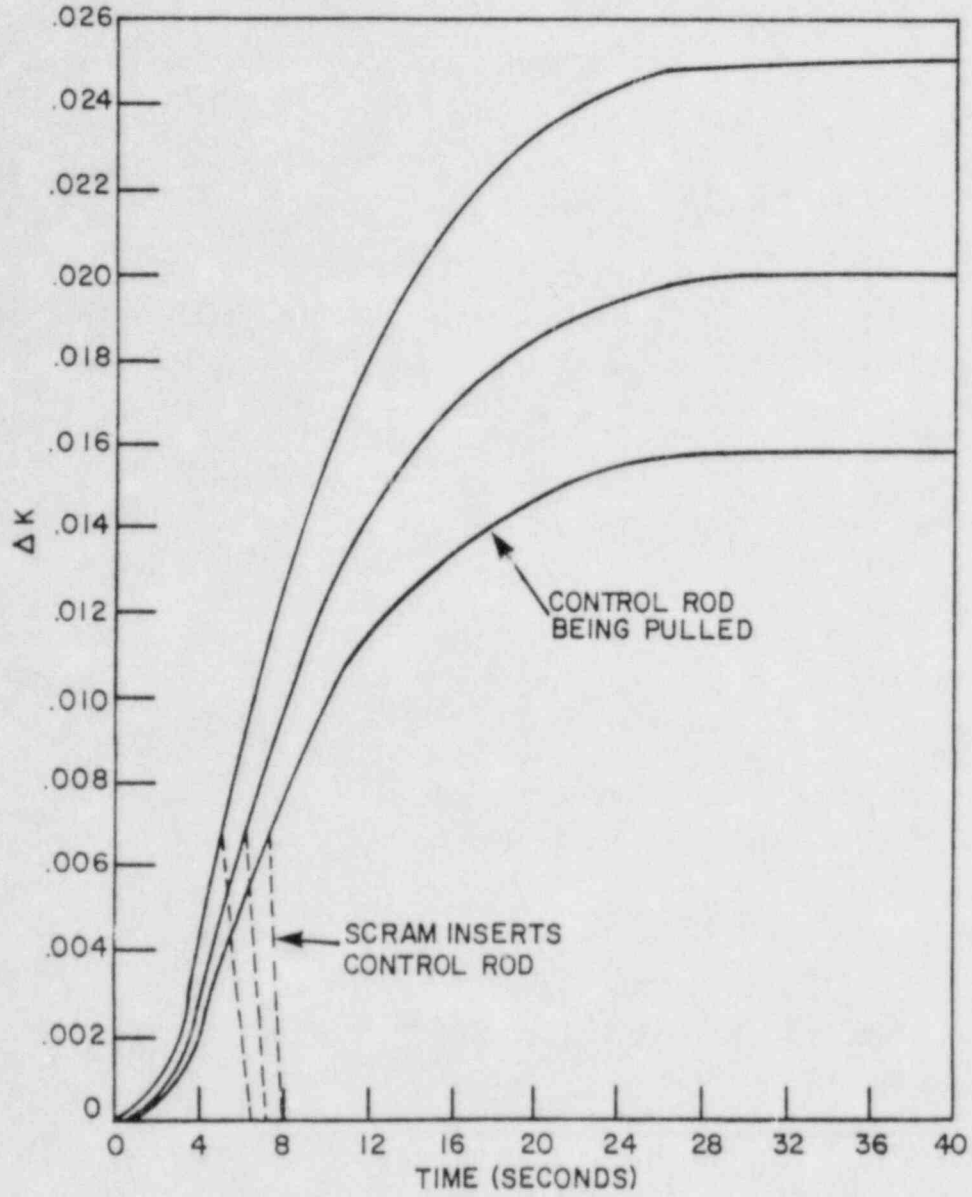

LA SALLE COUNTY STATION FINAL SAFETY ANALYSIS REPORT
FIGURE 15.4.1-1 POINT KINETICS CONTROL ROD REACTIVITY INSERTION

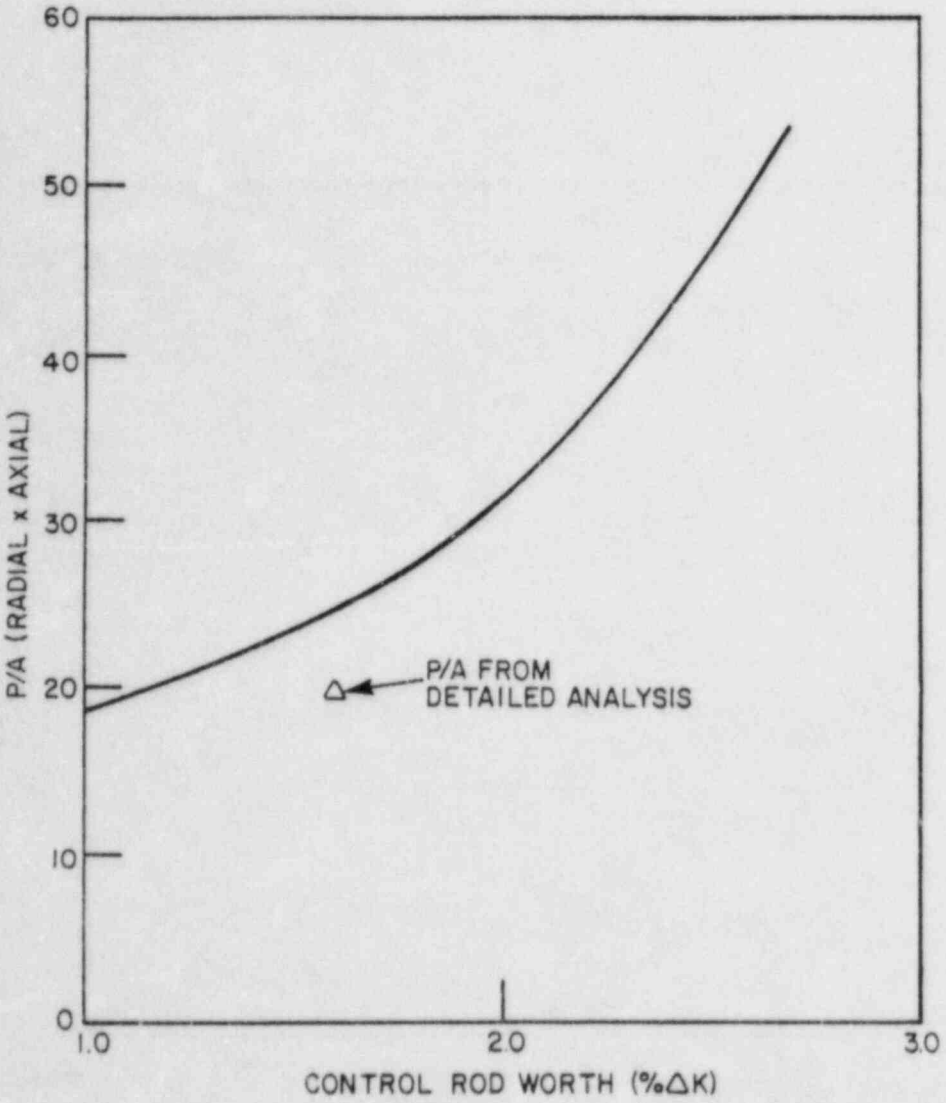

LA SALLE COUNTY STATION FINAL SAFETY ANALYSIS REPORT
FIGURE 15.4.1-2 P/A VS. ROD WORTH NEDO-10527 SUPPLEMENT 1[2] AND DETAILED ANALYSIS

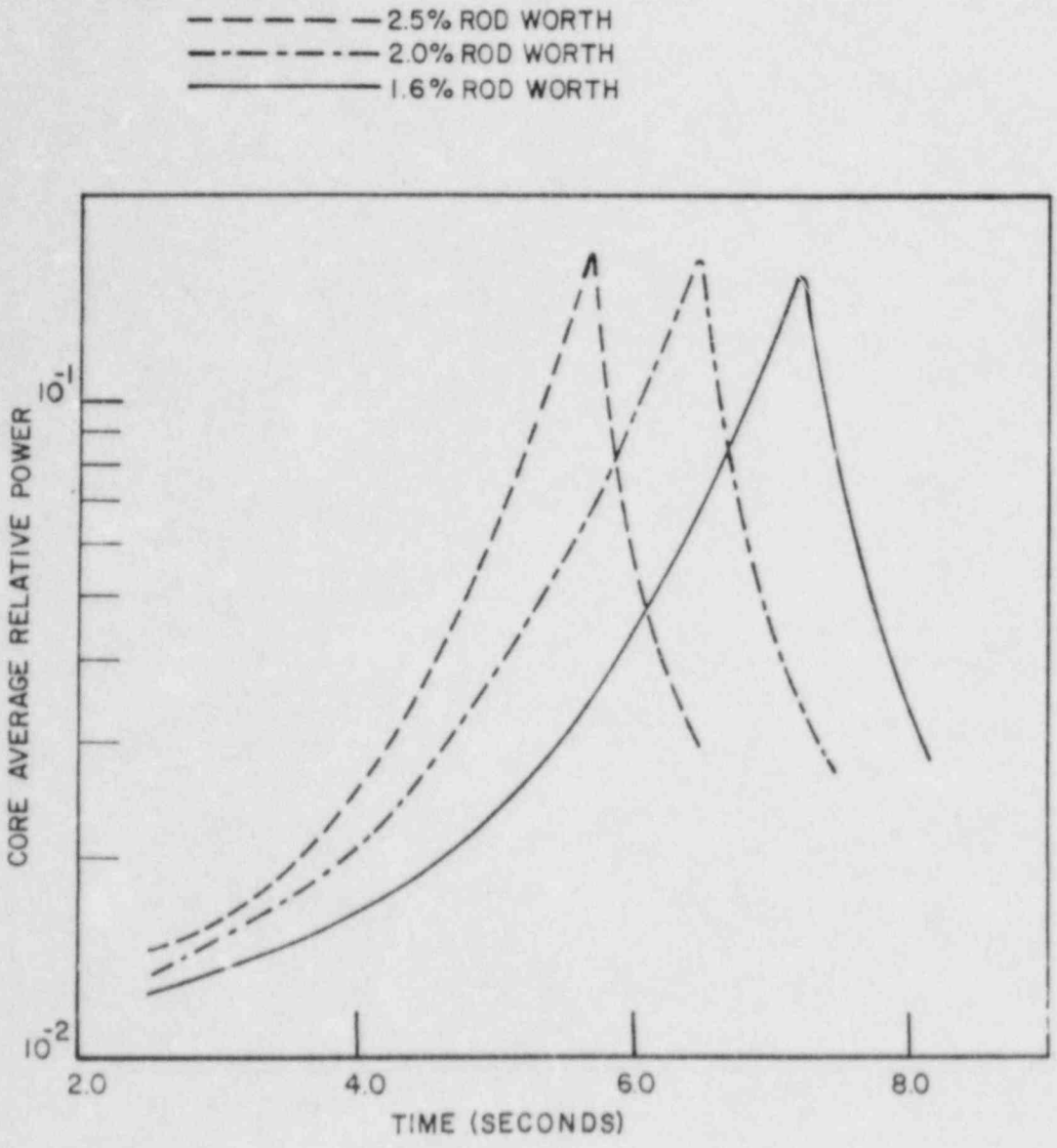

LA SALLE COUNTY STATION FINAL SAFETY ANALYSIS REPORT
FIGURE 15.4.1-3 CONTINUOUS RWE IN THE STARTUP RANGE CORE AVERAGE POWER VS. TIME FOR 1.6%, 2.0% AND 2.5% ROD WORTH'S (POINT MODEL KINETICS)

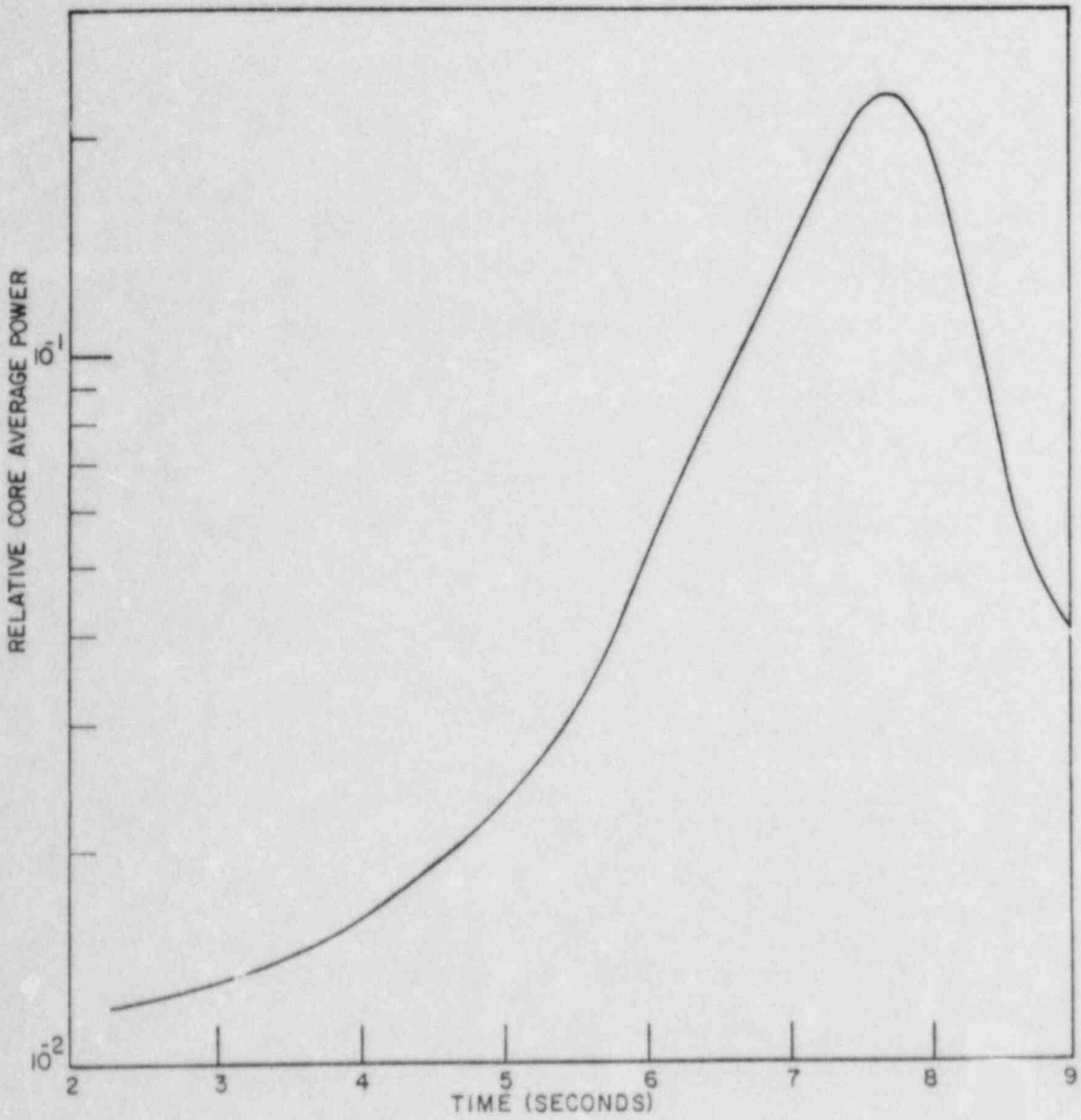

ASSUMPTIONS:

1. 1.6% Δk ROD
2. 0.3 fps WITHDRAWAL VELOCITY
3. IRM SCRAM FOR WORST BYPASS CONDITION
4. $P_o = 10^{-2}$ OF RATED
5. 1967 PRODUCT LINE TECH SPEC SCRAM RATE
6. EXPOSURE = 0.0 GWD/T

LA SALLE COUNTY STATION
FINAL SAFETY ANALYSIS REPORT

FIGURE 15.4.1-4

CONTINUOUS CONTROL ROD WITHDRAWAL FROM HOT STARTUP

15A.1.11 Continuous Control Rod Withdrawal During Power Range Operation

15A.1.11.1 Identification of Causes

While operating in the power range in a normal mode of operation the reactor operator makes a procedural error and withdraws the maximum worth control rod continuously until the rod block monitor (RBM) system inhibits further withdrawal.

15A.1.11.2 Sequence of Events and Systems Operation

While operating in the power range in a normal (except as noted in Section 15A.1.11.3.2) mode of operation, the reactor operator makes a procedural error and withdraws the maximum worth control rod continuously until the RBM system inhibits further withdrawal.

Under most normal operating conditions no operator action is required since the transient which would occur would be very mild. Should the peak linear power design limits be exceeded, the nearest local power range monitor (LPRM) would detect this phenomenon and sound an alarm. The operator must acknowledge this alarm and take appropriate action to rectify the situation.

If the rod withdrawal error is severe enough, the RBM system would sound alarms, at which time the operator would acknowledge the alarm and take corrective action. Even for extremely severe conditions (i.e., for highly abnormal control rod patterns, operating conditions, and assuming that the operator ignores all alarms and warnings and continues to withdraw the control rod), the RBM system will block further withdrawal of the control rod before fuel damage occurs.

Due to this positive reactivity insertion, the core average power will increase. More importantly, the local power in the vicinity of the withdrawn control rod will increase and potentially could cause localized cladding damage due to either achieving boiling transition or by exceeding the 1 percent plastic strain limit imposed on the cladding, which are the assumed transient failure threshold. The following list depicts the sequence of events for this transient:

	Event	Approximate Elasped Time
1.	Event begins -- Operator selects and withdraws at maximum rod speed the maximum worth control rod	0 sec
2.	Core average and local power increase	------
3.	Local power range monitors sound alarm	<5 sec
4.	Event ends -- by a RBM initiated rod block	<30 sec

15A.1.11.3 Core and System Performance

15A.1.11.3.1 Mathematical Model

For this transient the reactivity insertion is very slow; therefore, it is adequate to assume that the core has sufficient time to equilibrate (i.e., that both the neutron flux and heat flux are in phase). Making use of the above assumption, this transient is calculated using a steady-state three-dimensional coupled nuclear-thermal-hydraulic computer program. All spatial effects are included in the calculation.

The analytical methods and assumptions which are used in evaluating the consequences of this accident are considered to provide a realistic, yet conservative assessment of the consequences.

The basic code used for the Rod Withdrawal Error is the BWR Simulator Code as described in Section 4.3. This code calculates the nuclear responses and the instrument readings. A detector response code uses the instrument responses to predict the Rod Block Monitor action under the specified condition for the Rod Withdrawal Error.

15A.1.11.3.2 Input Parameters and Initial Conditions

The assumed error is a continuous withdrawal of the maximum worth rod at its maximum drive speed for a core operating at rated power. For purposes of conservatism, abnormal core conditions and the selection of an abnormal control rod pattern are assumed. The reactor is presumed to be in its most reactive state and devoid of all xenon. This ensures that the amount of excess reactivity which must be controlled by the movable control rods is maximum. Furthermore, it is assumed that the operator has fully inserted the maximum worth rod prior to its removal and selected the remaining control rod pattern in such a way as to achieve thermal limits in a fuel bundle in the vicinity of the rod to be withdrawn (see Fig. 15A.1.11-1). It should be

emphasized that this control rod configuration would be highly abnormal and could only be achieved by deliberate operator action or by numerous operator errors. Table 15A.1.11-1 presents the other parameters used in the analysis of this event.

The RBM has three trip levels (rod withdrawal permissive removed). The trip levels may be adjusted and are nominally 8 percent of reactor power apart. The highest trip level is set so that the safety limit is not exceeded. The lower two trip levels are intended to provide a warning to the operator. Settings are 107, 99, and 91 percent of initial, steady-state, operating power at 100 percent flow. The trip levels are automatically varied with reactor coolant flow to protect against fuel damage at lower flows. The variation is set to assure that no fuel damage will occur at any indicated coolant flow. The operator may encounter any number (up to three) of trip points depending on the starting power of a given control rod withdrawal. The lower two points may be passed up (reset) by manual operaion of a pushbutton. The reset permissive is actuated (and indicated by a light) when the RBM reaches 2 percent power less than the trip point. The operator should then assess his local power and either reset or select a new rod. The highest (power) trip point may not be reset.

15A.1.11.3.3 Results

The consequences of this transient are relatively mild and neither localized nor gross occurrence of boiling transition or violation of 1 percent plastic strain limit on the cladding occur. The variation in the MLHGR and MCPR, as a function of withdrawal of the highest worth rod, is presented on Figs. 15A.1.11-2 and 3, respectively. The bundles presented on Figs. 15A.1.11-2 and 3 represent the envelope of the MLHGR and the MCPR for each two-foot interval during the transient. The variation in the total reactor power is also shown on Fig. 15A.1.11-3. Although these figures show the change in thermal limits from the fully inserted to the fully withdrawn position, the control rod is automatically blocked at 4.5 feet, even under the worst set of assumptions. The variation in the signal response of the two independent channels is shown on Figs. 15A.1.11-4 and 5. With a set point of 107 percent, the rod is shown to block at 4.5 feet resulting in a ΔMCPR of (-) 0.128 and MLHGR of 13.5 percent kW/ft.

15A.1.11.4 Barrier Performance

An evaluation of the barrier performance was not made for this event since no radioactive material is released from the fuel.

15A.1.11.5 Radiological Consequences

An evaluation of the radiological consequences was not made for this event since no radioactive material is released from the fuel.

15A.1.12 Continuous Rod Withdrawal During Reactor Startup

15A.1.12.1 Identification of Causes

While operating in the power, source, and/or intermediate range of operation, the reactor operator makes a procedural error and withdraws the maximum worth control rod continuously.

15A.1.12.2 Sequence of Events and Systems Operation

Control rod withdrawal errors are not considered credible in the startup power range. The RSCS and the RWM prevent the operator from selecting and withdrawing an out-of-sequence control rod.

Continuous control rod withdrawal errors during reactor startup are precluded by the RSCS. The RSCS prevents the withdrawal of an out-of-sequence control rod in the 100 to 50 percent control rod density range and limits rod movement to the banked position mode of rod withdrawal from the 50 percent rod density to the desired power level. Since only in-sequence control rods can be withdrawn in the 100 to 50 percent control rod density and control rods are withdrawn in the banked position mode from the 50 percent control rod density point to the desired power level, there is no basis for the continuous control rod withdrawal error in the startup power range. See Section 15A.1.11 for description of continuous control rod withdrawal during power range operation. The bank position mode of the RSCS is described in Reference 4.

15A.1.12.3 Core and System Performance

The performance of the RSCS and RWM prevent erroneous selection and withdrawal of an out-of-sequence control rod, as described in Section 15A.1.12.2. Thus, the core and system performance is not affected by such an operator error.

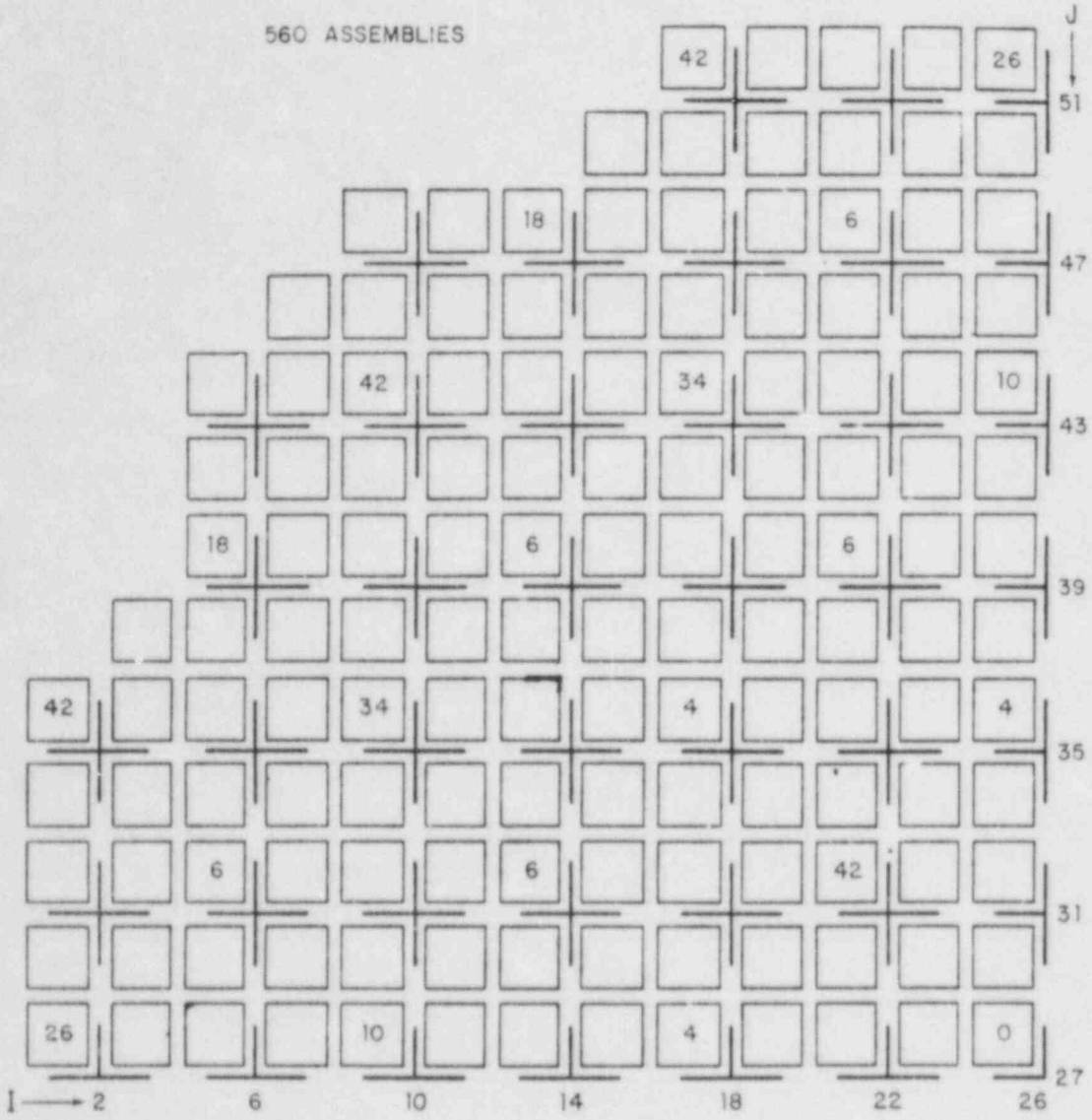

FIG. 15A.1.11-1

ROD PATTERN FOR RWE ANALYSIS
1/4 CORE SYMMETRY
SHOREHAM NUCLEAR POWER STATION-UNIT 1
FINAL SAFETY ANALYSIS REPORT

REVISION 12 - JULY 1978

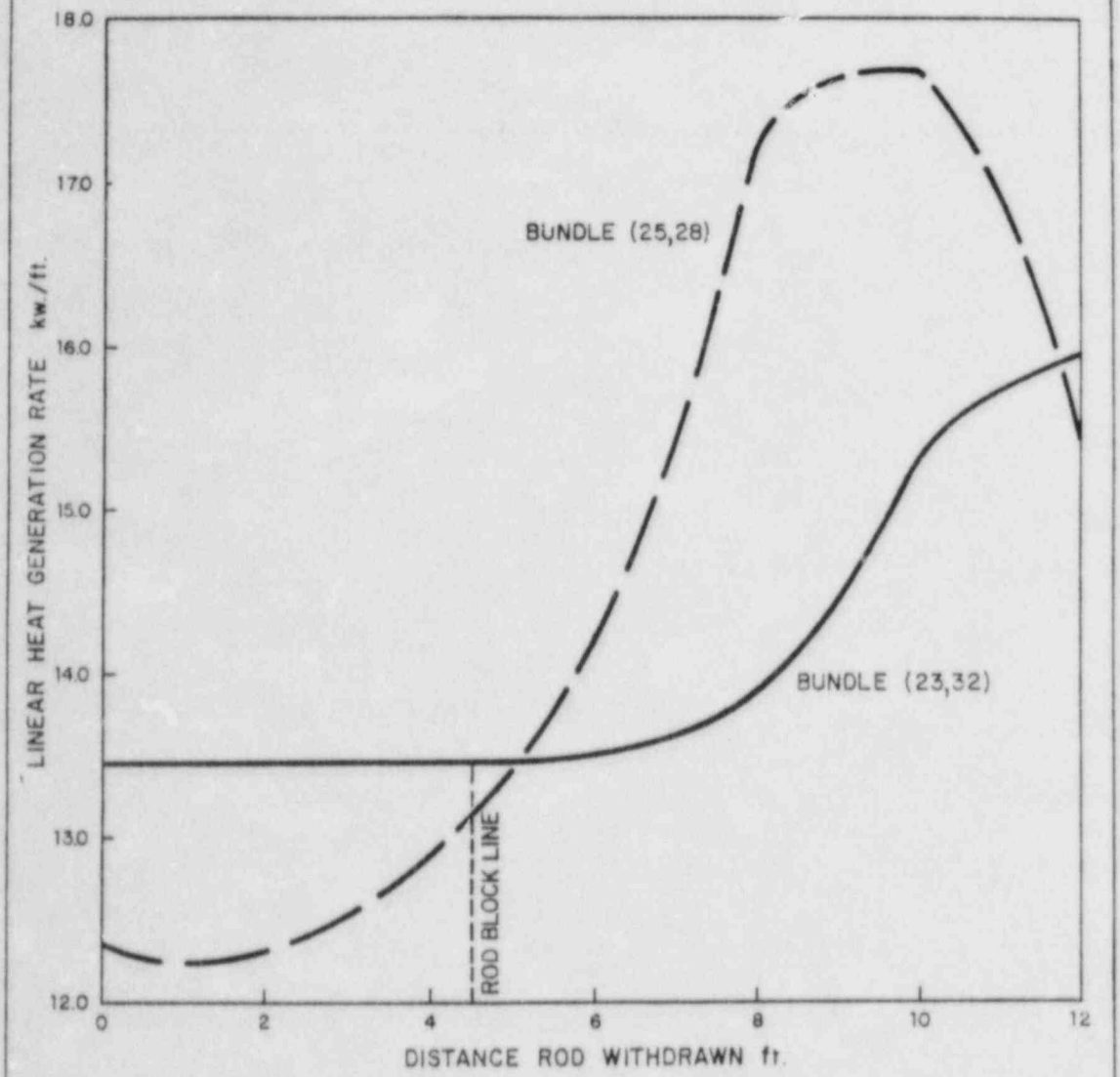

FIG. 15A.1.11-2

VARIATION OF MLHGR WITH THE DISTANCE ROD (26,27) IS WITHDRAWN DURING CONTINUOUS ROD-WITHDRAWAL ERROR

SHOREHAM NUCLEAR POWER STATION - UNIT 1
FINAL SAFETY ANALYSIS REPORT

REVISION 12 - JULY 1978

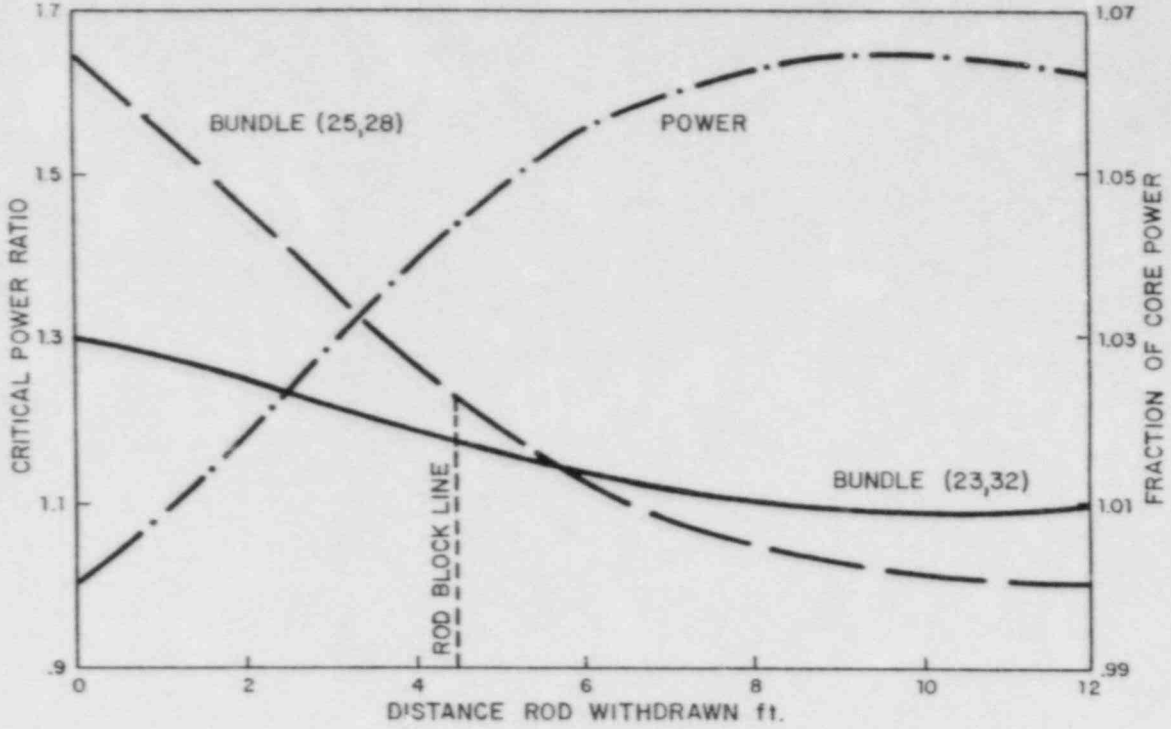

FIG. 15A.1.11-3

VARIATION OF CORE POWER AND MCPR WITH THE DISTANCE ROD (26,27) IS WITHDRAWN DURING CONTINUOUS ROD-WITHDRAWAL ERROR

SHOREHAM NUCLEAR POWER STATION - UNIT 1
FINAL SAFETY ANALYSIS REPORT

REVISION 12 - JULY 1978

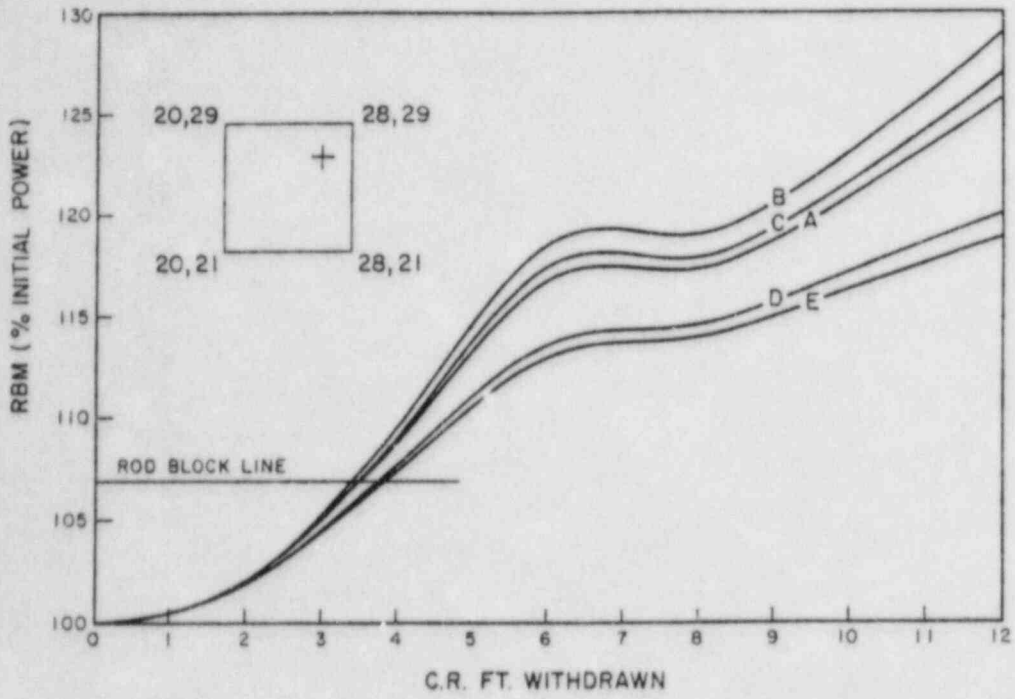

LEGEND

A NONE FAILED
B 20,21
C 28,21
D 28,29
E 28,29 AND 28,21

NOTE

SHOREHAM CYCLE 1

CONTROL ROD WITHDRAWAL IS BLOCKED AT 45 FT., BASED ON 1.07 SETPOINT

FIG. 15A.1.11-4

RBM RESPONSE TO CONTROL ROD MOTION-CHANNEL A&C

SHOREHAM NUCLEAR POWER STATION-UNIT 1
FINAL SAFETY ANALYSIS REPORT

REVISION 12-JULY 1978

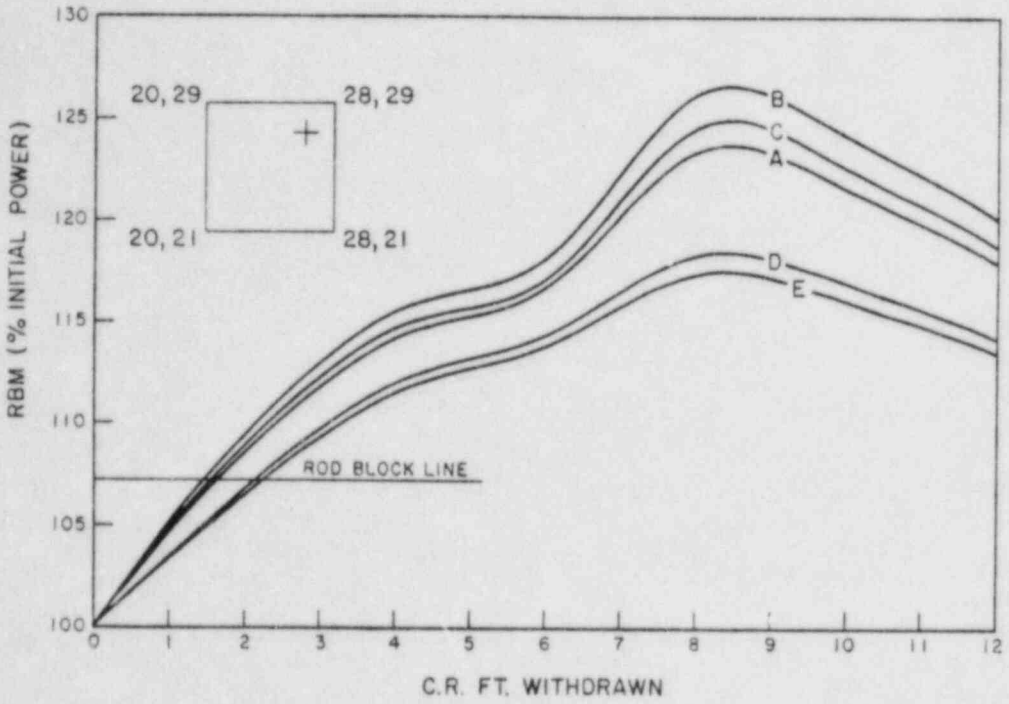

LEGEND

A NONE FAILED
B 20, 21
C 28, 21
D 28, 29
E 28, 29 AND 28, 21

NOTE

SHOREHAM CYCLE 1

CONTROL ROD WITHDRAWAL IS BLOCKED AT 3.0 FT., BASED ON 1.07 SETPOINT

FIG. 15A.1.11-5

RBM RESPONSE TO CONTROL ROD MOTION-CHANNEL B & D

SHOREHAM NUCLEAR POWER STATION-UNIT 1
FINAL SAFETY ANALYSIS REPORT

REVISION 12 - JULY 1978

APPENDIX E

PORTIONS OF THE ST. LUCIE NUCLEAR POWER STATION FINAL SAFETY ANALYSIS REPORT

15.1.5 LIMITING FAULT 3 EVENTS

15.1.5.1 Limiting Offsite Dose Event - Loss of Main Steam Outside Containment, Upstream of MSIV With Loss of Offsite Power as a Result of Turbine Trip

15.1.5.1.1 Identification of Event and Causes

All Limiting Fault-3 event groups and event group combinations resulting in an increased heat removal by the secondary system shown in Table 15.1.5-1 were compared to find the event resulting in the maximum offsite doses. The loss of main steam-large, outside containment, upstream of MSIV with loss of offsite power as a result of turbine trip and with technical specification primary to secondary leakage through the steam generator tubes was identified as the limiting LF-3 event.

The event groups and event group combinations evaluated and the significance of the offsite doses for each are indicated in Table 15.1.5-1. All events indicated as insignificant (I) would produce offsite doses well within the acceptance guideline in Table 15.0-4. All events indicated as significant (S) produce offsite doses within the acceptance guideline.

The loss of main steam-large, outside containment may occur due to a break in the 34 inch main steam line.

Breaks ranging from 0.056 ft^2 area up to the double-ended rupture of the 34 inch main steam line break are included in this event group. Events with break areas less than 0.056 ft^2 are classified in the small loss of main steam event group. The offsite doses were maximized by assuming an intermediate break (1.8 ft^2) which results in a minimum DNBR below 1.19. Technical specification tube leakage also increased the offsite doses. The loss of offsite power as a result of turbine trip causes the coastdown of all reactor coolant pumps. 7

Of the two event groups, loss of main steam-large inside containment and loss of main steam-large outside containment, in the LF-3 category, loss of main steam-large, inside containment will not cause a significant amount of steam release to the atmosphere and therefore will not result in significant offsite doses. Loss of main steam-large, outside containment with a loss of offsite power and a technical specification tube leakage is the limiting event combination, since the decreased RCS flow due to the loss of power results in degradation of fuel performance, and the technical specification tube leakage maximizes the release of activity to the atmosphere.

15.1.5.1.2 Sequence of Events and Systems Operation

Table 15.1.5.1-1 presents a chronological list and timing of system actions which occur following the large loss of main steam event outside containment with a loss of offsite power as a result of turbine trip.

The sequence of events and systems operation are identical to those presented in 15.1.5.3.2 and Figure 15.1.5.3-1 with the exception of the reactor trip set points and the response of systems actuated by the occur-

rence of high containment pressure. High containment pressure is not present in this event.

Table 15.1.5.1-2 contains a matrix which describes the extent to which normally operating plant systems are assumed to function during the transient. The operation of these systems is consistent with the guidelines of Subsection 15.0.2.3.

Table 15.1.5.1-3 contains a matrix which describes the extent to which safety systems are assumed to function during the transient.

15.1.5.1.3 Analysis of Effects and Consequences

a) Mathematical Models

The NSSS response to a loss of main steam with loss of offsite power as a result of turbine trip was simulated using the CESEC computer program described in Subsection 15.0-4. The transient minimum DNBR values were calculated using the TORC code which used the CE-1 CHF correlation described in Subsection 15.0-4.

b) Input Parameters and Initial Conditions

From the range of values for each of the principal process variables given in Subsection 15.0-3, a set of initial conditions contained in Table 15.1.5.1-4 was chosen that produces the lowest minimum DNBR. Additional clarification of the assumptions and parameters listed in Table 15.1.5.1-4 follows.

Maximum initial core power, maximum initial core inlet temperature, minimum initial core mass flowrate and initial RCS pressure are chosen to minimize the DNBR, and maximize offsite doses.

The moderator temperature coefficient and break size were varied to delay the occurrence of reactor trip either on low steam generator pressure or high core power level, thus maximizing the core heat flux. An intermediate break size corresponding to 1.8 ft^2 effective steam flow area per steam generator with a moderator temperature coefficient of -1.6×10^{-4} $\Delta\rho/F$ results in the lowest value of minimum DNBR and maximum degradation of fuel performance.

In order to further maximize the degradation in fuel performance and, thus, to maximize offsite doses, the time of turbine trip and the loss of offsite power, which caused four reactor coolant pumps to coastdown, is chosen so that the low reactor coolant flow trip condition occurs coincident with the low steam generator pressure reactor trip.

In this event, the turbine is assumed to trip prior to reactor trip due to depressurization of Main Steam System. The reactor trip on low hydraulic oil pressure is expected to occur during this event. In this analysis it is conservatively assumed that this trip does not occur prior to reactor trip on low reactor coolant flow or low steam generator pressure.

The Pressurizer Pressure Control System and the Pressurizer Level Control System are assumed to be in the manual mode of operation and, therefore, do not function to mitigate depressurization of the Reactor Coolant System (RCS). This results in low RCS pressure which minimizes the DNBR.

The highest one pin radial peak with the most top peaked axial power shape is chosen to minimize the DNBR during the transient.

c) Results

The dynamic behavior of important NSSS parameters following this event are presented on Figures 15.1.5.1-1 to 14. Table 15.1.5.1-1 summarizes some of the important results of this event and the times at which minimum and maximum parameter values discussed below occur. 7

A break in the main steam line outside containment causes an increase in steam flow, resulting in depressurization of the steam generators as shown on Figure 15.1.5-9. The pressure decrease initiates a low steam generator pressure trip and, subsequently, generates a main steam isolation signal (MSIS). MSIS closes the main steam isolation valves and main feedwater isolation valves isolating the intact steam generator while the steam generator connected to the ruptured line continues to blow down through the break.

The decreasing secondary pressure and temperature leads to an increase in primary to secondary heat transfer rate which causes the primary coolant (core average) temperature to decrease. Prior to reactor trip due to a negative moderator temperature coefficient, the decreasing core average temperature causes moderator reactivity to increase, resulting in an increase of core power. After reactor trip, the core power further decreases to decay power level as shown on Figure 15.1.5.1-1.

The increasing core heat flux and the decreasing reactor coolant flow rate result in a decreasing minimum DNBR as shown on Figure 15.1.5.1.8. The reactor trip causes the core heat flux to decrease resulting in a subsequent increase in minimum DNBR. The minimum DNBR experienced during a loss of main steam with a loss of offsite power as a result of turbine trip is 0.88 resulting in 3.1 percent of the fuel pins in DNB.

During this event, two sources of radioactivity contribute to the offsite dose, the initial activity in the steam generator inventory, which is assumed to be 0.1 μCi/cc dose equivalent I-131, and activity which is added to the steam generator during the transient due to assumed technical specification primary to secondary leakage through the steam generator tubes of 1 gallon/minute. 11

During the cooldown, steam releases from the intact steam generator via the MSVs and ADVs contribute to the offsite dose. 7

The offsite dose due to the loss of main steam-large, outside containment with loss of offsite power and with technical specification pri-

mary to secondary leakage through the steam generator tubes results in no more than a 70 rem two hour inhalation thyroid dose at the exclusion area boundary. The total offsite doses during this event are shown in Table 15.1.5.1-5. | 7 | 11

15.1.5.1.4 Conclusions | 7

This evaluation shows that the plant response to the loss of main steam-large outside containment with loss of offsite power as a result of turbine trip and with technical specification primary to secondary leakage through the steam generator tubes results in maximum offsite doses which are within the acceptance guideline in Table 15.0-4.

15.1.5.2 Limiting Reactor Coolant System Pressure Event

All Limiting Fault-3 event groups and event group combinations resulting in an increased heat removal by the secondary system shown in Table 15.1.5-1 are characterized by decreasing Reactor Coolant System (RCS) pressure. The peak RCS pressure which would occur during the most adverse of these events does not approach the acceptance guideline specified in Table 15.0-4. | 2

15.1.5.3 Limiting Fuel Performance Event - Loss of Main Steam With Loss of Offsite Power as a Result of Turbine Trip

15.1.5.3.1 Identification of Event and Causes

All Limiting Fault-3 (LF-3) event groups from the Increased Heat Removal by the Secondary System event type and the LF-3 event group combinations shown in Table 15.1.5-1 were compared to find the limiting fuel performance event. The loss of main steam-large, inside containment with loss of offsite power as a result of turbine trip was identified as the limiting LF-3 event.

The event groups and event group combinations evaluated and the significance of the approach to the fuel performance acceptance guidelines are indicated in Table 15.1.5-1. All event groups or event group combinations indicated as insignificant (I) produce fuel performance well within the acceptance guideline in Table 15.0-4. All events indicated as significant (S) produce a fuel performance within the acceptance guideline. | 2 | 2

The loss of main steam-large, inside containment may occur due to a break in the 34/36 inch main steam line. | 2

Breaks ranging from 0.056 ft^2 area up to the double-ended rupture of the 34/36 inch main steam line are included in this event group. Events with break areas less than 0.056 ft^2 are classified in the small loss of main steam event group. The potential for degradation in fuel performance was maximized by an intermediate size break (2.27 ft^2) (see Subsection 15.1.5.3.3 for details). The loss of offsite power as a result of turbine trip causes the coastdown of all reactor coolant pumps. | 2 | 2

Of all the event groups and event group combinations considered in the LF-3 category, loss of main steam events caused by large steam line breaks, both

inside and outside containment, result in maximum RCS pressure decrease and maximum core power increase prior to trip, both of which affect the fuel performance. Inside containment breaks are more adverse than outside containment breaks due to the assumed adverse impact of the steam environment on reactor trip setpoints. Loss of main steam-large, inside containment with a loss of offsite power as a result of turbine trip is the limiting event combination, since loss of power results in loss of all four reactor coolant pumps, which decreases the RCS flow and, consequently increases the degradation of fuel performance. 2

15.1.5.3.2 Sequence of Events and Systems Operation

Table 15.1.5.3-1 presents a chronological list and timing of system actions which occur following the large loss of main steam event, inside containment with a loss of offsite power as a result of turbine trip. Refer to Table 15.1.5.3-1 while reading this and the following section. The success paths referenced are those given on the sequence of events diagram (SED), Figure 15.1.5.3-1. This figure, together with Table 15.0-6, which contains a glossary of SED symbols and acronyms, may be used to trace the actuation and interaction of the systems used to mitigate the consequences of this event. The timings in Table 15.1.5.3-1 may be used to determine when after the initiating event, each action occurs.

The sequence presented demonstrates that the operator can cool the plant to cold shutdown during the event. 2

The sequence of events and systems operations described below represents the way in which the plant was assumed to respond to the event initiator. Many plant responses are possible, however, certain responses are limiting with respect to the acceptance guidelines for this section. Of the limiting responses, the most likely one to be followed was selected.

Table 15.1.5.3-2 contains a matrix which describes the extent to which normally operating plant systems are assumed to function during the transient. The operation of these systems is consistent with the guidelines of Subsection 15.0.2.3.

Table 15.1.5.3-3 contains a matrix which describes the extent to which safety systems are assumed to function during the transient.

The success paths in the sequence of events diagram, Figure 15.1.5.3-1, are as follows:

Reactivity Control:

A reactor trip signal (RTS) is automatically generated by the Reactor Protective System on either low reactor coolant pump flow, low steam generator pressure, low electrohydraulic control oil pressure, or high containment pressure. The RTS opens the reactor trip circuit breakers to de-energize the control element drive mechanism (CEDM) bus power supply interrupting power to the CEDM holding coils, allowing the control element assemblies to fall into the core. The closure of the MSIVs and MFIVs, as discussed under the Secondary System Integrity success path, limits the extent of cooldown of the reactor coolant thereby limiting moderator reactivity insertion caused by the

negative MTC. After the reactor trip, a safety injection actuation signal (SIAS) is generated by the Engineered Safety Features Actuation System (ESFAS) on low pressurizer pressure. Negative reactivity is inserted when the borated water from the refueling water tank (RWT) is supplied by the high pressure safety injection (HPSI) pumps. The SIAS switches the charging pump suction from the volume control tank to the boric acid makeup tank (BAMT). The charging pumps are manually loaded onto the safety bus and started. The RCS boron concentration is increased to the cold shutdown level by replacing the RCS volume shrinkage with borated water.

Reactor Heat Removal:

The Reactor Coolant System provides natural circulation to remove core heat following coastdown of the reactor coolant pumps. The steam generators provide primary to secondary heat transfer where the heat is removed by the blowdown of the steam generators. After a period of reverse heat transfer, the intact steam generator serves as the heat sink for normal primary to secondary heat transfer. Additional heat removal is provided through the injection of cold water from the RWT following SIAS, as discussed under the Primary System Integrity success path. The Shutdown Cooling System (SCS) is manually actuated when the RCS temperature and pressure have been reduced to 350 F and 275 psia, respectfully. The SCS provides sufficient flow to cool the RCS to cold shutdown conditions. 2

Secondary System Integrity:

Upon decrease in the steam supply to the turbine, the Turbine Control System is assumed to generate a turbine trip signal (TTS). The TTS causes the digital electrohydraulic control system to close the turbine stop and control valves.

A main steam isolation signal (MSIS) is generated by the ESFAS upon the sensing of low steam generator pressure in the affected SG or on high containment building pressure. The MSIS isolates both SGs by closing their main steam isolation valves and feedwater isolation valves. 3 When the RCS temperature is stabilized, the operator actuates the auxiliary feedwater (AFW) pumps and opens the appropriate AFW discharge valves to supply feedwater from the condensate storage tank to the intact SG. The AFW control valve is manually regulated to maintain the SG level. The operator closes the moisture separator reheater block valves. To initiate cooldown, the atmospheric dump valves (ADV) of the SG with intact piping are opened. When offsite power is restored, the operator starts the circulating water pumps, clears the MSIS and blocks the MSIS from the affected SG to be opened, and actuates the hogging ejectors to restore condenser vacuum. The steam bypass control system is then actuated to cool the plant, terminating the release to the atmosphere. When steam pressure drops too low to maintain condenser vacuum, the operator opens the atmospheric dump valves (ADVs) and controls the dumping of steam to the atmosphere until shutdown cooling entry conditions are reached. When the ADVs are actuated, use of the SBCS is terminated and the main steam isolation valves are closed in preparation to break vacuum. 2

Primary System Integrity:

Initially, the pressurizer assists in the control of the RCS pressure and

volume changes during the transient by compensating for the contraction of the RCS fluid. Eventually the pressurizer empties and void forsmation in the reactor vessel head compensates for any additional contraction of the RCS fluid. The SIAS closes the letdown isolation valves and switches the charging pump suction from the VCT to the BAMT. The HPSI pumps restore the pressurizer level. When the RCS boron concentration has been increased to the cold shutdown level, the operator switches the charging pump suction from the BAMT to the RWT. Whe operator throttles the HPSI pumps when pressurizer level has been re-established. During cooldown, the charging pumps are started and operated as required to maintain the pressurizer level. The charging pumps initially take suction from the BAMT until the RCS has been increased to the cold shutdown boron concentration, at which time the charging pump suction is realigned to the refueling water tank. As the RC pressure is reduced, the operator blocks the safety injection actuation signal to prevent its inadvertent actuation. The safety injection tanks are depressurized by draining or venting and then are isolated to permit further depressuization of the RCS. After the reactor coolant pumps have been stopped, the operator uses the auxiliary spray to reduce pressurizer pressure. 2

Containment Integrity:

The containment absorbs and contains the initial mass and energy release. The SIAS actuates the Containment Cooling System fans to circulate and cool the containment atmosphere. A containment spray actauation signal (CSAS) is generated by the ESFAS on high-high contaminment pressure activating the containment Spray System to provide further cooling of the containment atmosphere.

Plant Habitability:

The CIAS isolates the control room from the external atmosphere and starts the emergency cooling fans. The SIAS stops the normal Reactor Auxiliary Building exhaust fans and starts the normal Reactor Auxiliary Building supply fans (if not already operating) and the Emergency Core Cooling System (ECCS) area exhaust fans. Air flow is diverted from non-essential areas of the Reactor Aux iliary Building to the ECCS pump rooms to provide environmental control of these essential areas and to divert the exhaust air from the Reactor Auxiliary Building through a high efficiency filter. (Isolation of the control room is not necessary for this event.)

Radioactive Effluent Control:

The SIAS isolates non-essential CCW and the letdown line. A containment isolation actuation signal (CIAS) is generated by the ESFAS on high containment pressure. The CIAS isolates a number of lines leading to and from containment including the containment sump pump discharge lines, and the steam generator blowdown lines. The Containment Spray System provides a vehicle for distributing hydrazine from the Iodine Removal System. A low level signal isolates the spray chemical storage tank, terminating the hydrazine addition. (The Iodine Removal System is automatically actuated but does not mitigate the consequences of this event.)

Maintenance of AC Power:

A low voltage on the 4.16 kV safety buses generates an undervoltage signal which starts the diesel generators. The non-safety buses are automatically separated from the safety buses and all loads are shed. After each diesel generator set has attained operating voltage and frequency, its output breaker closes connecting it to its safety bus. ESF equipment is then loaded in sequence onto this bus. The SIAS opens the diesel generators' output breakers and sheds all loads from the safety buses. As the diesel generators are up to speed, their output breakers reclose and the ESF equipment is again sequenced onto the safety buses. After offsite power has been restored, the operator may manually transfer the 4.16 kV non-safety buses to the startup transformers and loads the buses as required. The diesel generators are stopped when the load transfer is completed. 2

15.1.5.3.3 Analysis of Effects and Consequences

a) Mathematical Models

The NSSS response to a loss of main steam with loss of offsite power as a result of turbine trip was simulated using the CESEC computer program described in Subsection 15.0.4 . The transient minimum DNBR values were calculated using the TORC code which uses the CE-1 CHF correlation described in Subsection 15.0.4.

b) Input Parameters and Initial Conditions

From the range of values for each of the principal process variables given in Subsection 15.0.3, a set of initial conditions contained in Table 15.1.5.3-4 was chosen that produces the lowest minimum DNBR. Additional clarification of the assumptions and parameters listed in Table 15.1.5.3-4 follows.

Maximum initial core power, maximum initial core inlet temperature, minimum initial core mass flowrate and initial RCS pressure are chosen to minimize the DNBR. 2

The moderator temperature coefficient and break size were varied to delay the occurrence of reactor trip either on low steam generator pressure or high core power level, thus maximizing the core heat flux. An intermediate break size corresponding to 2.27 ft^2 effective steam flow area per steam generator with a moderator coefficient of -1.3×10^{-4} $\Delta\rho/F$ results in the lowest value of minimum DNBR and maximum degradation of fuel performance.

In order to further maximize the degradation in fuel performance the time of turbine trip and the loss of offsite power, which causes four reactor coolant pumps to coast down, is chosen so that the low reactor coolant flow trip condition occurs coincident with the low steam generator pressure reactor trip. 2

In this event, the turbine is assumed to trip prior to reactor trip due to depressurization of Main Steam System. The reactor trip on low hydraulic oil pressure would occur during this event. In this analy-

sis it is conservatively assumed that this trip does not occur prior to reactor trip on low reactor coolant flow or low steam generator pressure.

The Pressurizer Pressure Control System and the Pressurizer Level Control System are assumed to be in the manual mode of operation and, therefore , do not function to mitigate depressurization of the Reactor Coolant System. This results in low RCS pressure which minimizes the DNBR.

The highest one pin radial peak with the most top peaked axial power shape is chosen to minimize the DNBR during the transient.

c) Results

The dynamic behavior of important NSSS parameters following this event are presented on Figures 15.1.5.3-2 to 15. Table 15.1.5.3-1 summarizes some of the important results of this event and the times at which minimum and maximum parameter values discussed below occur.

A break in the main steam line inside containment causes an increase in steam flow, resulting in depressurization of the steam generators as shown on Figure 15.1.5.3-10. The pressure decrease initiates a low steam generator pressure trip and, subsequently, generates a main steam isolation signal (MSIS). MSIS closes the main steam isolation valves and main feedwater isolation valves isolating the intact steam generator while the steam generator connected to the ruptured line continues to blow down through the break. The pressure in the intact steam generator increases rapidly at first, following MSIS, followed by a gradual increase consistent with the core decay heat removal rate.

The decreasing secondary pressure and temperature leads to an increase in primary to secondary heat transfer rate which causes the primary coolant (core average) temperature to decrease. Due to an increase in heat flux, caused by loss of RCP flow, the core average temperature increases to a peak and then decreases due to reactor trip. After trip, core average temperature increases at a rate consistent with the decay heat addition to the RCS and limited heat removal by the intact steam generator. The variation in core average temperature is shown on Figure 15.1.5.3-5. The overall cooldown of the primary system leads to a depressurization of the RCS as shown on Figure 15.1.5.3-4.

Due to a negative moderator temperature coefficient, the decreasing core average temperature causes moderator reactivity to increase, resulting in an increase of core power. Subsequently, increasing core average temperature causes moderator reactivity to decrease resulting in a decrease in core power. After reactor trip, the core power further decreases to decay power level as shown on Figure 15.1.5.3-2.

The increasing core heat flux and the decreasing reactor coolant flow rate result in a decreasing minimum DNBR as shown on Figure 15.1.5.3-9. The reactor trip causes the core heat flux to decrease resulting in a subsequent increase in minimum DNBR. The minimum DNBR

experienced during a loss of main steam with a loss of offsite power as a result of turbine trip is 0.603, resulting in 7.6 percent of the fuel pins in DNB.

15.1.5.3.4 Conclusion

This evaluation shows that the plant response to a loss of main steam with a loss of offsite power as a result of turbine trip produces a fuel performance which is within the acceptance guideline in Table 15.0-4.

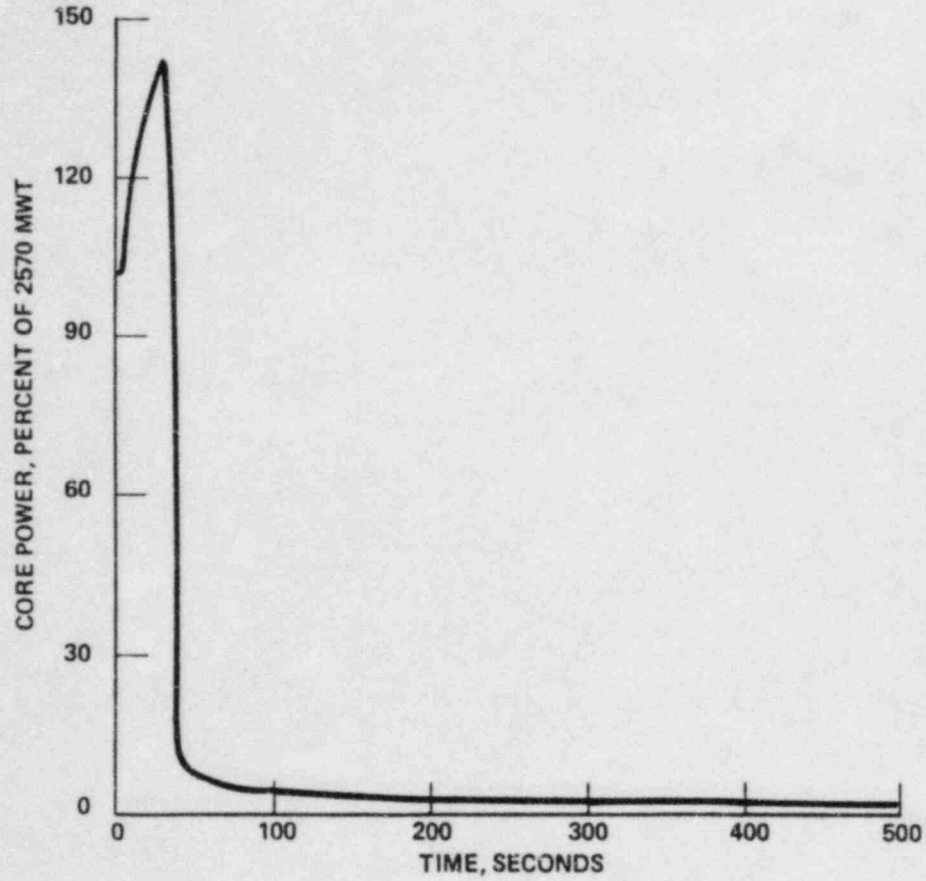

AMENDMENT NO. 6 (9/81)

FLORIDA POWER & LIGHT COMPANY
ST. LUCIE PLANT UNIT 2

CORE POWER VS TIME

FIGURE 15.1.5.3-2

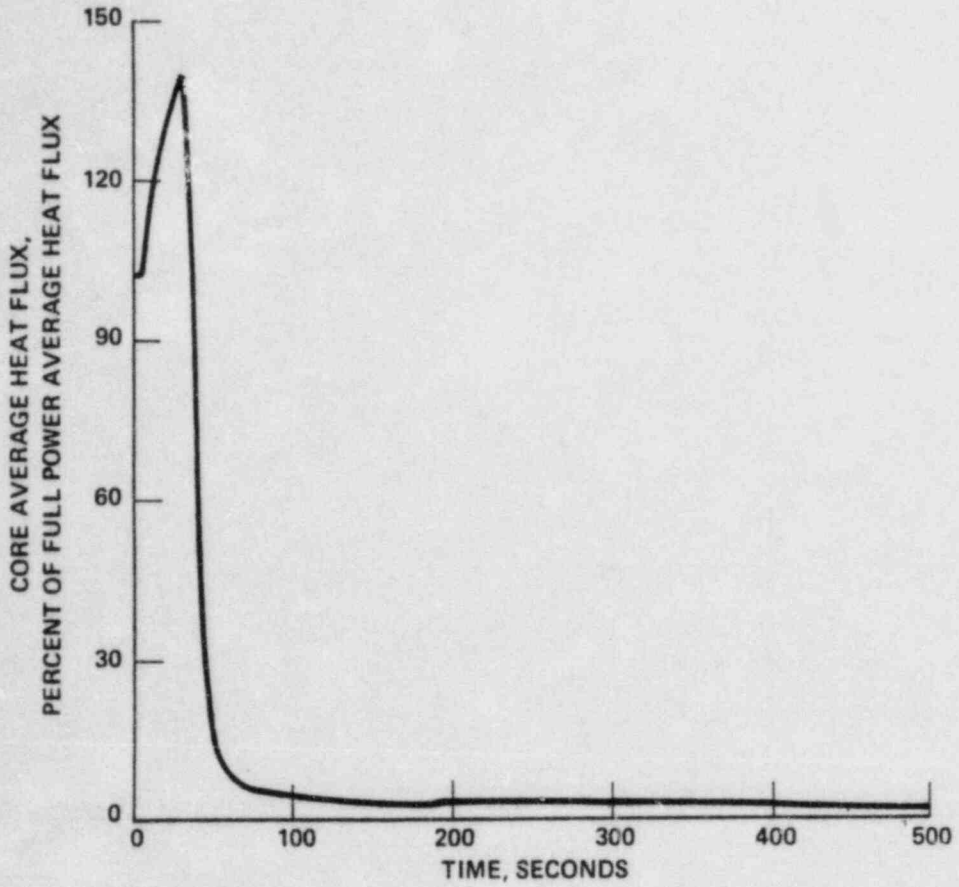

FLORIDA POWER & LIGHT COMPANY
ST. LUCIE PLANT UNIT 2

CORE AVERAGE HEAT FLUX
VS TIME

FIGURE 15.1.5.3-3

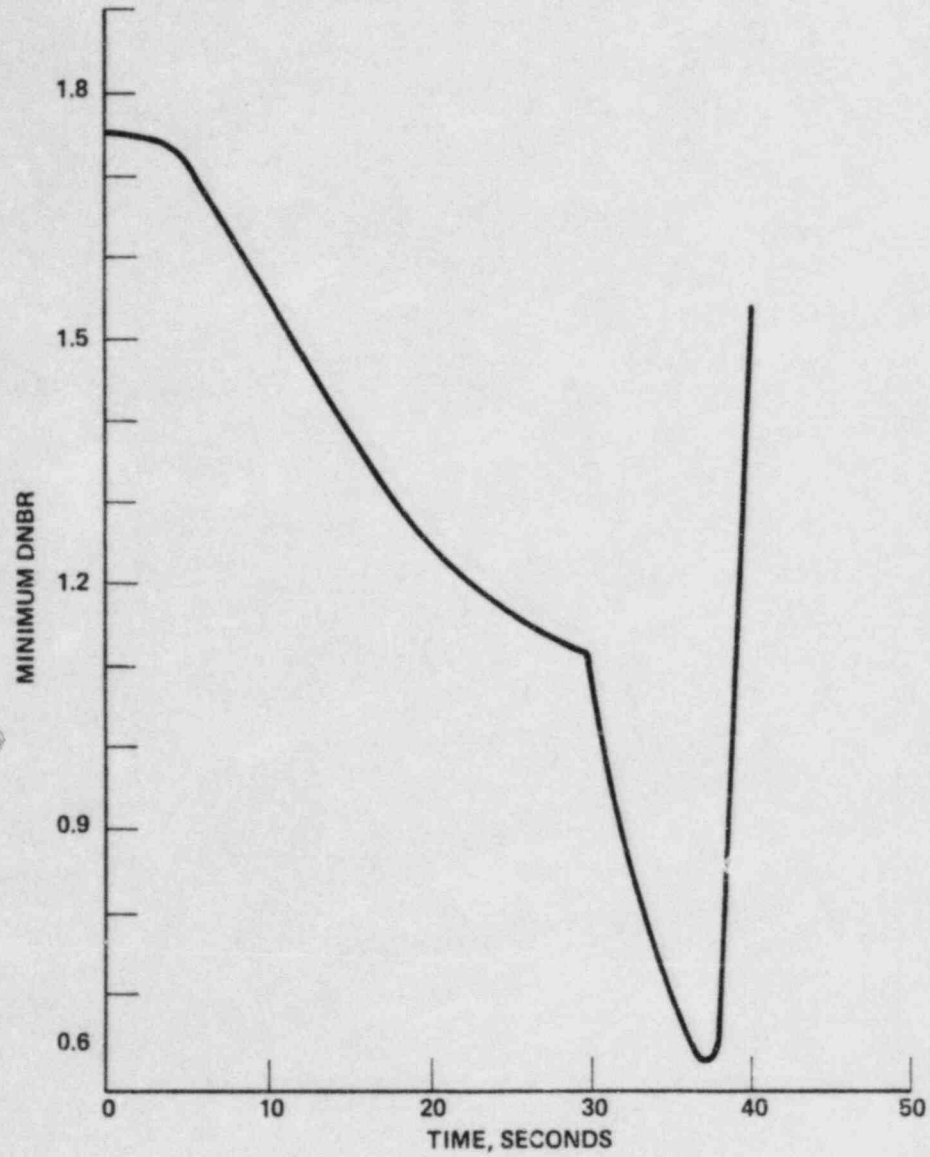

FLORIDA POWER & LIGHT COMPANY
ST. LUCIE PLANT UNIT 2

MINIMUM DNBR VS TIME

FIGURE 15.1.5.3-9

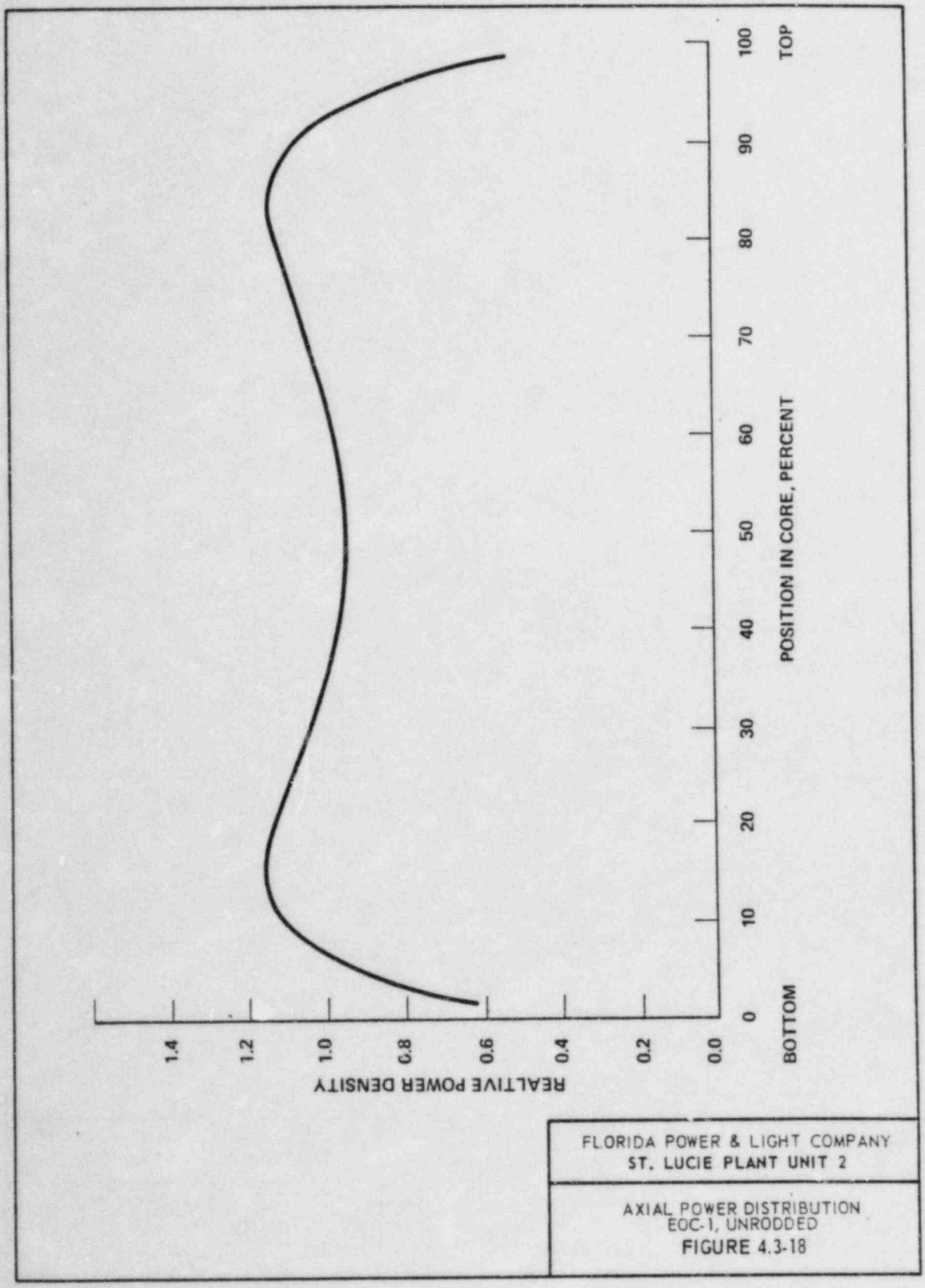

FLORIDA POWER & LIGHT COMPANY
ST. LUCIE PLANT UNIT 2

AXIAL POWER DISTRIBUTION
EOC-1, UNRODDED
FIGURE 4.3-18

EG&G Idaho, Inc.
P.O. Box 1625
Idaho Falls, Idaho 83415